TOWARDS A FEW CYCLE PULSES FROM FIBER LASERS BASED ON VARIOUS NONLINEAR PULSE PROPAGATION

A Dissertation

Presented to the Faculty of the Graduate School

of Cornell University

in Partial Fulfillment of the Requirements for the Degree of

Doctor of Philosophy

by

Hui Liu

January 2014

© 2014 Hui Liu

ALL RIGHTS RESERVED

TOWARDS A FEW CYCLE PULSES FROM FIBER LASERS BASED ON VARIOUS NONLINEAR PULSE PROPAGATION

Hui Liu, Ph.D.

Cornell University 2014

The advantage of fiber lasers is self-evident. Fiber is relatively low cost, flexible for compact design, has a large surface area to volume ratio for efficient heat dissipation, is alignment free, and provides good spatial beam quality due to its properties as a waveguide. It can be highly user friendly due to the minimum maintenance and much lower cost. The performance increases in fiber lasers have allowed them to reach applications in the fields of manufacturing with lasing machining, multi-photon biological imaging, and laser surgery. Moreover, fiber laser has rich nonlinearity so it provides a good play ground for nonlinear phenomena study, such as Rogue waves.

Before 5 years ago, fiber laser had been dominated by soliton lasers [47] [9], which gives good performance for solid state laser but has limited performance for fiber lasers due to the accumulated large nonlinear phase due from strong confined wave propagation within the small core of the fiber and relative large local dispersion to generate short pulses according to the area theorem. The ordinary soliton fiber laser has limited pulse energy of 0.1 nJ. For dispersion managed (DM) soliton fiber lasers, although the nonlinearity could be controlled to some extend by temporal pulse broadening inside the cavity, which results an order of magnitude increase of energy, it is still hard for fiber laser to compete with solid state lasers in energy. Recent developments in the field of fiber lasers over the past five years , particularly the dissipative soliton lasers at nor-

mal dispersion regime [1] showed a different nonlinear solution which does not constrained by soliton area theorem, have enabled fiber lasers to compete with solid state lasers in terms of energy around 100 fs regime.

To compete with solid state lasers, fiber lasers also must be able to achieve short pulses down to a few cycles. Solid state gain media have gain bandwidths of hundreds of nanometers while the bandwidth of doped fiber is around 40 nm, which fundamentally limits the shortest pulses available from fiber source based on commonly used mode locking mechanisms. Since the gain will act like a filter to limit the possible average cavity solution both both soliton and dissipative soliton lasers. Another difficulty is the relative large net dispersion of fiber lasers compared with solid state lasers, which starts to place additional limits on the pulse durations below 100 fs. Although 100 fs pulses can be routinely generated from fiber lasers, pulses as short as a few cycles are harder to stabilize than in solid state lasers.

Over the past few decades, fiber lasers were typically made with Er-doped fiber and later with Yb-doped fiber. Tm fiber lasers have drawn people's attention due to its potential applications for high harmonic generation, mid-IR pumping source and many other areas. In this thesis, fiber lasers with different gain medium, Erbium, Ytterbium and Thulium, will be presented with the effort of generating short pulses through the use of different mode locking mechanisms. The extended self-similar propagation, which is different from previous average cavity analysis, will be introduced as a route to few cycle pulse generation. Pulses as short a 6 cycles have been generated for both Yb and Er lasers. The extended self-similar propagation can occur in either a piece of highly nonlinear fiber through passive self-similar propagation of parabolic pulses in normal dispersion fiber or through a segment of dispersion decreasing fiber, which

has a mathematical analogy to self- similar propagation in a gain fiber. The design guide for this type of cavity will be given, and energy scaling of this cavity with large core fibers will be discussed.

BIOGRAPHICAL SKETCH

Hui Liu was born in Taiyuan, Shanxi, China in 1984. Her parents had always imagined her being a writer, a doctor, or a lovely housewife until she got into the first Science Experimental Classes in her province. Three years of immersion with all kinds of academic training and competition revealed the beauty of science to her and made her think of a path in science.

Unsatisfied with the exploration of science in high school, she continued her study as an optoelectronics major at Tianjin University, which is close to her hometown as her parents wished. By the end of college, she decided to go aboard to look at the world in her own view and seek the most advanced research experience. Luckily, she ended up at Cornell University to work on a MEng Professor Frank Wise's group, where she enjoyed not only the fascinating physics, particularly in nonlinear optics, but also the group of decent scientists and friends to work with. She then continued to stay in the group to pursue her PhD in Applied and Engineering Physics. Her journey will continue in Professor Michelle Sander's group at Boston University as a postdoctoral researcher to work on applications of ultrafast science.

To my family and Taige, for their constant support and unwavering love.

ACKNOWLEDGEMENTS

First and foremost, I thank to my advisor, Professor Frank Wise, for his teachings in both academic study and life lessons. His kindness and understanding encouraged me to come all the way today. He taught me how to do research from scratch as well how to be a self-respecting while self-criticizing scientist. I would also like to thank my committee members, Professor Alexendar Gaeta and Professor Michal Lipson, for their support and guidance in various aspects of my academic life.

I am also grateful to have a group of colleagues to work and study with. They are: Shian Zhou, Andy Chong, Will Renninger, Simon Lefrancois, Khanh Kieu, Heng Li, Zhi Zhao and Erin Stranford, Logan Wright, Yuxin Tang and Zhanwei Liu. I enjoyed the time I spent with everyone.

Finally, I am also thankful to my parents and Taige for their love and support.

TABLE OF CONTENTS

Biographical Sketch . . . iii
Dedication . . . iv
Acknowledgements . . . v
Table of Contents . . . vi
List of Figures . . . ix

1 Introduction **1**
1.1 Organization of the thesis . . . 4
1.2 Nonlinear attractors to generate short pulses from fiber laser . . . 5
1.2.1 Soliton . . . 6
1.2.2 Dissipative Solitons . . . 8
1.2.3 Similaritons . . . 10
1.3 Colorful Fiber Laser . . . 13
1.4 Mode Lockers . . . 13
1.4.1 Saturable Absorbers . . . 14
1.4.2 Spectral Filters . . . 19

2 Er Fiber Laser **24**
2.1 High Energy Soliton Fiber Laser . . . 24
2.1.1 Introduction . . . 24
2.1.2 Increase Output Ratio . . . 25
2.1.3 Increase Cavity Length . . . 27
2.1.4 Conclusion . . . 28
2.2 Dissipative Soliton Fiber Laser . . . 29
2.2.1 Introduction . . . 29
2.2.2 Simulation . . . 30
2.2.3 Experiment . . . 31
2.2.4 Conclusion . . . 33
2.3 Amplifier Similariton Fiber Laser . . . 33
2.3.1 Introduction . . . 34
2.3.2 Numerical Simulation . . . 35
2.3.3 Experimental Results . . . 39
2.3.4 Discussion . . . 40
2.3.5 Conclusion . . . 41
2.4 Enhanced bandwidth generation based on self similar evolution . . . 41
2.4.1 Introduction . . . 42
2.4.2 Numerical Simulation . . . 44
2.4.3 TOD Impact . . . 47
2.4.4 Experimental Results and Discussion . . . 49
2.4.5 Future work for enhanced bandwidth generation from Er fiber laser . . . 52
2.5 Conclusion . . . 53

3 Yb Fiber Laser **54**
3.1 Pulse generation without gain bandwidth limitation in a laser with self similar evolution . . . 54
3.1.1 Introduction . . . 54
3.1.2 Numerical Simulations . . . 58
3.1.3 Experiment . . . 59
3.1.4 Discussion . . . 64
3.1.5 Conclusion . . . 65
3.2 Extended Self-Similar Pulse Evolution in a Laser with Dispersion-Decreasing Fiber . . . 65
3.2.1 Introduction . . . 66
3.2.2 DDF Theory . . . 67
3.2.3 Numerical Simulation . . . 69
3.2.4 Experiment . . . 71
3.2.5 Conclusion . . . 74
3.3 Sub 10-fs pulse generation from DDF . . . 74
3.3.1 DDF laser features . . . 74
3.3.2 Octive Span DDF Laser . . . 76
3.3.3 Limitations of DDF Laser Cavity . . . 77
3.3.4 Future work for DDF lasers . . . 78
3.4 Scaling with CCC fiber . . . 79
3.4.1 Introduction . . . 79
3.4.2 Numerical Study . . . 79
3.4.3 Initial Experiment . . . 81
3.5 Conclusion . . . 81

4 Tm Fiber Laser **83**
4.1 Introduction . . . 83
4.2 Tm Soliton Laser . . . 84
4.2.1 Experiment . . . 84
4.2.2 Tm Soliton Laser with a Filter . . . 86
4.2.3 Dispersion Managed (DM) Tm Soliton . . . 87
4.3 Large Normal Dispersion Tm Laser . . . 89
4.3.1 Introduction . . . 89
4.3.2 Experiment . . . 90
4.3.3 Discussion . . . 92
4.3.4 Conclusion . . . 94
4.4 Conclusion and Future Direction . . . 94

5 Future Directions **97**
5.1 Spectral Compression within Gain Attractor . . . 97
5.2 Experimental Design of a Laser with Spectral Compression . . . 101
5.3 ”Hybrid” Evolution . . . 102
5.3.1 DM Soliton and Amplifier Similariton . . . 102

5.3.2 Dissipative Soliton and Amplifier Similariton 106
5.4 Conclusion 107

Bibliography **109**

LIST OF FIGURES

1.1 Illustration of self similar evolution in passive fiber(left) and amplifier(right) . . . 12
1.2 Illustration of saturable absorption . . . 14
1.3 Absorption of a fiber taper embedded in a SWCNT-polymer composite as a function of the average input power. Inset: diagram showing an embedded fiber taper used as a SA. . . . 16
1.4 The loop mirror configuration . . . 17
1.5 The transfer function of a NOLM input power in the units of kilowatt-meters . . . 17
1.6 Standard NPE set up for a fiber laser cavity. HWP: half waveplate and QWP: quarter-waveplate. . . . 18
1.7 BF bandwidth vs. the thickness of the quartz plate. 1T= 0.5mm. 20
1.8 Schematic of a typical Gaussian filter as used in a fiber laser . . . 22

2.1 Experimental setup of all fiber soliton laser . . . 26
2.2 Cavity slope efficiency with different output coupling. . . . 27
2.3 Cavity length with different output energy. . . . 28
2.4 Simulation Result of Er dissipative soliton laser.(a) Mode-locked spectrum. (b) Calculated transform limited pulse. . . . 31
2.5 Experimental setup of Er dissipative soliton laser . . . 31
2.6 Experimental Results: (a) spectrum, (b) interferometric autocorrelation of the dechirped pulse. . . . 33
2.7 Schematic . . . 35
2.8 Filter Impact on amplifier similariton lasers. (a)Filter bandwidth v.s. transform limited pulse. (b) Filter bandwidth v.s. pulse energy. Black line: Lucent fiber. Redline: Redfern fiber. Green line: Er110 fiber . . . 37
2.9 Simulation Result. Left: Mode locked spectrum. Right: Calculated transform limited autocorrelation . . . 38
2.10 Pulse evolution inside the cavity. Left: evolution of pulse duration and bandwidth. Right: pulse shape evolution compared with a parabolic pulse with the same peak power and energy. . . 38
2.11 Experimental setup. . . . 39
2.12 Experimental Results.(a) Mode locked spectrum.(b): Dechirped autocorrelation. (c) Spectrum before the gain and after the grating filter. (d) RF spectrum. . . . 40
2.13 Numerical Simulation. (a) Cavity Schematic. (b) Pulse spectrum evolution. A, B, C : the spectrum from different positions in the cavity. . . . 44
2.14 Pulse evolution inside the cavity. (a):Pulse bandwidth and duration evolution. (b): M matric evolution. . . . 45

2.15 Impact of net dispersion from gain segment with controlled all fiber lengths and nonlinearity. β_2 of the gain segment is varied artificially from 77 fs^2 to 20 fs^2. 46
2.16 Simulation Results.(a): Broadest simulated spectrum. (b) Calculated zero phase transform limit pulse from spectrum (inset) . . . 47
2.17 Simulation with and without TOD.(a):Chirped pulse without TOD. (b)Spectrum without TOD.(c):Chirped pulse TOD. (d):Spectrum withTOD. 48
2.18 Simulated pulse and spectrum with zero TOD for other parts of the cavity except for UNHA7. The TOD values are set to be -51 fs^3 (a)(b) and 51 fs^3(c)(d) 49
2.19 Simulated spectrum without TOD for the whole cavity(left) and without TOD for the fiber after the gain only (right). 50
2.20 Experimental Setup. PBS is a 50:50 1550 *nm* polarization beam splitter. QWP is quarter wave plate. HWP is half wave-plate. HNLF is high nonlinear fiber. PBC is 980 *nm* polarization beam combiner. 50
2.21 (Experiment Result. (a)Mode locked spectrum. Black line is linear scale. Blue line is log scale. Red line is the log scale spectrum of Er-doped gain. (b) Dechirped autocorrelation 51
2.22 (TOD impact on the dechirped pulse. Black line: dechirped pulse. Red line: simulated autocorrelation by adding TOD from grating to the calculated transform limited pulse. 52

3.1 Schematic of the simulated laser. HNLF: Highly nonlinear fiber. . 59
3.2 Comparison of simulation to experiment at the indicated locations in the cavity. Simulations assume 2 m length of PCF, along with parameters given in text. Top row: simulated chirped pulses. The inset is the numerical transform-limited pulse from location C. Middle row: simulated spectra. Bottom row: experimental spectra. 60
3.3 Fiber laser schematic. QWP: quarter-waveplate; HWP: half-waveplate; PBS: polarizing beam-splitter. 61
3.4 Experimental results. a) spectrum after the PCF, b) output spectrum and c) output autocorrelation signal after phase correction by MIIPS for a 25-fs pulse. 62
3.5 Experimental Results of shortest pulse. a) spectrum after the PCF, b) output spectrum and c) output autocorrelation signal after phase correction by MIIPS for a 21-fs pulse. 63
3.6 Schematic and Pulse spectrum at different location of the cavity. 70

3.7 DDF cavity properties. (a).Broadest bandwidth generated with various length of DDF. (a)Simulation (black line) and experiment results (Red line: calculated transform limited pulse from spectra. Green Line: Dechirped pulse) with different length of DDF.(b)The amount of chirp for a cavity of fixed DDF initial dispersion β_{20} with various DDF length. Red dotted line is the calculated theoretical value of the constant chirp from DDF. 70
3.8 Mode locked Simulation Result. (a):Simulated spectrum and its transform limited pulse (inset). (b): Chirped pulse and its spontaneous frequency. 71
3.9 Pulse evolution inside the cavity. Left: pulse duration and bandwidth evolution. Right:Pulse shape evolution compared with a parabolic shape with same peak power and energy. $M^2 = \int[|u| - |p|]^2 dt / \int |u|^4 dt$, where u is the pulse being evaluated and p is a parabola with the same energy and peak power.M=0.14 represents Gaussian shape. M<=0.06 represents parabolic shape 72
3.10 Experiment Setup. PBS: polarization beam splitter. 72
3.11 Generic spectrum evolution at different location of the cavity.(a) Spectrum from gain.(b) Spectrum from PCF.(c) Spectrum from PBS. (d) Comparison of spectrum from PCF and combined spectrum from PBS and grating reflection. 73
3.12 Experiment Results. (a): Mode locked spectrum. (b): Dechirped autocorrelation(black line) and calculated transform limited autocorrelation with 600 fs^2 TOD (Redline). 74
3.13 Impact of loss on DDF lasers. 75
3.14 Pump power impact on pulse bandwidth and energy. 76
3.15 DDF Simulation Results. (a): Mode locked spectrum in both linear(black) and log (red) scale. (b): Calculated transform limited autocorrelation. 77
3.16 Simulated mode locked results with different combination of 2.7 m CCC fiber and other single mode fiber. 80
3.17 Simulated mode locked results with the highest peak power. (a) Mode locked spectrum. (b) Calculated zero phase transform limited autocorrelation. 80
3.18 Simulated mode locked results with different combination of 2.7 m CCC fiber and other single mode fiber. 82

4.1 Experimental Setup. The Filter was added later. 84
4.2 Experimental Result. (a):Mode locked spectrum.(b) Autocorrelation 85
4.3 Experimental Result of Tm soliton laser With a filter. Left: Mode locked spectrum. Right: Autocorrelation. 87
4.4 DM Tm Soliton Experimental Setup with a 15T filter. 88

4.5 Experimental Result. (a):Mode locked spectrum.(b) Autocorrelation . . . 88
4.6 Experimental Setup . . . 90
4.7 Experimental Results.Left: Mode locked spectrum in log scale. Right: Autocorrelation . . . 91
4.8 Simulation Results. (a) Mode locked spectrum. (b) Autocorrelation of calculated zero phase pulse. (c) M parameter evolution within the cavity. (d) Chirped pulse . . . 93
4.9 Simulation Results of a cavity made from Advalue Photonics normal dispersion fiber.(a) Mode locked spectrum.(b) Calculated transform limited pulse. (d) Chirped pulse and its spontaneous frequency. (d) Autocorrelation of transform limited pulse . . . 96

5.1 Spectral compression within a laser schematic . . . 98
5.2 Schematic of an extended self similar laser with spectral compression . . . 98
5.3 (a) Pulse shape evolution inside the cavity. (b) Pulse bandwidth and duration evolution. (c) Mode locked spectrum. (d) Calculated transform limited pulse. . . . 99
5.4 Dispersion regimes of mode locking lasers . . . 100
5.5 (a) Schematic of self similar laser with spectral compression near zero GVD. (b) Mode locked spectrum. (c) Calculated transform limited pulse . . . 101
5.6 Experiment Setup . . . 102
5.7 Simulation Results of amplifier similariton laser with spectral compression. (a) Spectrum compression laser mode locked spectrum (b) Spectrum compression laser calculated transform limited pulse. (c) Narrow filter cavity mode locked spectrum. (d) Narrow filter cavity calculated transform limited pulse. . . . 103
5.8 Controlled spectral compression study by changing the GTI bounces. Left: spectral compression bandwidth v.s total bounces. Right: Net cavity dispersion v.s. total bounces . . . 104
5.9 Laser performance with controlled net cavity dispersion . . . 104
5.10 Simulated mode locked results from the cavity with 22 GTI bounces. Left: mode locked spectrum. Right: Calculated transform limited pulse. . . . 105
5.11 Pulse evolution from the cavity with 22 GTI bounces. Left: pulse duration evolution. Right: spectrum bandwidth evolution. . . . 106
5.12 Simulated output pulse (black line) and a parabola pulse with the same peak power and energy(red line) . . . 106
5.13 Simulation of pulse evolution of Er dissipative soliton laser from Section 3.2. Left: bandwidth and pulse duration evolution. Right: M parameter evolution to compare with parabolic pulse. M≤0.06 indicates parabolic pulse. . . . 107

CHAPTER 1

INTRODUCTION

The development of ultrafast sources and technology has opened doors for basic scientific research in areas such as chemistry and biology and in technological development such as telecommunication and micro-machining. For example, the shortest pulse will determine the fastest movement we can catch and study. Although continuous wave (CW) lasers are widely used in machining, pulses as short as 100 fs are found to give the best cutting in terms of quality and efficiency, which is very useful for high precision manufacturing of things such as medical devices. The growth of these fields also promotes the study of ultrafast science to understand fundamental limits and to develop new sources based on new understanding.

Until recently, solid state lasers, well represented by the Ti:sapphire laser, dominated the market of ultrafast tools. Its material and spectroscopic properties enables both high energy and short pulses. The shortest pulses it can generate, enabled by its large gain bandwidth, is 3 fs at 800 nm. The amplified system can reach *mJ* level. However, the high cost and demanding maintenance of solid state lasers set barriers to their potential users and widespread applications.

Fiber lasers have intrinsic advantages over solid state lasers in terms of cost, compactness, and required maintenance. The growth of the telecommunications industry helped provide various fiber components at low cost. The bending property of fiber makes lasers made from it much more compact at all repetition rates. As a natural waveguide, the alignment of the laser is minimized to simple collimator alignment or even reduced to none for all fiber cavity. Fiber

also has a large surface area to volume ratio, which acts to dissipate heat efficiently and eliminates the need for cooling in most fiber lasers. Those properties are very user friendly and result in low maintenance. Thus, fiber lasers have great potential to be routinely used for a variety of applications and even in clinical settings.

The limitations of fiber lasers are also a result of the properties of fiber. The tight confinement of the light within the fiber gives large accumulated nonlinear phase, which bounds the highest energy fiber lasers can achieve without care. But the strong nonlinearity of fiber also allows it to exhibit rich nonlinear phenomena, which make fiber lasers an appropriate medium in which to study nonlinear science, such as Rogue Wave. Fiber lasers also have relative large dispersion due to the length of the fiber needed to make a cavity. Another drawback of fiber lasers is that there are a limited choice gain media, which all have much narrow gain bandwidths than solid state lasers. The gain bandwidth will fundamentally limit the shortest pulse available from fiber oscillators without innovative ideas.

The potential advantages of fiber have motivated researchers to overcome the problems associated with fiber. Rapid progress has been made in the field of fiber lasers to the point where their performance is catching up with solid state lasers quickly. New discoveries in science and technology have enables these advances.

Recently a dissipative soliton laser has been presented by Andy Chong [1] and co-workers. It shows that a solution of cubic Ginzburg-Landau equation (CGLE) exists in a normal dispersion fiber laser which offers comparable performance to solid state lasers in the 100 fs regime. The system requires a spectral

filter to support the solution for the dissipative process and to help to stabilize the cavity. This type of laser has already been used for several biological imaging applications and is on the market at 1/3 or even less the cost of a comparable solid state laser. However, it is hard for dissipative soliton lasers to go below 80 fs since the nonlinear phase in this type of laser is controlled through the of use large normal dispersion to linearize the phase. Analytical solutions show that less net cavity dispersion is required to achieve shorter pulse durations. Thus, the minimum normal dispersion of the cavity limits the shortest pulse this laser can generate.

Fiber lasers based on self-similar propagation in the gain fiber have also been recently demonstrated [2] [3]. The gain fiber attractor supports a parabolic pulse with quadratic nonlinear phase that can be fully compensated by linear chirp. This type of laser generates shorter pulses than are achievable with a dissipative soliton laser. However, due to the limited gain bandwidth, the shortest pulses that can be are around 40 fs for an Yb-doped laser since the gain bandwidth will act like a filter and interrupt the self-similar propagation, which eventually leads to wave breaking.

Overcoming the gain bandwidth limitation and continuing the self-similar propagation is a route to generate few cycle pulses with fiber laser. Two methods are presented in this thesis to extend the self-similar propagation within the fiber oscillator. One is with highly nonlinear normal dispersion fiber that utilizes passive parabolic propagation in the normal dispersion fiber [4] . The other uses dispersion decreasing fiber (DDF), which is mathematically equivalent to a piece of gain fiber but without the gain bandwidth limit [5]). Both methods have generated pulses as short as 20 fs in Yb-doped fiber lasers. The

broadest spectrum from an Er-doped laser was generated with a highly nonlinear normal dispersion fiber after the gain. The DDF cavity exhibits better phase control of the pulse and can be a route to pulses down to 10 fs. Optimization of the DDF cavity, combined with energy scaling by using larger-core fiber, predict performance directly comparable with solid state lasers in terms of both pulse duration and pulse energy.

1.1 Organization of the thesis

The rest of the thesis is organized as follows. Chapter 1 will introduce different nonlinear attractors in fibers and their manifestation in fiber oscillators as a background to mode locking fiber lasers. This discussion will include soliton, dissipative soliton, and amplifier similariton lasers. The theoretical limits of each attractor will be discussed. Fiber lasers with different wavelengths will be summarized briefly with the focus on Erbium, Ytterbium, and Thulium gain. The crucial components in fiber lasers needed to assist mode locking will be introduced. The rest of the thesis will be presented as a catalog of different wavelength lasers based on my works in the Wise group, although the same mode locking mechanisms hold for all wavelengths, although each different regime has its own feature and problems to overcome. Chapter 2 introduces short pulses generation from Er-doped fiber lasers including soliton lasers, dissipative soliton lasers, amplifier similariton lasers, and enhanced bandwidth generation based on self-similar propagation. Design guides for each type of laser will be presented for different application purposes. Chapter 3 introduces Yb-doped fiber lasers with the emphasis on the DDF laser. The theory and design guide for the DDF laser will be shown. It will also demonstrate the initial

work on energy scaling of extended amplifier similariton lasers with a passive fiber. Chapter 4 introduces Tm-doped fiber lasers including a Tm soliton laser and a Tm large normal dispersion fiber laser. Initial simulations with a normal dispersion Tm fiber will also be presented as a starting point for future experiments.

1.2 Nonlinear attractors to generate short pulses from fiber laser

A piece of fiber ($k2>0$) can be modeled by the well know nonlinear Schrodinger equation(NLSE).

$$\frac{\partial A}{\partial z} = \frac{g}{2}A - i\frac{\beta_2}{2}\frac{\partial^2 A}{\partial t^2} + i\frac{\beta_3}{3}\frac{\partial^3 A}{\partial t^3} + i\gamma(|A|^2)A \tag{1.1}$$

where g is the gain, for passive fibers this term can be taken off. β_2 is the second order dispersion, γ is the nonlinear coefficient, For pulses longer than 100 fs, the third order dispersion term is negligible.

In the anomalous dispersion regime, for both passive and active fiber, the bright soliton exists, which is a strong nonlinear attractor formed from the balance of nonlinearity and dispersion. This topic and its applicationwill be introduced in section 1.2.1.

In the normal dispersion regime, passive fiber, exhibit a parabola solution, shown by Anderson [6] that is not a nonlinear attractor and cannot form a parabola pulse by itself. There is also a solution called dark soliton but it will be be covered in this thesis. For gain fiber, a solution called amplifier similariton

exists as demonstrated by Fermann [7] which can attractor pulses with any initial shape to its local attractor to be a parabolic pulse shape and propagate self similarly afterward. These two types of self similar solutions will be discussed in section 1.2.3.

There is another more complex equation called the cubic-quintic Ginzburg-Landau equation (CQGLE) for fiber system. This equation add higher order nonlinearity(saturable absorption), gain filtering(or any kind of filtering) and to the basic NLSE. Those two additional terms correspond to commonly used components in practical laser systems. This equation has an analytical solution called a dissipative soliton which will be covered in 1.2.2.

1.2.1 Soliton

Soliton in Anomalous Dispersion Fiber

Soliton (also called bright soliton) is the famous attractor with the balancing of nonlinear phase and anomalous dispersion. It maintains its shape and energy along the propagation once it is formed. It has many solutions for each integer value of

$$N = \gamma P_0 (t_0)^2 / |\beta_2. \tag{1.2}$$

For N>1, those are called high order soliton. Here and in this thesis, we focus on the case of $N = 1$ fundamental soliton,which was described by the equation (1.3) and its solution shown below (1.4):

$$\frac{\partial A}{\partial z} = -i\frac{\beta_2}{2}\frac{\partial^2 A}{\partial t^2} + i\gamma(|A|^2)A \tag{1.3}$$

$$A(t,z) = A_0 Sech(t/t_0)e^{iz/2} \tag{1.4}$$

By plugging the solution to NLSE, we have a simple relation between the pulse parameters and the system parameters as described what is called soliton area theorem below [8]:

$$E_\tau = \frac{|\beta_2|}{\gamma t_0} \tag{1.5}$$

The soliton solution has been widely observed in different physical systems. The fundamental soliton has the property of maintaining its shape along the fiber once it is formed and is such a strong attractor that it can tolerate large perturbation, such as gain and loss , and come back to its initial shape.Therefore it is naturally a good candidate to make a feed back laser simply by splicing the fiber to make a loop. A soliton will fit the periodic boundary condition easily and a saturable absorber will help to form the pulse from noise after many round trips. Once the laser reaches steady state, the solution propagates as it would in passive fiber.

Simple as it is, soliton lasers dominated the field of mode locking fiber laser for more than 2 decades and has found applications in many areas such as in telecommunications system. The limit of soliton lasers is that, according to the area theorem, the pulse energy is clamped by balancing nonlinearity and dispersion, which usually ends up being 0.1 nJ for a standard 6 μm single mode fiber. There have been many method used to increase the pulse energy. The commonly used one is to use large core fiber with less nonlinearity. In this thesis, an exploration of the perturbation tolerance of soliton lasers will be carried out in Section 2.1 as a way to get high energy soliton lasers.

Dispersion Managed Soliton

A group at MIT proposed a method to overcome the soliton energy clamping by introducing a breathing solution of NLSE [9] with β_2 and γ vary along the propagation.

$$\frac{\partial A}{\partial z} = -i\frac{\beta_2(z)}{2}\frac{\partial^2 A(z)}{\partial t^2} + i\gamma(z)(|A|^2)A \tag{1.6}$$

The laser has both normal and anomalous dispersion segments inside the cavity. The pulse will be broadened and narrowed twice in the time domain as a way to manage the nonlinearity by reducing the peak power. The spectrum of the pulse will keep the same inside the cavity. The system output energy when the pulse reaches the shortest pulse duration and the pulse is mostly chirped inside the cavity. This avoid excessive nonlinear phase accumulation. Although the pulse is now a breathing solution, its periodic evolution makes it still easy to make a laser cavity. This method can increase the pulse energy by a order of magnitude. More importantly, the laser works around net zero dispersion so this method is and has been a way to generate very short pulses.

1.2.2 Dissipative Solitons

The study and development of dissipative soliton have drawn much attention in the past few years. First of all, it is a solution that is well known in the mathematical field but hardly paid attention to in the physical science, especially in the field of lasers. People have been so focused on the two soliton solutions that dispersion compensate was always used in order to receive high performance. Second, the performance of dissipative soliton has orders of magnitude increase compared with traditional soliton, which makes it directly compara-

ble to solid state lasers. As a further motivation predicted by analytical theory, pulses without energy limit are possible at the condition known as dissipative soliton resonance.

The major difference between dissipative solitons and solitons is the process of essential dissipative within the laser cavity, which is facilitated by a filter as shown in both the equation and experiment. The laser cavity has a spectral breathing factor of 5. The physical explanation of the spectral filter is that it cut the highly chirped pulse in both temporal and spectral domain to ensure the pulse satisfies the periodic boundary condition.

Dissipative solitons are solutions of CQGLE which has the following non-dimensional form of

$$U_z = gU + (1 - i\frac{D\Omega}{2})U_{tt} + (\frac{\alpha}{\gamma} + i)|U|^2U + \frac{\delta}{\gamma^2}|U|^4U, \tag{1.7}$$

Where D is the GVD, g is the net gain and loss, Ω is the filter bandwidth squared, α is a cubic saturable absorber term, δ is a quintic saturable absorber term, γ refers to the cubic refractive nonlinearity of the medium, U is the product of the electric field envelope and $\sqrt{\gamma}$, z is the propagation coordinate and t is the product of the local time and $\sqrt{\Omega}$. This equation admits the following exact solution:

$$U = \sqrt{\frac{A}{\cosh(\frac{t}{\tau}) + B}}e^{-i\frac{\beta}{2}\ln(\cosh(\frac{t}{\tau})+B)+i\theta z}. \tag{1.8}$$

Although the solution looks complicated, the dissipative soliton that will be introduced in this thesis is for the range -1<B<1. Laser operating at this regime are commonly known as All Normal Dispersion (Andi) lasers. This type of laser can routinely generate 100 fs pulse with a few nJ. Energy scaling of this laser has so far made a 31 fs, 84 nJ pulse [10] although the pulse quality was sacrificed due

to the gain bandwidth limit.

The other regimes of B have not been explored extensively but they could have potentially very interesting physics and performance. For example, when B>1, it has a flat top rectangularly shaped highly chirped pulse. Although it is hard to dechirp in practice, it is believed to be a route to dissipative soliton resonance for unlimited energy.

1.2.3 Similaritons

Passive Simlaritons

Anderson and coworkers [6]has found a wave-breaking free solution of normal dispersion fiber:

$$A^2(t,0) = A_0^2(1 - \frac{t}{\tau}^2) \tag{1.9}$$

It is a self similar solution since the form is invariant upon propagation, which can be understood intuitively as the parabola shape of the pulse will generate parabolic phase in time domain due to self phase modulation (SPM). For a highly chirped parabola pulse, it also has parabolic spectrum shape which is the same phase shape GVD will add to the spectrum domain. The phase of the pulse keeps its shape in both time and spectrum domain along probation and so is the pulse shape itself. The parabola pulse shape in time domain is more important as it is usually the nonlinear phase caused by SPM that causes wave breaking. Self-similar evolution is a powerful technique to avoid distortion of optical pulses that propagate nonlinearly. Pulses with a parabolic intensity profile and linear frequency chirp can propagate without wave breaking within a

normal dispersion, which is an attractive feature for many applications.

As mentioned before, this type of solution is not a nonlinear attractor so it is suitable to make a mode lock a laser from this mechanism. However, it could be used as part of the cavity to manipulate the pulse propagation with the present of other mode locking mechanism.

Amplifier Similariton

With the gain term g present and normal dispersion β_2>0 in the NLSE,

$$\frac{\partial A}{\partial z} = \frac{g}{2}A - i\frac{\beta_2}{2}\frac{\partial^2 A}{\partial t^2} + i\gamma(|A|^2)A \tag{1.10}$$

Fermann and coworkers [7] has found an asymptotic solution of

$$A(z,t) = A_0(z)\sqrt{1-(t/t_0(z))^2}e^{i(a(z)-b(z)t^2)} \quad for \;\; t \le t_0(z) \tag{1.11}$$

For an amplifier with constant gain, this asymptotic solution is a nonlinear attractor which means when the initial condition (mainly the energy) is close enough to the attractor range, they will all be evolving into the self-similar solution. The difference between Anderson self similar pulse and amplifier similariton is shown is Fig. 1.1.

A useful feature of these pulse is that the chirped self-similar pulses (sometimes referred as "similariton") can be compressed to the Fourier-transform limit by simply passing them through a dispersive delay. More importantly, the bandwidth of the pulse can increase exponentially without wave breaking limit except the gain bandwidth limit, which could be avoided by other methods described in Chapter 2 and Chapter 3.

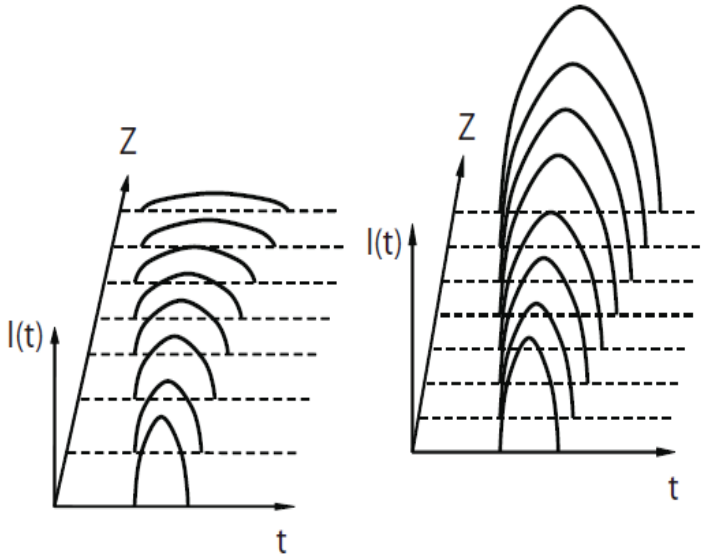

Figure 1.1: Illustration of self similar evolution in passive fiber(left) and amplifier(right)

Although the self similar amplifier has been developed for more than a decade, it was hard to make a feedback laser from amplifier similariton because the monotonic evolution of the pulse in a local attractor makes it hard to fit into a feedback loop. Recently, Oktem [2] demonstrated a soliton similariton Er laser with a soliton formation before the gain as the right initial condition for the gain attractor. Renninger [3] used a narrow filter (4 nm) to cut back the highly chirped pulse to its initial condition which allows it to reach parabola pulse within the gain segment. Both methods demonstrate the feasibility of stabilize the local attractor in a laser cavity and the gain attractor itself works as a key mechanism to mode lock the laser.

1.3 Colorful Fiber Laser

The wavelength of the fiber laser is dependent on the fiber doping with rare earth ions based on stimulated emission from excited atoms or ions such as erbium (Er3+), neodymium (Nd3+), ytterbium (Yb3+), thulium (Tm3+), or praseodymium (Pr3+). Although fiber lasers with all these doping have been reported, for mode locking lasers, Er and Yb are the two well developed medium. For the past few years, the improvement of Tm doped gain fiber has drawn much attention to developing mode locked Tm laser. Raman fiber laser is another way to generate different frequencies with the gain medium based on stimulated Raman scattering. Mode locked Raman Soliton laser [11] and Raman self similar laser [12] have been reported.

In this thesis, we will focus on the three most actively studied mode locking gain medium: Er, Yb and Tm. Different mode locking regime will be demonstrated in Er laser. New development for fiber lasers at 1 μm and 2 μm will be presented.

1.4 Mode Lockers

Despite of all the nonlinear attractor and mode locking mechanism, for most fiber lasers with limited length of fiber, some assists such as saturable absorbers are needed to start the pulse from noise; for cavities with more dramatic evolution, pulses needed to be brought back by extra force such as spectral filter to be self sustained within a loop. Once the laser reach steady state, all those components works together for pulse shaping and stabilize the cavity.

1.4.1 Saturable Absorbers

Saturable absorbers have the nonlinear property of transmitting higher intensity light more than lower intensity light. Therefore, they help to select the pulse from the noisy background and gradually build up the pulse through many round trips. The principle of saturable absorption (SA) is illustrated in Fig.1.2 below. Any component or physical process that has such a nonlinear

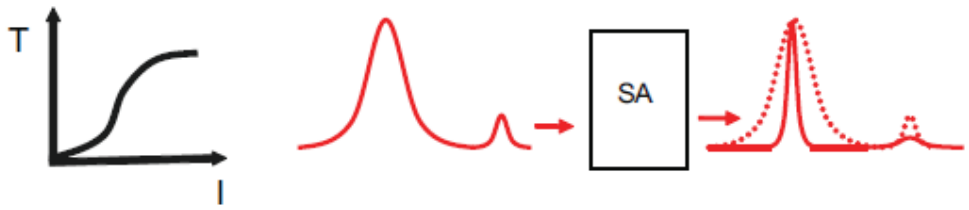

Figure 1.2: Illustration of saturable absorption

loss property can be used as a saturable absorber. For example, the Kerr lens effect is used as an SA for many solid state lasers. The most commonly used SAs in fiber lasers are: carbon nanotube (CNT) absorbers, nonlinear loop mirrors, semiconductor saturable absorber mirrors (SESAMs), and nonlinear polarization evolution (NPE). Among these, NPE has the fastest response time and largest saturation depth, so it is mainly used in the work of this thesis.

SESAM

SESAMs are formed from a Bragg mirror on a saturable absorbing semiconductor material. These can be modeled by the equation below when their recovery

time is much shorter than the pulse duration:

$$R = 1 - T_0/(1 + \frac{|A(t)|^2}{P_{sat}} \tag{1.12}$$

where T_0 is the transmission at low intensity and $P_(sat)$ is the saturation energy. SESAM has been developed for many years and are widely used in fiber lasers in both Yb and Er system. There are commercially available with different modulation depths and fast response times. Batop is one of the SESAM companies where details and reviews of SESAM could be found.

SESAMs have the advantage of simple implementation, but they are relative expensive and subject to damage at high powers and with extended use. In addition, it has fixed modulation depth and therefore will allow limited accessible modes.

Single-Walled Carbon Nanotube(SWCNT) Absorbers

The optical property of SWCNTs has have been demonstrated less than a decade ago, but they have already attracted a lot interest particularly in the field of ultrafast fiber lasers as a fast, inexpensive, fiber-integrated SAs. Depending on the diameter of the nanotube, it they can work as saturable absorbers at a large range of wavelengths. There are many ways to a fiber formatted make SWCNT SAs in a fiber format, including depositing the carbon nanotubes on the end of the fiber and or around the a tapered fiber. The technology of making a robust, high power SWCNT is still under development,. But but progresses have has been made so that they are now be used reliably in low power operation at 1.55 um. SWCNTs can not tolerate long time operation due to optical bleaching. An all fiber Er-doped mode locked laser with a SWCNT SA will be introduced

in Chapter 2. Fig.3 shows the saturable absorber absorption property from of a fiber formatted SWCNT [13].

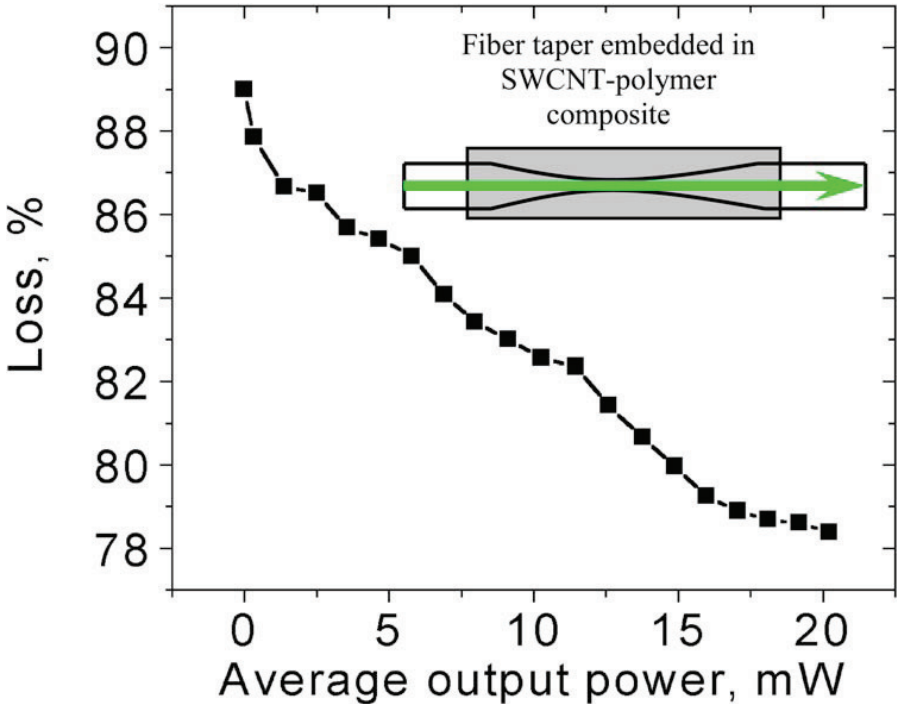

Figure 1.3: Absorption of a fiber taper embedded in a SWCNT-polymer composite as a function of the average input power. Inset: diagram showing an embedded fiber taper used as a SA.

Nonlinear Optical Loop Mirrors(NOLMs

NOLMs were proposed initially as a switching device based on the nonlinear phase induced by self phase modulation(SPM) [14]. The configuration of a NOLM is shown in Fig.1.4.

The lengths of the two paths are the same. When the output rationα is NOT 1/2, nonlinearity will make the phase accumulation different for the two paths.

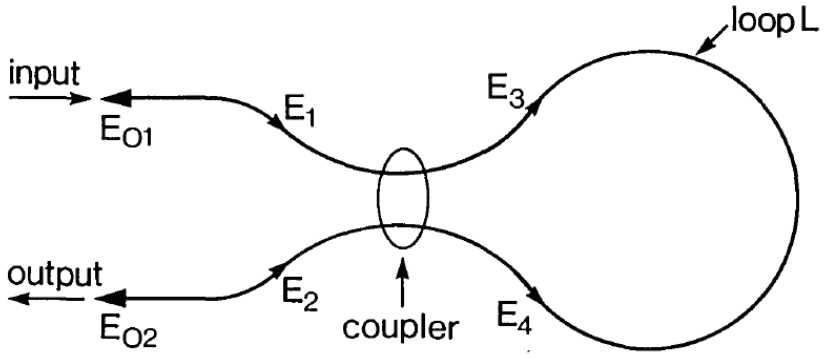

Figure 1.4: The loop mirror configuration

The transmission curve can then be expressed as:

$$|E_(02|^2 = |E_(IN)|^2[1 - 4\alpha(1 - \alpha)]. \tag{1.13}$$

Fig.1.5 shows the transmission curve with different value of α:

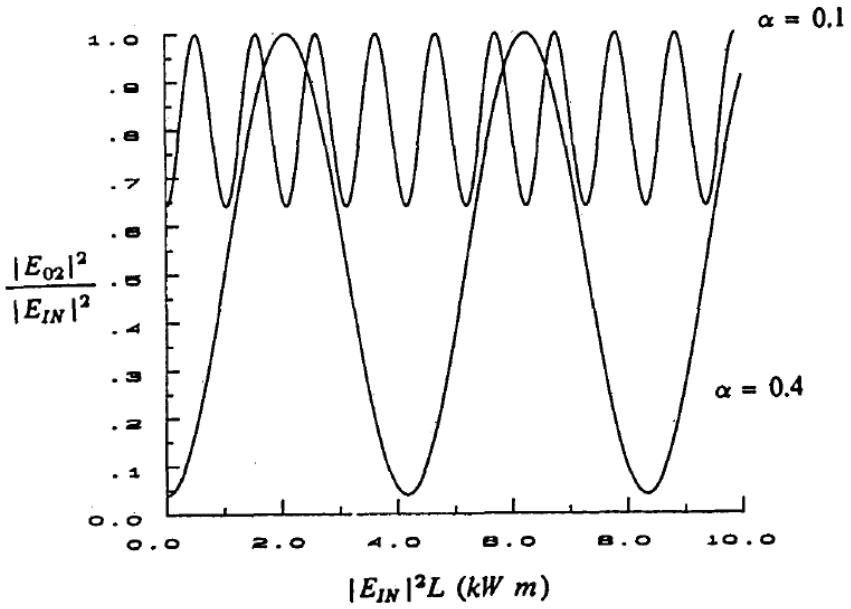

Figure 1.5: The transfer function of a NOLM input power in the units of kilowatt-meters

To reduce the fiber lengths needed, gain fibers are used to make nonlinear amplifying loop mirrors (NALMs).The advantages of NOLMs are their fiber integration, robustness, and very low cost. However, practical implementations of NOLMs as SAs in fiber lasers show that they tend to mode lock relative long pulses(>300 fs) [15].

Nonlinear Polarization Evolution

The detailed theoretical analysis of NPE is difficult. But it can be intuitively understood as an artificial SA that forms as a result of self-phase modulation and cross phase modulation(XPM) of two orthogonally polarized light components. The typical NPE implementation in a fiber laser cavity is shown in Fig.1.6. When the total length of the fiber cavity is too long(comparable to fiber beat length), the performance of NPE mode locked lasers will be compromised. The differ-

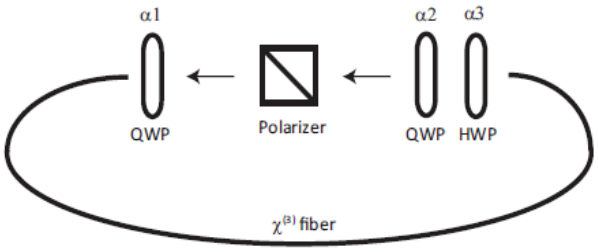

Figure 1.6: Standard NPE set up for a fiber laser cavity. HWP: half waveplate and QWP: quarter-waveplate.

ence of rotation angle $\Delta\phi$ for the two circular polarization modes $E_{\pm}$=E_x±-iE_y can be written as:

$$\Delta\phi = \frac{\gamma L}{3}(|E_+|^2 - |E_|^2). \tag{1.14}$$

To guarantee angle rotation happens, a polarizer and a quarter wave plate are used to ensure elliptical polarization. After the pulse accumulates nonlinear phase within the fiber to rotate its polarization orientation, an half and a quarter wave plate adjust the polarization to match the polarizer. The polarization mismatch between pulses and the polarizer also determine the output ration of the laser cavity. The output from the polarizer after a round trip is shown below:

$$I = \frac{1}{2}[1 - sin(2\alpha_1)sin(2\alpha_2) + cos(2\alpha_1)cos(2\alpha_2)cos(2(\alpha_1 + \alpha_2 - 2\theta_2 + \delta\phi))]. \quad (1.15)$$

where α,θ are the angles of quarter wave plate and half wave plate respectively. The last term of the transmission function is where the SA function happens when proper angels of the wave plates are set. See Ref [16], and Taura's thesis for more detailed analysis and other configuration of NPE as a SA.

1.4.2 Spectral Filters

Spectral filters can help pulse shaping by removing side lobes on the spectrum and to some extent by helping select the pulse from noise. The spectral filters used most for fiber lasers have a bandpass transmission curve. This is especially important for dissipative soliton mode locking as it is an essential component for supporting the solution. Filters are also used heavily in amplifier similariton lasers as the most convenient way to stabilize the feedback loop. But other methods such as soliton formation and spectral compression can also be used to stabilize amplifier similariton lasers. In general, a proper spectral filter is always found to be helpful in mode locking fiber lasers even it is not the major mode locking mechanism.

Birefringence Filters(BFs)

The principle behind BFs is the phase shift of orthogonal polarization states of light upon propagation through a birefringent material. The phase shift is wavelength dependent. When the beam has a wavelength dependent polarization rotation, it will have a wavelength dependent loss after a linear polarizer. In fiber lasers, BFs are formed by a birefringent plate and a polarizer which is also used as the output. The phase shift from the birefringent plate and its transmission function after a linear polarizer can be expressed as follows, when the angle of the polarizer with respect to the principle axis of the birefringent plate is 45 degrees.

$$\Delta\phi = \frac{2\pi}{\lambda}(n_e - n_o)dT = cos^2(\Delta\phi/2) \tag{1.16}$$

The thickness of the birefringent plate determines the period of the transmission curve and therefore decide the bandwidth of the filter. The Measured BF bandwidth versus the thickness of the quartz plate at 1um is shown in Fig.1.7 below.

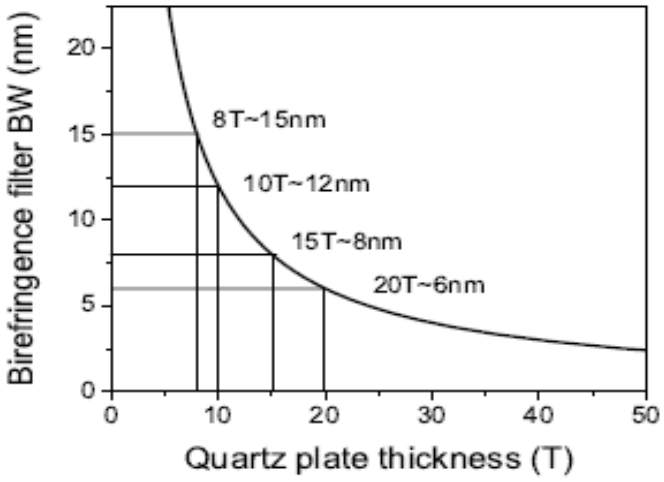

Figure 1.7: BF bandwidth vs. the thickness of the quartz plate. 1T= 0.5mm.

Interference Filters

Interference filters can form bandpass filters, long pass filters, or low pass filters. They function by transmitting one or more spectral bands while reflective to others. An interference filter has multiple layers of dielectric material with different refractive indices. The different wavelengths will experience different transmissions due to the influence of constructive and destructive interference. The filter is usually operated at normal incidence , while increasing the incident angle will tune the center wavelength of the spectral filter. The transmission curve can be expressed as:

$$\lambda_c = \lambda_0 \sqrt{1 - \frac{sin^2\theta}{n^2}} \tag{1.17}$$

where θ is the incident angle, λ_c is the center wavelength of transmission curve, λ_0 is the center wavelength at normal incidence and n is the refractive index of the material between two dielectric walls.

One practical draw back to the interference filter is that the peak transmission is low, usually less than 70 percent, which introduces extra loss to the cavity. But it is still used widely in fiber laser cavities to assist mode locking [**?**, 2].

Gaussian Filters

The extra structure of a filter can affect the performance of the laser and even prevent it from mode locking. The motivation behind using a Gaussian filter is that it has a clean single peak without periodic or secondary structure as in many other filters. In addition, a gaussian shaped pulse is generally used in nonlinear pulse probation analysis.

One way to make a Gaussian filter is to use a dispersive element such as a grating or prism and a single mode filter as shown in Fig.1.8 below. The beam

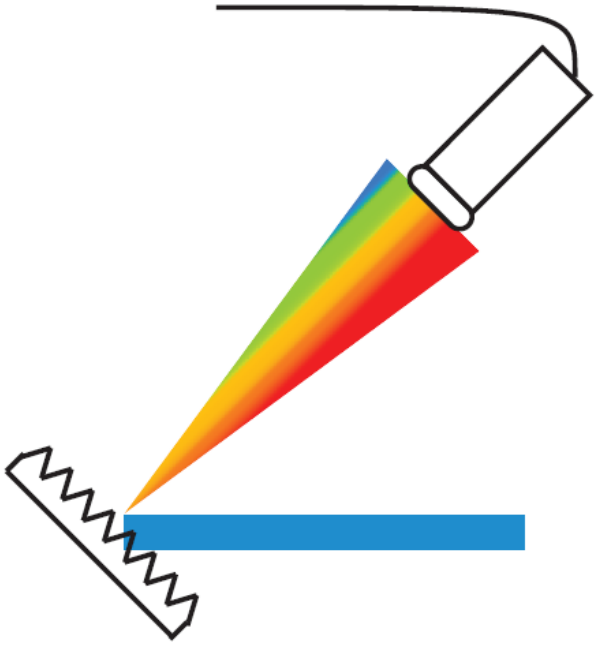

Figure 1.8: Schematic of a typical Gaussian filter as used in a fiber laser

becomes wavelength dependent spatially, and the single mode fiber has a Gaussian mode. The combination of the two components will generate a filter with a Gaussian profile. The bandwidth of the filter is dependent on the dispersion, beam size, fiber size, and the distance between the two components. Generally, increasing the beam size, dispersion, and distance between the two will decrease the filter bandwidth. Increasing the fiber size will result increasing the filter bandwidth. Changing the incident angle to the dispersive element or the position of the fiber can tune the center wavelength of the filter. This technique can generate filters as narrow as a couple of nm, which is suitable for amplifier similariton laser cavities. There is typically a 30 % loss from a grating due to the reflection and higher order diffraction, which so far can be tolerated by most

mode locked lasers but will become the limit of performance eventually. In the future, less lossy Gaussian filters need to be developed.

CHAPTER 2

ER FIBER LASER

It is a natural gift that the spontaneous emission of Erbium doped fiber happens to overlap with the most widely used telecom windows around 1.55 μm. The losses of silica fibers are lowest in this region. Although the fiber dispersion is usually anomalous but can be tailored with great flexibility by methods like dispersion shifted fiber or simply changing the core size the increase the waveguide dispersion. The booming of the optical fiber communication prepared various components at 1.55 μm regime as long as developed tools and technique for fibers in general. Therefore, compared with other wavelength, Er-doped fiber laser is the easiest candidate to make a real all fiber compact laser. This wavelength regime is not only important for telecommunication but could also be used to big-imaging and many other applications as an eye-safe operation wavelength regime.

2.1 High Energy Soliton Fiber Laser

2.1.1 Introduction

For the soliton operation, fiber laser has its disadvantage of confining the light in a small core, which results in excessive nonlinear phase shift. Therefore the energy from soliton fiber laser is usually limited to 100 pJ for standard single mode fiber cavity as predicted by soliton area theorem.

The soliton area theorem shows the case of fundamental soliton, which has

constant shape of the temporal intensity profile. A higher-order soliton

$$u(0,\tau) = Nsech(\tau), \tag{2.1}$$

is a soliton pulse which exceeds the energy of a fundamental soliton by a factor of square of an integer number. It will experience temporal variation periodically. So for a feedback cavity, it is possible to have high order soliton within the laser cavity as long as the nonlinear phase can be managed.

To increase soliton laser energy, besides dispersion control, two simple methods are used for energy scaling:

1. Increasing output ratio. Since soliton is a very strong attractor, the output ratio is increased from 50% to 99% to see how much loss a soliton laser can tolerate.

2. Lower repetition rate, it could be simply understood as for the average power, lower repetition rate will generate higher pulse energy. It can also be understood in an integral way as a large net anomalous cavity will support higher energy.

2.1.2 Increase Output Ratio

The schematic of the laser is shown in Fig.2.1. The total length of the Redfern gain fiber is 3 m (β_2 =50 fs^2/mm, A_{eff}=14μm^2. The rest of the cavity is made of SMF28 (β_2 = 23 fs^2/mm, A_{eft}=79 μm^2)with 2 m as fiber pigtails from other components. Most of the SMF28 fiber is spliced before the gain and after non-polarized fiber formatted isolator, where the cavity repetition rate is varied by adding more fibers. The first output has ratio varied from 50% to 99%. The second output has ratio of 15% as a monitor.

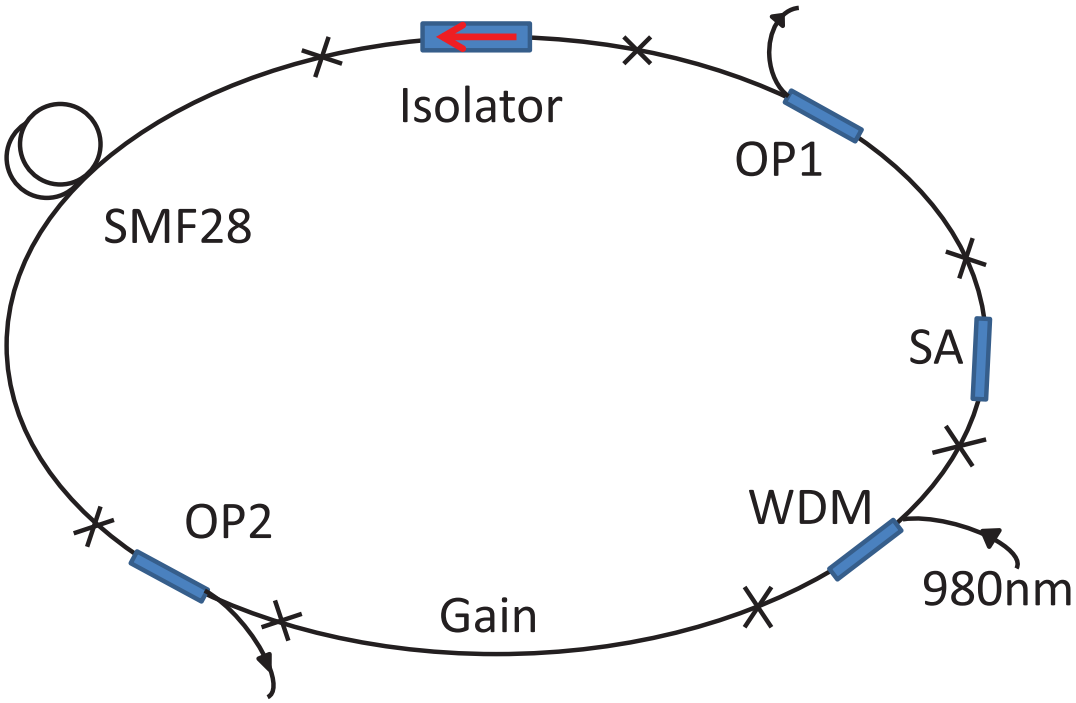

Figure 2.1: Experimental setup of all fiber soliton laser

Increase output ratio

The initial cavity has total of 9 m of fibers with 4 m SMF28 before the gain. The output coupler 1 ratio is increased until no stable mode locking can be observed. Changing the output coupling does not affect the overall slope efficiency as much as shown in Fig.2.2. The highest single pulse energy increases from 0.13 nJ from 95% output cavity to 0.37 nJ from 99% output cavity. Higher ratio than 99.5% (99%+50%) from output1 no longer supports mode locking. The pulse duration is around 600 fs for all the output ratios.

This results demonstrated that soliton is indeed a robust solution for the fiber laser cavity. High loss (output) as much as more than 99% can be tolerated for

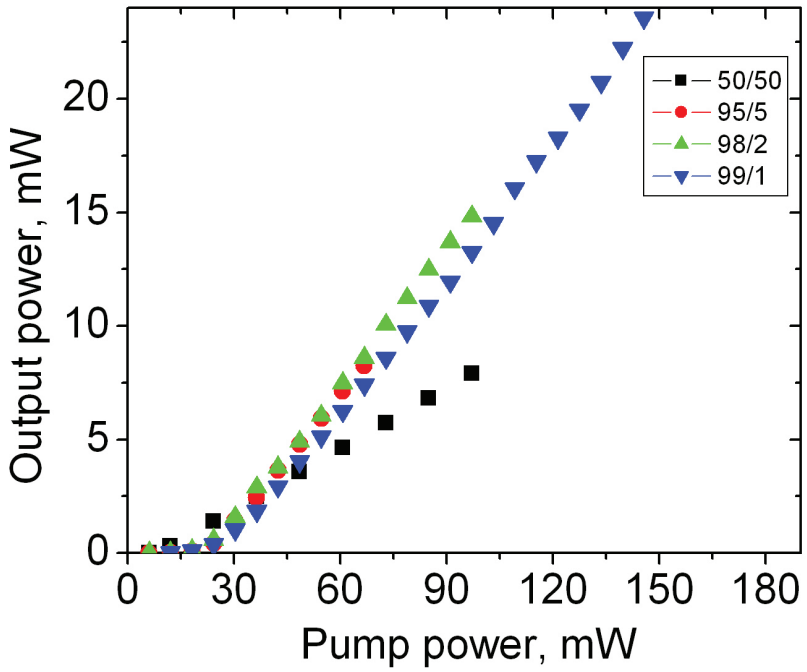

Figure 2.2: Cavity slope efficiency with different output coupling.

this type of cavity especially with an all fiber format. This simple method can be used to scale soliton energy by a factor of 4 easily. Ultimately the maximum output (loss) the cavity can handle would be equal the 20 dB gain.

2.1.3 Increase Cavity Length

With a 99% coupler, the cavity length is increased from 9 m to 40 m by adding 10 m and then 20 m SMF28 fibers before the gain. The energy increases from 0.37 nJ to 1.4 nJ as shown in Fig.2.3.

Further increase cavity length will results in not stable mode locking. It could be due to reaching fiber beat length or the limit of scalable pulse energy. This cavity is not for the best design to get the highest energy since the small

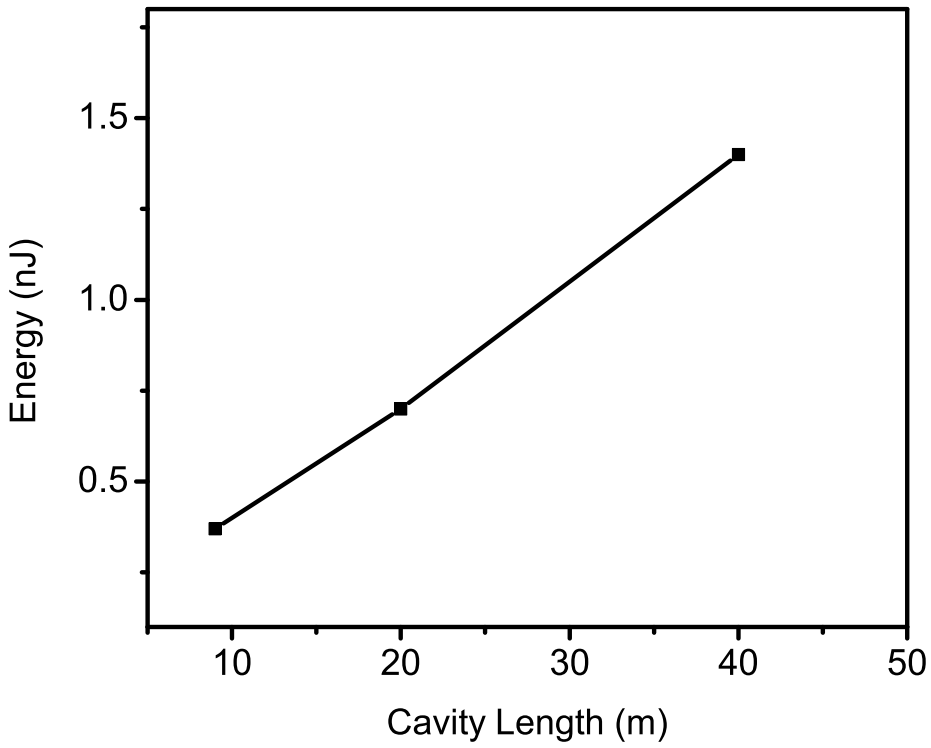

Figure 2.3: Cavity length with different output energy.

core normal dispersion gain segment will limit the pulse energy by having the highest energy and shortest pulse together in the smallest core segment in the fiber cavity. However, the concept works well as an initial demonstration and this laser has had applications in telecommunication lab, quantum optics lab and quantum dot lab.

2.1.4 Conclusion

A demonstration of scaling the mode locking soliton pulse energy from a standard telecom fiber components is done by two simple methods: increase output

ratio and increase cavity length. The limit of two methods are shown and the pulse energy increases more than 10 times. The performance is limited by the gain fiber, which is a small core (4 μm), large normal dispersion fiber. By replacing the gain fiber to be a standard doped anomalous dispersion gain fiber, higher energy as much as 3 nJ can be expected (refer to Khanh Kieu's thesis).

2.2 Dissipative Soliton Fiber Laser

2.2.1 Introduction

Dissipative soliton laser. is a relative new concept compared with soliton laser. It was first demonstrated with Yb-doped fiber laser by Andy Chong and co works [1] since at 1 μm, it is natural to have all normal dispersion values. It has potential to create high pulse energy above soliton or dispersion-managed soliton energies. In contrast to soliton formation, the pulse-shaping mechanism of ANDi lasers is based on the chirped pulse spectral filtering (CPSF) that occurs with an intra-cavity spectral filter [1]. The removal of anomalous-dispersion components from the laser provides fundamental and practical advantages. High pulse energy (above 20 nJ) with 150 fs dechirped pulse duration has been demonstrated with Yb-doped ANDi fiber lasers [18]. Meanwhile, an erbium (Er)-doped fiber laser with only normal dispersion elements was also reported [19]. This so-called gain- guided soliton fiber laser relies on the limited bandwidth (BW) of the gain medium for the pulse-shaping. It was an important to step to increase the pulse energy since the pulse energy is expected to be larger with increasing net normal cavity dispersion. However, un-

like the Yb ANDi lasers, the gain-guided soliton laser only created picosecond pulses. To create shorter pulses, a gain-guided soliton Er fiber laser with a dispersion map and large net normal dispersion (0.07 ps^2) was created [20]. However, the dechirped pulse duration (1 ps) was still in the picosecond range. It was recently shown that the mode-locked spectral BW and the dechirped pulse duration are strong functions of the spectral filter parameters in ANDi fiber lasers [21]. This motivates investigation of the role of the spectral filter in Er fiber lasers. By inserting an appropriate spectral filter within the Er fiber laser, femtosecond dechirped pulses with high pulse energies are expected. Here we present the result of the femtosecond Er fiber laser with a spectral filter at large net normal cavity dispersion (0.1 ps^2). The laser produces 220 fs pulses after dechirping. These results demonstrate the successful translation of the CPSF mechanism to Er fiber lasers. The pulse energy is 1 nJ, but is expected to improve significantly with an optimal design.

2.2.2 Simulation

The simulation is designed to have a cavity with similar net dispersion and cavity design of the Yb Andi laser [21]. The total length of passive normal dispersion metro core fiber (β_2=10 fs^2, A_{eff}=50 μm^2) is about 16 m. The 3 m gain fiber has β_2=50 fs^2 and A_{eff}=14 μm^2. It is distributed before and after gain fiber at ratio of 4:1 as the case of Yb Andi laser. The mode locked simulation result is shown in Fig.2.4. The pulse energy from simulation is 1.4 nJ, with spectrum bandwidth of 29 nm and calculated zero phase transform limited pulse of 217 fs. The spectrum has steep side and some structures on the edge. The spectral breathing ratio of the pulse is 2.

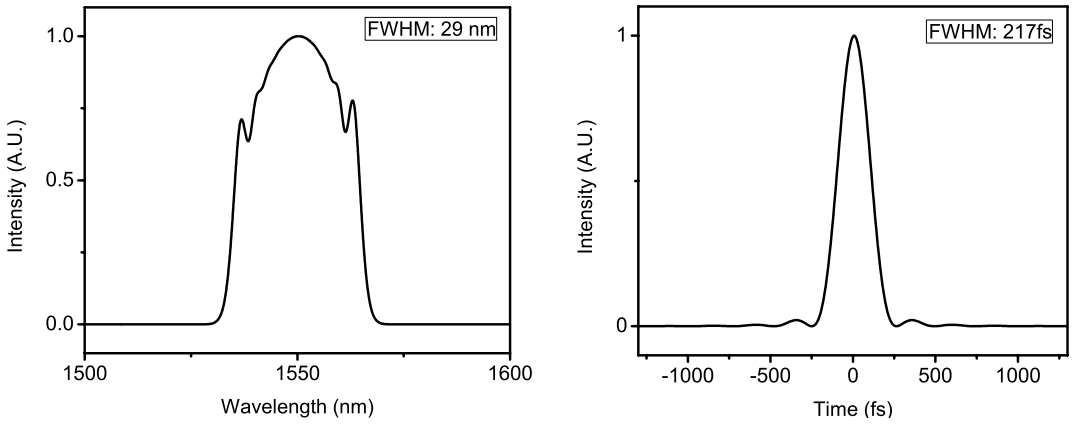

Figure 2.4: Simulation Result of Er dissipative soliton laser.(a) Mode-locked spectrum. (b) Calculated transform limited pulse.

2.2.3 Experiment

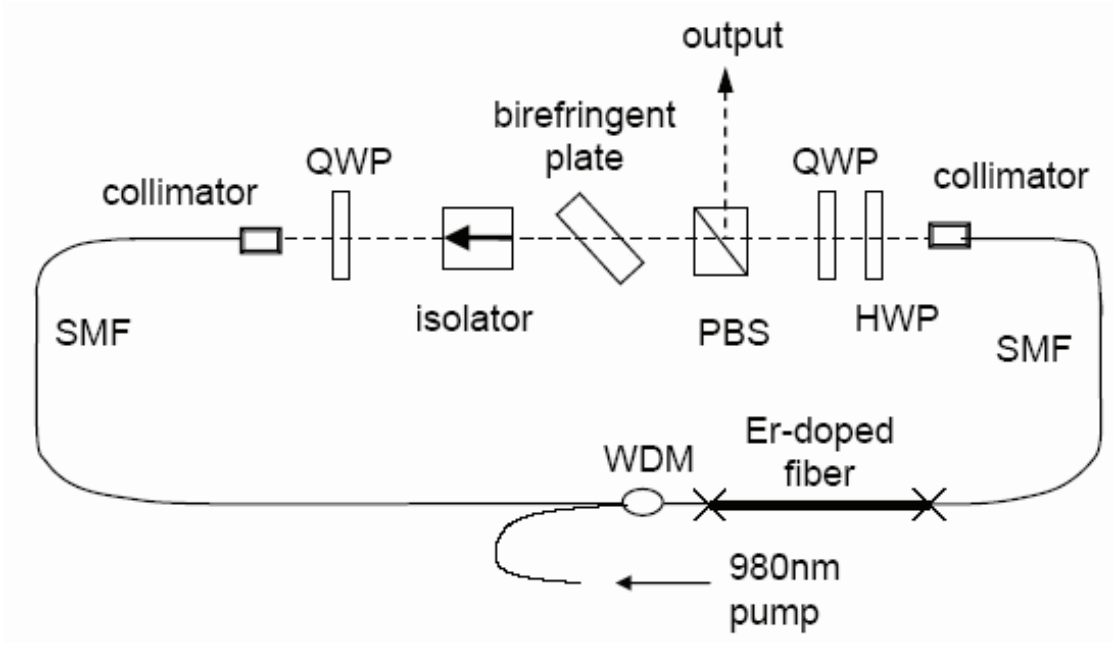

Figure 2.5: Experimental setup of Er dissipative soliton laser

Fig.2.5 shows the experimental setup. Guided by simulation, the fiber lasers consists of 12 m of single-mode fiber (SMF) with normal dispersion at 1550 nm, 3 m of Er-doped gain fiber (Redfern fiber with normal dispersion), and an-

other 3 m of SMF. Because commercially-available wavelength-division multiplexers (WDM) and collimators are anomalously dispersive at 1550 nm, some short anomalous dispersion segments are unavoidable. However, the laser has a very weak dispersion map; the anomalous dispersion segments compensate only 10% of the normal dispersion. The pulse evolution will be essentially that of an ANDi laser. The net cavity dispersion is 0.1 ps^2. Nonlinear polarization evolution (NPE) provides some self-amplitude modulation. A birefringent filter with 15 nm BW is used to implement CPSF, and provides the dominant self-amplitude modulation. The repetition rate of the laser is 9.9 MHz. By adjusting the waveplates, stable, self-starting mode-locked operation is obtained. Fig.2.6 shows the experimental results. 10 mW mode-locked average power corresponds to 1 nJ pulse energy. The pulse energy is pump limited. The spectrum shows the characteristic sharp peaks around its edges resembling the ANDi fiber laser modes as expected. The measured dechirped pulse duration is 220 fs. The interferometric autocorrelation shows noticeable side-lobes, which arise from the steep sides and structure of the spectrum. The CPSF action of the intracavity spectral filter makes a noticeable improvement of the dechirped pulse duration. The net cavity dispersion is larger than in the gain-guided soliton fiber laser [19], yet this laser successfully creates femtosecond pulses. The demonstration of femtosecond Er fiber laser operation at large net cavity dispersion is an important step to achieve femtosecond-duration and high energy pulses from Er fiber lasers. Since the physics in Yb fiber lasers and Er fiber lasers is essentially the same, by choosing proper laser design parameters, we expect Er fiber lasers to generate high pulse energies with the CPSF mode-locking mechanism, as demonstrated in Yb fiber lasers [18]. The future work will focus on optimizing the pulse energy from the laser.

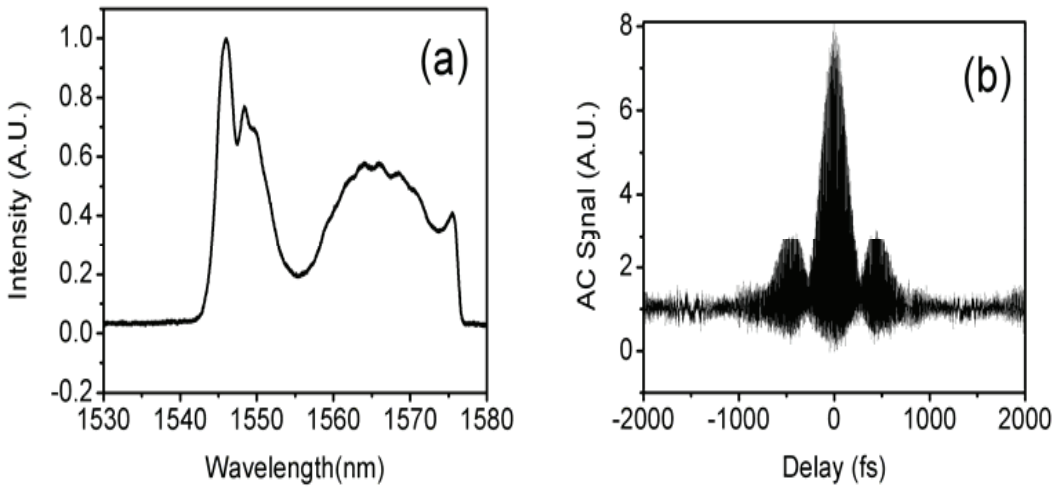

Figure 2.6: Experimental Results: (a) spectrum, (b) interferometric autocorrelation of the dechirped pulse.

2.2.4 Conclusion

Femtosecond pulse (1 nJ, 220 fs) generation from an erbium-doped fiber laser with intracavity spectral filtering and large normal dispersion is demonstrated. Higher pulse energy with femtosecond duration from the Er fiber laser should be achievable with appropriate laser design parameters.

2.3 Amplifier Similariton Fiber Laser

We demonstrated a large normal dispersion Er-doped fiber laser based on self-similar pulse evolution in the gain fiber. The cavity is stabilized by the local nonlinear attractor in the gain fiber through the use of a narrow filter. This type of mode locking mechanism allows the for the manipulation of the cavity design for various applications by operating at various levels of pulse chirp, repetition

rate, and bandwidth. This laser produces 1.8 nJ pulses with 60 nm bandwidth that are dechirped down to 82 fs with an external grating pair.

2.3.1 Introduction

Parabolic pulse generation has always been of interest since parabolic pulses evolve self-similarly in fiber and convert the nonlinear phase into linear chirp and therefore avoid wave breaking from excessive nonlinear phase. Parabolic self-similar pulse propagation within an amplifier was first demonstrated by Fermann [7], which triggered the development of self-similar fiber oscillators. Ilday and coworkers [22] built a passive self-similar fiber laser that generated parabolic pulses within the passive normal dispersion fiber before the gain fiber. However, the gain fiber did not act as a nonlinear local attractor and the overall spectral breathing in this system is small.

Recently Oktem and coworkers [2] developed a soliton-similariton Er-doped fiber laser to demonstrate the co-existence of two nonlinear attractors in one laser. Soliton formation works along with a bandpass filter to prepare a proper seed pulse before the amplifier, along the pulse to reach the asymptotic parabolic pulse solution by the end of gain fiber. Renninger and coworkers [3] used a narrow filter to prepare the initial pulse before the gain and generate parabolic pulses from an Yb-dobed fiber oscillator. The filter alone replaced soliton formation to assist similariton generation in the gain fiber and provides freedom to manipulate the cavity design for other performance targets [23].

Although the co-existence of two attractors in soliton similariton laser [2] is scientifically interesting, the requiring soliton formation brings another degree

of restraint to the laser design. It will be beneficial to have a self similar laser without unavoidable anomalous fiber.

Here an Er-doped amplifier similariton laser stabilized by a narrow filter only is reported. It demonstrates the implementation of self-similar propagation in the gain fiber at 1550 nm and achieves 1.8 nJ pulses with 60 nm bandwidth that are de-chipred down to 82 fs.

2.3.2 Numerical Simulation

Numerical simulations of the nonlinear Schrodinger equation are based on the split-step Fourier method were used to guide the experimental design and understand the intra-cavity pulse evolution. The schematic of the simulated cavity is shown in Fig. 2.7.

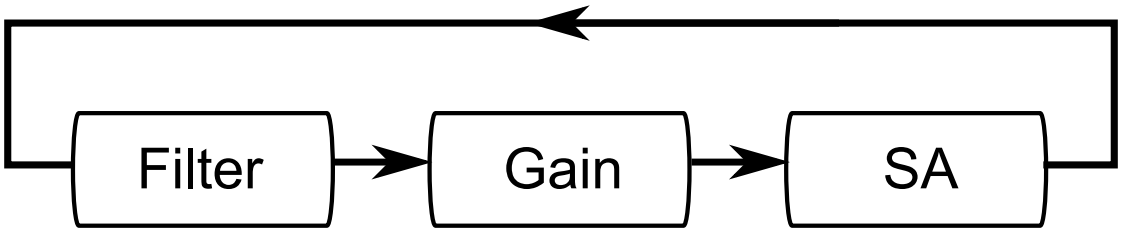

Figure 2.7: Schematic

A strong saturable absorber with a modulation depth of 1 is used to select the pulse from noise and assist mode locking. When the cavity is in the steady-state, the gain fiber works as an attractor to draw the pulse to its asymptotic solution of a parabolic pulse. The self-similar evolution is cut back to its initial condition by the narrow filter before the gain segment. The proper choice of

filter is important to have the attraction happen within the limited gain length.

In order to select an appropriate filter, we consider the self-similar evolution in the gain fiber, as described in [7]. The gain fiber we use is a 290 cm long Redfern fiber with a dispersion of around 50 fs^2/mm and a mode field diameter of 4.2 μm. The equation below calculates the proper initial pulse duration assuming the asymptotic solution is reached at the end of gain fiber. The gain bandwidth sets the limit of the reasonable spectral bandwidth. For erbium gain, this is 40 nm. The gain per length is 1.75 /m, calculated from simulation, assuming a small signal gain of 30 dB.

$$\begin{aligned} &\Omega_p = 5\text{THz} \\ &T_{opo}(0) = 3\frac{\beta_2}{\gamma}\left(\frac{2}{3}\Omega_p^2\right)^{\frac{1}{3}} \end{aligned} \tag{2.2}$$

where Ω_p is the gain bandwidth, $T_{opo}(0)$ is the optimum initial pulse duration that will enter into the nonlinear attractor quickest, γ is the nonlinear coefficient of the fiber, β_2 is the constant dispersion of the fiber, g is gain per length, and z is the length of the fiber, For a 40 nm gaussian pulse at 1.55 μm, this is about 5 THz.

Here we assume the pulse reaches the parabolic solution by the end of the gain fiber. Plugging in the parameters experimentally appropriate parameters to these equations, the calculated initial pulse duration is about 460 fs, which corresponds to a bandwidth of 7 nm for a transform limited Gaussian pulse. For a chirped pulse, the bandwidth will be narrower.Various filter bandwidths ranging from 1 nm to 10 nm were tried in simulation. It shows that for given gain fiber, there is a most suitable filter to get the highest energy and shortest pulse from the oscillator as shown in Fig.2. 8.

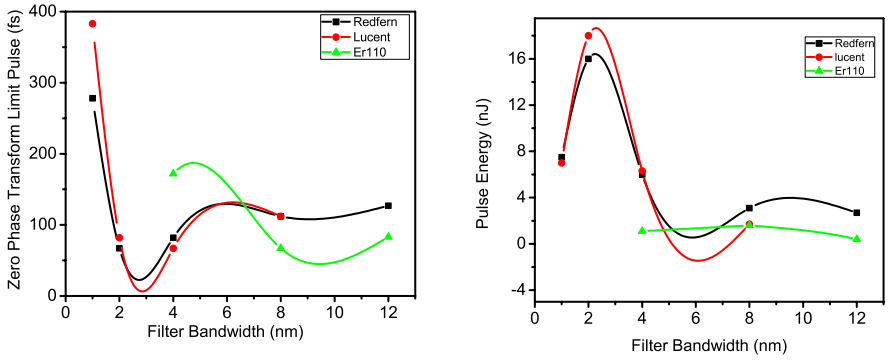

Figure 2.8: Filter Impact on amplifier similariton lasers. (a)Filter bandwidth v.s. transform limited pulse. (b) Filter bandwidth v.s. pulse energy. Black line: Lucent fiber. Redline: Redfern fiber. Green line: Er110 fiber

Considering the experimentally realizable bandwidths, a 4 nm Gaussian filter is picked for this demonstration to set a clean and proper initial condition for the gain segment. The rest of cavity consist of a total of 90 cm of anomalous dispersion step-index fiber (SMF28) as fiber collimator and coupler pigtails (70 cm at the input end and 20 cm at output end), and 54 cm of normal dispersion fiber (OFS 980) right after gain from the wave-division multiplexer (WDM) pigtail. The cavity has a net normal dispersion with magnitude 0.15 ps^2. The simulated results are shown in Fig.2.9.

The simulated results has 4.2 nJ, 53 nm bandwidth (37 nm in RMS), corresponding to an 82 fs transform limited pulse. The pulse evolution is also studied as shown in Fig.2.10.

Where metric $M^2 = \int [|u| - |p|]^2 dt / \int |u|^4 dt$, u is the pulse being evaluated and p is a parabola with the same energy and peak power. M=0.14 represents a Gaussian shape. M <=0.06 represents a parabolic shape. The pulse evolution shows clearly that within the gain fiber, the pulse is experiencing dramatic growth in

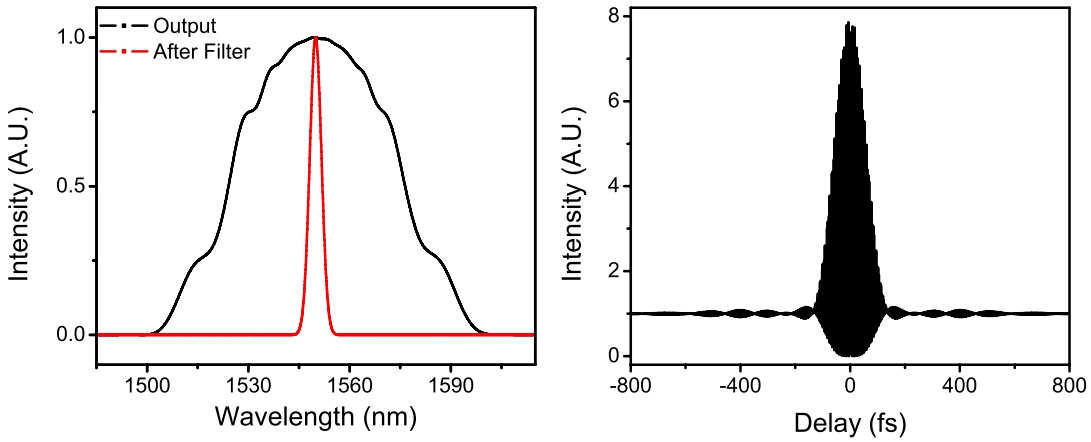

Figure 2.9: Simulation Result. Left: Mode locked spectrum. Right: Calculated transform limited autocorrelation

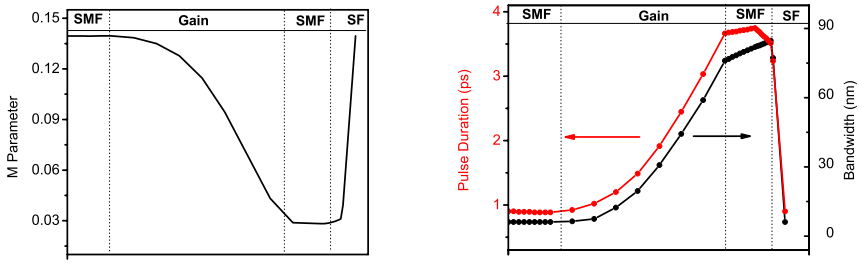

Figure 2.10: Pulse evolution inside the cavity. Left: evolution of pulse duration and bandwidth. Right: pulse shape evolution compared with a parabolic pulse with the same peak power and energy.

both the temporal and spectral domains while it attracts towards the parabolic pulse shape as predicted by the local nonlinear attractor. The narrow spectral filter is able to stabilize the feed back loop and satisfy both the boundary condition for the cavity and for the initial input condition for the gain fiber.

An interesting feature of this laser is that the pulse chirp is not sensitive to the net dispersion before the gain. It can be understood as the gain attractor

will put an amount of fixed chirp on top of the asymptotic solution according to the analysis for the amplifier equation below. However, the chirp on the output pulse is influenced by the fiber after the gain.

$$\phi(z,T) = \phi_0 + 3\gamma(2g)^{-1}A_0^2(z) - g(6\beta_2)^{-1}T^2 \tag{2.3}$$

2.3.3 Experimental Results

The experiment was constructed guided by the simulation and the schematic is shown in Fig.2.11. A 600 /mm grating and a 0.5 mm collimator forms a 4 nm gaussian filter. A half waveplate is placed before the grating to adjust the polarization state to get the maximum diffraction efficiency from the grating. Half and quarter waveplates combined with a polarization beam splitter are used to form a saturable absorber based on nonlinear polarization evolution (NPE). The laser is co and counter pumped with 54 cm of step-index fiber (OFS980) from the WDM pigtail before and after the gain fiber. The repetition rate of the laser is 40 MHz.

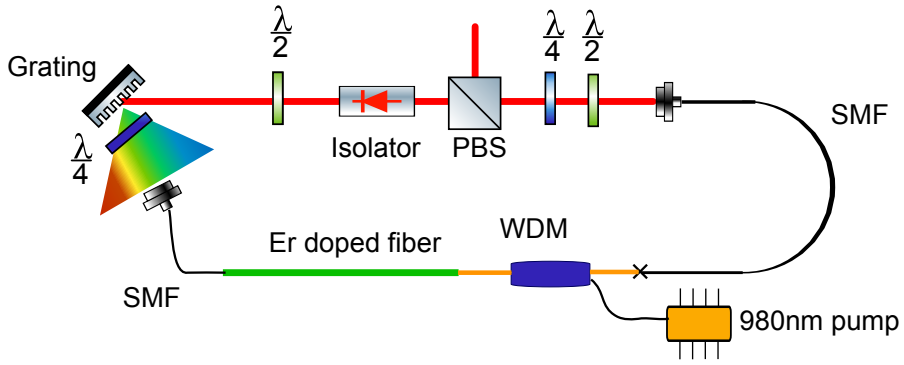

Figure 2.11: Experimental setup.

Mode locking is achieved by adjusting the waveplates and is very easy to

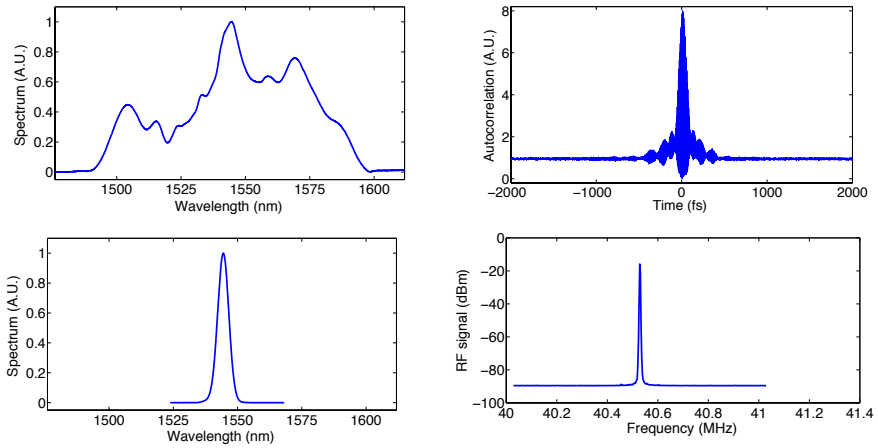

Figure 2.12: Experimental Results.(a) Mode locked spectrum.(b): Dechirped autocorrelation. (c) Spectrum before the gain and after the grating filter. (d) RF spectrum.

obtain. The mode locked pulse is self-starting at the 40 MHz repetition rate and has 140 mW of output power, corresponding to a pulse energy of 3.5 nJ. The dechirped pulse duration after a dispersive delay line (grating pair) is 75 fs. The chirp of the pulse referred from the dispersion delay line is 44,400 fs^2, which is much less than the net cavity dispersion as the case in Yb amplifier similariton laser [3]. Considering the 4 nm filter, the pulse bandwidth has a strong spectral breathing ratio of more than 10 times, as predicted by simulation. The side lope of the AC is from the TOD from the grating.

2.3.4 Discussion

This is the first demonstration of using a narrow filter to stabilize self-similar evolution in an Er-doped laser cavity. As is expected, the gain bandwidth set the limitation for the shortest pulse the laser could generate. The simple design of the cavity allows for future manipulation of the cavity such as putting a dis-

persion map within the cavity. The laser is currently pump limited with two single mode diodes. The performance of the laser could be improved by using a even narrow filters (2 nm) and higher pump power in the double cladding fiber version. More systematic study of this type of design will be presented in future work.

2.3.5 Conclusion

We have demonstrated an amplifier similariton laser stabilized by a narrow filter at 1550 *nm* with large net normal dispersion. The laser is stable and easy to mode locking. The pulse experiences a spectral breathing ratio of 13 within the cavity. The generated pulse duration is 75 fs with 3.5 nJ of chirped pulse energy.

2.4 Enhanced bandwidth generation based on self similar evolution

As mentioned earlier, the gain bandwidth of Er-doped fiber limits the shortest pulse that could be generated from amplifier similariton laser. However, the strong nonlinear attractor of gain segment and a narrow filter allows the dramatic evolution of the pulse inside the cavity. Therefore, the idea to broaden the spectrum even future after the gain is tested in this section based on the passive similariton propagation [6]. A large normal dispersion Er-doped fiber laser with enhanced bandwidth generation stabilized by self similar attraction in the gain segment and a narrow filter is demonstrated as a new route to generate few cycle pulses. The laser generates 37 fs dechirped pulse with 2.5 nJ.

2.4.1 Introduction

Fiber lasers have caught up with solid state laser performance in terms of energy over the past five years due to the development of dissipative soliton lasers at normal dispersion. However, to compete with solid state lasers in pulse duration, fiber lasers have the intrinsic limitations of large dispersion, large nonlinearity and narrow gain bandwidth. So far the methods used for short pulse generation in Er-doped fiber lasers have all exploited minimizing the net cavity dispersion. Dispersion-managed (DM) soliton lasers with near zero net cavity dispersion can generate very short pulses [24], but their stability around zero dispersion has to be compromised. The bandwidth of a DM soliton is fundamentally limited by small breathing ratio and gain bandwidth. On the other hand, the DM solution cannot tolerate large nonlinear phase accumulation and therefore has limited pulse energy. In addition, mode locking is hard to achieve around zero dispersion regime and its performance is not well predicted by simulation. In contrast, dissipative soliton fiber lasers [1] with large normal dispersion achieve high energy but rarely generate pulses below 100 fs. In fact, the way to generate shorter pulse in dissipative soliton laser is also to minimize total cavity dispersion [25]. By minimizing the cavity dispersion via limiting the fiber length, a 50 fs all normal dispersion Er-doped fiber laser was reported [26]. The performance of both DM soliton and dissipative soliton lasers is fundamentally limited by two factors: the net dispersion of the minimum fiber required to build the cavity and relatively narrow gain bandwidth since both Yb- and Er-doped silica fiber has about one-quarter gain bandwidth of Ti:sapphire.

A new type of pulse solution based on self similar evolution in the gain fiber was demonstrated recently in fiber oscillators [2, 3, 27]. Both Oktem and Ren-

ninger's cavities can support strong spectral breathing due to the strong nonlinear attractor of gain segment. Amplifier similariton pulse evolution works to linearize the nonlinear phase by attracting to a parabolic pulse shape. Therefore, these lasers can tolerate even more nonlinear phase shift and generally generate much shorter pulse than a dissipative soliton laser. However, the self-similar evolution will eventually be disrupted by the gain bandwidth, limiting the shortest pulse this type of cavity can generate with Erbium gain [2] to be around 100 fs. Aguergaray [27] built the self similar laser based on Raman gain with kilometers of fiber. Although Raman gain bandwidth is much larger than the doped fiber, the shortest pulse generated from this type of laser is 6 ps.

One of the advantages of a parabolic pulse is wave-breaking free operation in a normal dispersion medium as is the case in Anderson s parabolic pulse compression [6]. Chong *et. al* [4]proposed a fiber laser design based on extending the self similar propagation in the gain fiber and further in a high nonlinear normal dispersion passive fiber after the gain. The strong spectral breathing (a factor of 30) is stabilized by the local gain attractor and a 4 nm Gaussian filter placed before the gain segment. The net dispersion and thus total fiber length do not limit the minimum pulse duration in this evolution. Therefore various repetition rates are possible to meet different applications. More importantly, understanding the evolution in this type of cavity allows for manipulation of the laser design for various motivations.

Here we present an all fiber Er-doped fiber laser with self similar evolution within the gain and enhanced bandwidth generation in the high nonlinear fiber after the gain. We show both simulated and experimental result. The laser exhibits more than 20 times spectral breathing and the generated largest spectra

and shortest pulses from Er-doped fiber laser seen to date. The mode locked spectra supports 30 fs transform limited pulses, and they can be dechirped to 33 fs with a pair of grating with secondary structures caused by TOD from fibers and grating.

2.4.2 Numerical Simulation

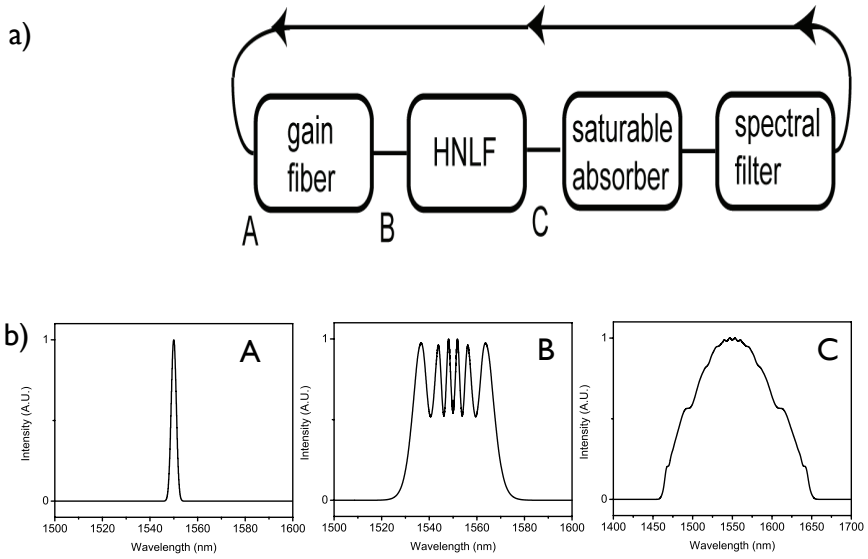

Figure 2.13: Numerical Simulation. (a) Cavity Schematic. (b) Pulse spectrum evolution. A, B, C : the spectrum from different positions in the cavity.

The schematic of the cavity and generic spectral evolution are shown in Fig.2.13. The cavity has two major fiber segments: gain fiber and high nonlinear fiber after the gain. A saturable absorber and a narrow filter (2-12 nm) are used to initiate mode locking and stabilize the cavity. Fig.2.13 (b) shows the spectrum evolution at different locations of the cavity. A narrow filter shapes

the pulse to be a few nm Gaussian before the gain (A), then the pulse entered into parabola regime and experienced first strong bandwidth growth by the end of the gain fiber (B) as in the case of amplifier similariton laser [3] . It is significantly broadened in both temporal and spectral domain in the high nonlinear fiber after and is then cut back by the filter to make the feedback.

The pulse experienced wild evolution within the cavity compared with all previous existing lasers as shown in Fig.2.14 The pulse evolution can be quantified with the metric, $M^2 = \int[|u| - |p|]^2 dt / \int |u|^4 dt$, where u is the pulse being evaluated and p is a parabola with the same energy and peak power. In the gain fiber, the pulse evolves from a Gaussian profile (M=0.14) after the spectral filter to a parabola (M≤0.06) as shown in Fig.2.14(b). Within the cavity, spectrum bandwidth and pulse duration grows together in both the gain fiber and the high nonlinear fiber after. This dramatic evolution shows the robustness of the mode locking mechanism: the nonlinear attractor of gain segment and narrow filter. The tolerance of this evolution indicate a large freedom of manipulation of the laser cavity for different application.

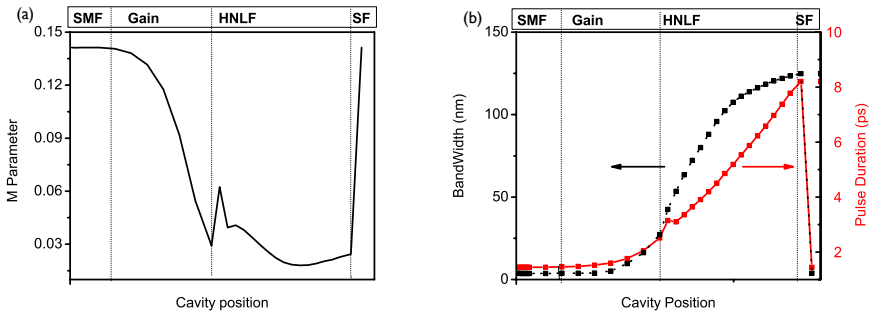

Figure 2.14: Pulse evolution inside the cavity. (a):Pulse bandwidth and duration evolution. (b): M matric evolution.

Systematic simulation has been done with various filter bandwidth, gain

fiber and high nonlinear fiber.The cavity is designed to optimize the total broadening while keeping the chirp nearly linear. The net cavity dispersion is always large normal(>0.06 ps^2). The controlled simulation shows that although the net cavity dispersion does not affect the bandwidth, for the fixed length of high nonlinear fiber, the less net dispersion from gain segment, the broader spectrum it can generate as shown in Fig.2.15 This can be understood as pulse with lower chirp broadening faster in the presence of nonlinearity.

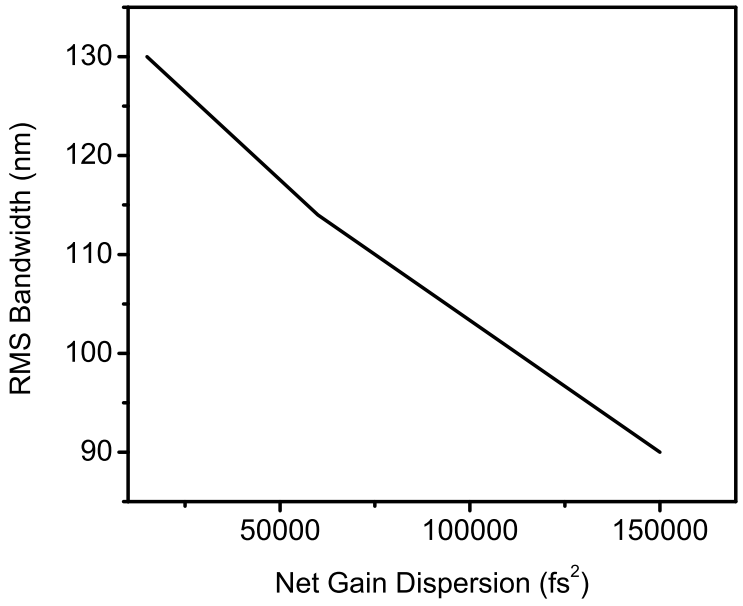

Figure 2.15: Impact of net dispersion from gain segment with controlled all fiber lengths and nonlinearity. β_2 of the gain segment is varied artificially from 77 fs^2 to 20 fs^2.

One of the broadest simulated result carried out with realistic experiment parameters is from a cavity with 80 cm of normal dispersion gain fiber (β_2=19 fs^2 and β_3=50 fs^3, A_{eff}=29μm^2), a total of 50 *cm* of SMF 28 fiber (β_2=-23 fs^2 and β_3=86fs^3, A_{eff}=70μm^2) from collimator fiber pigtail, a total of 60 cm of passive normal-dispersion fiber OFS980(β_2=4.5 fs^2 and β_3=109 fs^3, A_{eff}=44μm^2) from

WDM right before and after gain. It is followed by 2.5 m of highly-nonlinear fiber UHNA7(β_2=31 fs^2 and β_3=-51 fs^3, A_{eff}=8 μm^2). For this gain fiber, a 8 nm filter is used to reach the best performance. The cavity has net dispersion of 0.08 ps^2.

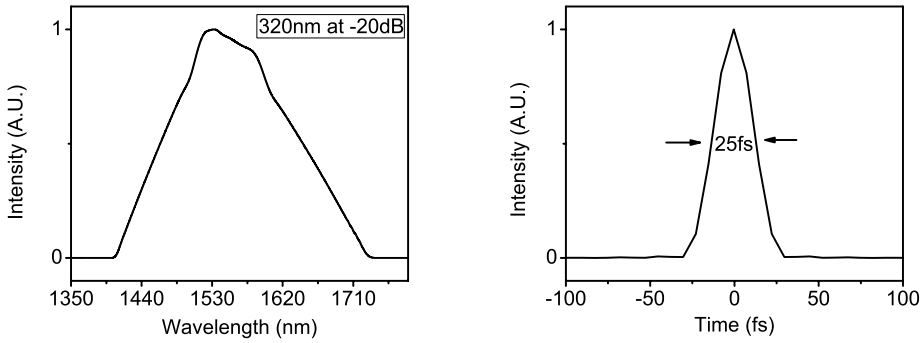

Figure 2.16: Simulation Results.(a): Broadest simulated spectrum. (b) Calculated zero phase transform limit pulse from spectrum (inset)

The mode-locked result has spectrum (Fig.2.16)broad enough to support a 25 fs pulse. The asymmetric feature of the spectrum is due to large TOD from the cavity. The spectral breathing ratio is more than 20 in one round trip. The large net normal cavity dispersion shows a departure from other mode locking mechanisms that rely on minimizing the cavity dispersion to generate short pules. Indeed, the length of the cavity is more than 100 times the dispersion length.

2.4.3 TOD Impact

Even at such large net normal dispersion, TOD influences the laser performance by causing asymmetric features of both the pulse and spectrum (Fig.2.17). These asymmetric feature will eventually disrupt the self similar evolution and leads

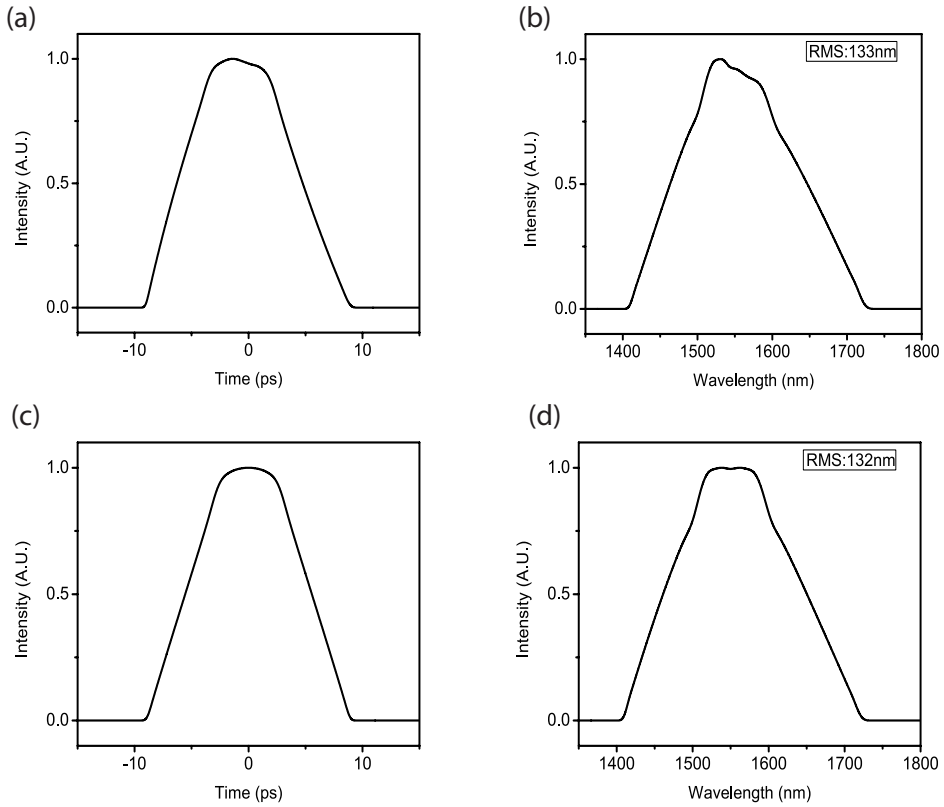

Figure 2.17: Simulation with and without TOD.(a):Chirped pulse without TOD. (b)Spectrum without TOD.(c):Chirped pulse TOD. (d):Spectrum withTOD.

to wave breaking. Controlled study shows that it is the TOD after the gain that matters to the pulse propagation, where the spectrum get broad enough for local TOD to be comparable with GVD. Different sign of TOD cause different asymmetry (Fig.2.18). However, some part of TOD could assist to generate broader spectra by compensating nonlinearity after the gain(Fig.2.19). The with some TOD inside the cavity (Fig.2.19), the pulse bandwidth broaden by a little more than 10%. Therefore managing the TOD, especially the TOD after the gain will be the next step to minimize its impact on wave breaking but maximum its function to overcome nonlinearity. It can also be engineered to match the dispersion delay line outside the cavity to fully compensate TOD on top of the pulse.

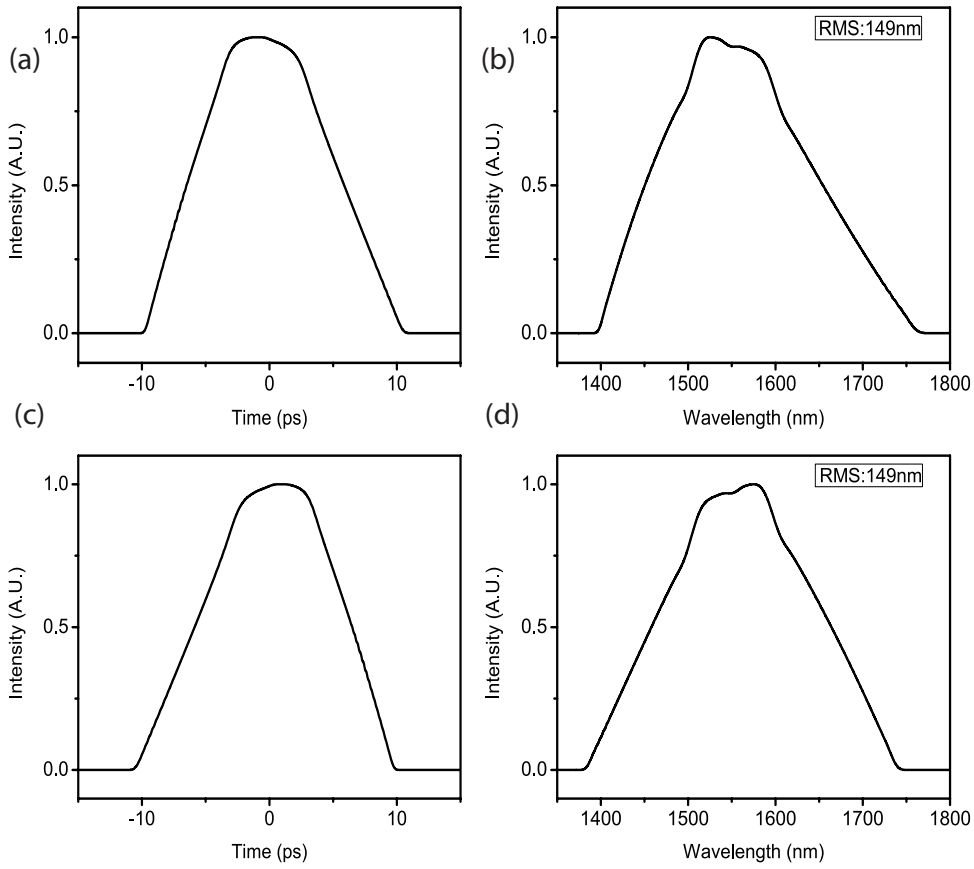

Figure 2.18: Simulated pulse and spectrum with zero TOD for other parts of the cavity except for UNHA7. The TOD values are set to be -51 fs^3 (a)(b) and 51 fs^3(c)(d)

2.4.4 Experimental Results and Discussion

A laser cavity guided by simulation mentioned above was built as shown in Fig. 2.20 Nonlinear polarization evolution(NPE) is used as the saturable absorber to fully access the mode locking states. A 300/mm grating and 0.5 mm beam size collimator create the Gaussian filter. Despite the low slope efficiency of 10%, due in part to splicing and filtering losses, the laser exhibits stable, self-starting mode locking for various filter bandwidths. The repetition rate of the laser is

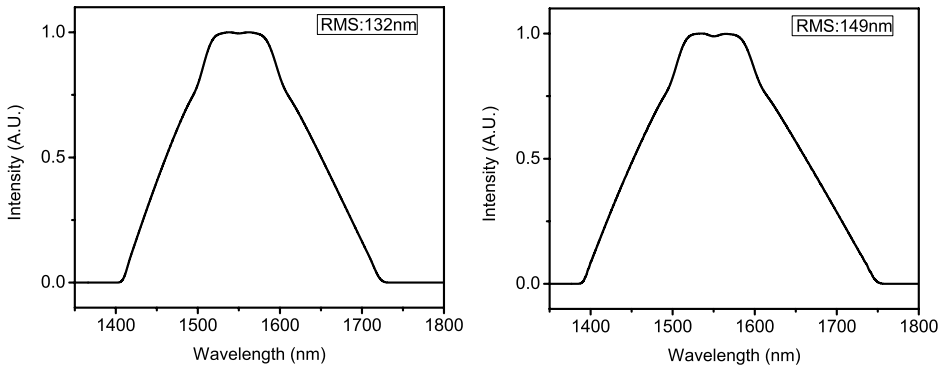

Figure 2.19: Simulated spectrum without TOD for the whole cavity(left) and without TOD for the fiber after the gain only (right).

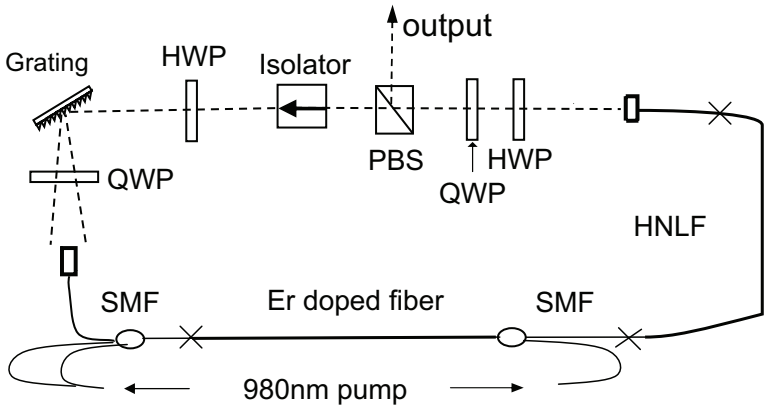

Figure 2.20: Experimental Setup. PBS is a 50:50 1550 *nm* polarization beam splitter. QWP is quarter wave plate. HWP is half wave-plate. HNLF is high nonlinear fiber. PBC is 980 *nm* polarization beam combiner.

around 42 MHz.

The performance of the laser (Fig.2.21) matches the simulation in terms of bandwidth and pulse energy. The spectrum from the polarization beam splitter tends to have modulation on top which we suspect is due to intrinsic NPE filtering. The laser is pumped by 3 single mode diodes that provide up to 1.3 mW of pump power, which gives 200 mW maximum CW power. The laser is cur-

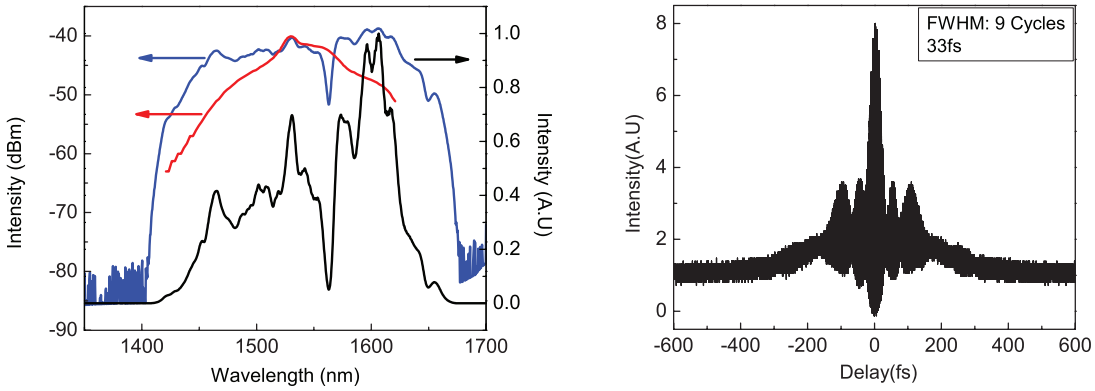

Figure 2.21: (Experiment Result. (a)Mode locked spectrum. Black line is linear scale. Blue line is log scale. Red line is the log scale spectrum of Er-doped gain. (b) Dechirped autocorrelation

rently power limited due to gain saturation. The dechirped pulse duration is 33 fs, which is 10% beyond the transform limit. Calculations show that excessive TOD is responsible for the uncompensated phase shown as the secondary structure in autocorrelation(Fig.2.22). The pulse chirp is 54,000 fs^2, much less than the net cavity dispersion, which is a signature of self-similar evolution [3]. The chirped pulse energy is 1.6 nJ.

So far simulation and experimental studies of this cavity shows two major limits to the spectrum broadening : the nonlinear phase accumulation in the high nonlinear fiber after the gain and the loss due to the strong filtering. The first problem can be avoided by using a dispersion decreasing fiber after the gain to control the dispersion as will be reported in another paper. The later problem could be potentially solved by spectrum compression [28]. The length, dispersion and nonlinearity of the gain fiber determine the range of filter to use in order to support self similar evolution and separate the laser from dissipative soliton.

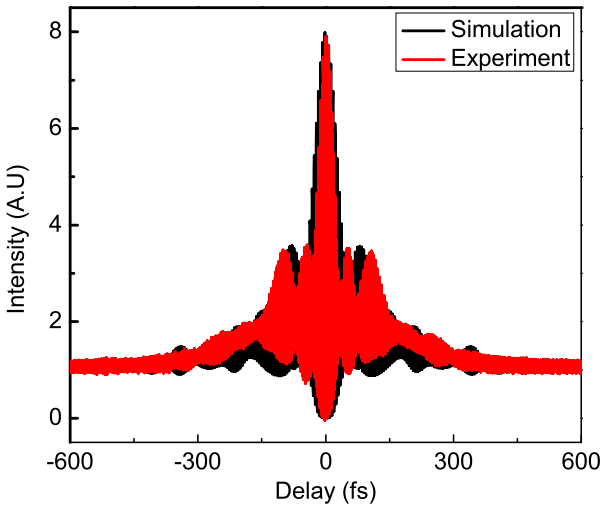

Figure 2.22: (TOD impact on the dechirped pulse. Black line: dechirped pulse. Red line: simulated autocorrelation by adding TOD from grating to the calculated transform limited pulse.

2.4.5 Future work for enhanced bandwidth generation from Er fiber laser

1. Systematic study the design guide of laser. Such as the best match between gain fiber and high nonlinear fiber.

2. Use more efficient gain fiber. The cavity is currently limited by pump power due to gain saturation. Higher pump power will give broader spectrum and more energy. Also from the study in Section 2.4, shorter gain fiber with a bigger filter will give even broader spectrum.

3. TOD control in dechirping stage.

4. Spectral compression to replace filter to reduce cavity loss and to make a

more integrated laser cavity.

5. Use CNT SA to replace NPE to make an all fiber formatted cavity.

2.5 Conclusion

An Er fiber laser based on similariton formation in the gain segment and enhanced bandwidth generation in passive fiber is demonstrated as a new route to generate short pules in Er-doped fiber lasers. This laser generates pulses down to 6 cycles(33 fs) with 1.6 nJ pulse energy. The laser is currently limited by gain saturation.

CHAPTER 3

YB FIBER LASER

This chapter focus on the extension of Yb amplifier similariton laser [3]. Two type of self similar extension (passive self similar and DDF self similar solution) within the fiber laser cavity will be introduced in this chapter. The future direction of those two methods will be discussed.

3.1 Pulse generation without gain bandwidth limitation in a laser with self similar evolution

With existing techniques for mode-locking, the bandwidth of ultrashort pulses from a laser is determined primarily by the spectrum of the gain medium. Lasers with self-similar evolution of the pulse in the gain medium can tolerate strong spectral breathing, which is stabilized by nonlinear attraction to the parabolic self-similar pulse. Here we show that this property can be exploited in a fiber laser to eliminate the gain-bandwidth limitation to the pulse duration. Broad (~200 nm) spectra are generated through passive nonlinear propagation in a normal-dispersion laser, and these can be dechirped to ~20-fs duration.

3.1.1 Introduction

The shortest light pulse that can be generated by a laser oscillator will always be of fundamental interest to the field of ultrafast science, and it will determine the time resolution or bandwidth of many measurements. A critical factor in the design of an ultrashort-pulse laser is the bandwidth of the gain medium.

Almost all lasers that generate few-cycle (~10 fs) pulses exploit the huge ($2\pi\times44$ rad THz) gain bandwidth of titanium-doped sapphire. Spectra that exceed the gain bandwidth, and pulses that approach a single cycle in duration, have been generated through nonlinear spectral broadening and preferential output coupling of the edges of the spectrum [29].

Much of our understanding of mode-locked lasers comes from analytic solutions of equations based on the assumption of small changes in a pulse as it traverses the cavity [30]. The intracavity pulse evolution in even a 10-fs Ti:sapphire laser is not dramatic, because the crystal comprises roughly one characteristic dispersion length (L_D) of propagation: $L_D = \tau^2/|\beta_2| \sim 1$ mm, where τ is the pulse duration and β_2 is the second-order dispersion coefficient. When the approximations of the model break down, perturbative [31] and numerical analyses are employed.

Fiber oscillators have not reached the few-cycle regime. Few-cycle pulses can be generated by pulse compression or by interfering the spectra of two separate continuua seeded by a fiber laser [32]. Direct generation from an oscillator should impact applications by improving the stability, and reducing the complexity and cost of the source. Applications would include generation of seed pulses for attosecond science, frequency metrology, and nonlinear microscopy [33], among others.

The gain bandwidth of ytterbium-doped silica fiber [34] is about one-quarter that of Ti:sapphire. Significant gain typically extends over 100-150 nm, with the short-wavelength limit of the gain determined by the pump absorption band. The cut-off wavelength, below which the fiber supports multiple transverse modes, may present an ultimate limitation to the bandwidth of a fiber laser:

even small higher-order-mode content significantly reduces the multi-pulsing threshold of modelocked fiber lasers [35]. Single-mode fiber (SMF) designed to operate near 1 μm typically has a cut-off wavelength near 900 nm. Modelocked Yb fiber lasers produce bandwidths up to ~120 nm at the -20-dB points, and pulses as short as ~30 fs [36, 37]. Broader output spectra can be produced with noise bursts [38,39], which are not self-consistent solutions of the laser cavity. The gain bandwidth will present a clear challenge to the generation of 10-fs pulses. A fiber laser typically includes around 1 m of fiber. $L_D \sim 2$ mm for a 10-fs pulse, so a 10-fs fiber laser will comprise hundreds of dispersion lengths. The pulse evolution in such a laser will likely involve extreme spectral and temporal changes. Whether such dramatic evolution can be controlled is an important question.

Here we describe a new approach to the design of fiber lasers, which decouples the pulse bandwidth from the limitations of the gain spectrum. In a resonator with large normal dispersion, spectral broadening in fiber after the gain segment produces output bandwidths that substantially exceed the gain bandwidth. The overall evolution is stabilized by filtering and the nonlinear attraction to the self-similar solution in the gain medium. Bandwidths approaching 200 nm and pulses as short as 21 fs (the shortest from a fiber laser to date) are generated in initial experiments. This demonstration introduces a class of fiber lasers with clear potential for few-cycle pulse generation, and more broadly for producing a range of useful output pulses. In contrast to prior work aimed at generation of the shortest pulses, this approach cannot be understood within averaged-cavity models [30].

Self-similar evolution is a powerful technique to avoid distortion of optical

pulses that propagate nonlinearly. Pulses with a parabolic intensity profile and linear frequency chirp,

$$A(z,t) = A_0(z)\sqrt{1-(t/t_0(z))^2}e^{i(a(z)-b(z)t^2)} \tag{3.1}$$

for $t \leq t_0(z)$ are asymptotic solutions of the nonlinear Schrodinger equations that govern pulse propagation in passive [6] or active [7] fiber with positive nonlinear refraction and normal group-velocity dispersion (GVD). These pulses accumulate substantial nonlinear phase shifts without undergoing wave-breaking or more-dramatic distortions such as pulse fission. For an amplifier with constant gain, the asymptotic solution is a nonlinear attractor; a range of inputs to the amplifier evolve to the self-similar solution [7]. The chirped self-similar pulses (sometimes referred as "similaritons") can be compressed to the Fourier-transform limit by passing them through a dispersive delay.

Short-pulse lasers based on self-similar pulse propagation in their gain segments were recently reported [2, 3, 27, 40]. Spectral breathing occurs in these lasers, with the bandwidth varying by an order of magnitude as the pulse traverses the resonator. Strong filtering stabilizes the evolution by allowing a short pulse to evolve to the parabolic solution before the end of the gain fiber [3]. A remarkable feature of these lasers is that the similariton is a local nonlinear attractor in the gain segment of the laser. The pulse can change dramatically, or it can be intentionally manipulated, in the rest of the cavity, as long as the input to the amplifier can approach the asymptotic solution. This property of the amplifier similariton evolution will be a valuable degree of freedom in the design of high-performance instruments.

The spectral bandwidth of a similariton grows exponentially in an amplifier. However, the self-similar evolution is disrupted when the pulse bandwidth ap-

proaches the gain bandwidth of the amplifier, and this limits the pulse energy and duration that can be achieved [41]. The generation of pulses shorter than 30-40-fs from a self-similar amplifier based on Yb fiber will be difficult. Spectral broadening in a similariton-soliton laser [2] will likely be limited by soliton fission in the anomalous-dispersion segment. It may be possible to extend or continue self-similar pulse evolution beyond an amplifier. For example, a fiber with lower dispersion and/or higher nonlinear coefficient than the gain fiber can induce substantial spectral broadening. The linearly-chirped parabolic pulse produced by the amplifier will maintain close to a parabolic shape and linear chirp in the passive fiber. This evolution is related to the parabolic pulse compression scheme discussed by Anderson [6].

3.1.2 Numerical Simulations

Although self-similar propagation in gain and passive fibers are well-known, prior studies of single-pass propagation from a given initial condition do not address whether the evolution will develop from noise in a system with feedback. Numerical simulations were performed to assess the feasibility of the desired evolution. The simulated cavity (shown conceptually in Fig. 3.1 and with experimental detail in Fig. 3.3) contains 30 cm of SMF (β_2 = 230 fs^2/cm), 80 cm of Yb-doped gain fiber, and another 20 cm of SMF. We assume that 35% of the light is coupled into a segment of passive fiber with β_2 = 400 fs^2/cm a and nonlinear coefficient 5 times larger than that of the gain fiber. These parameters correspond to a photonic-crystal fiber (PCF). After the passive fiber, 80% of the energy is coupled out, and the remaining 20% traverses a saturable absorber and a Gaussian filter with 3-nm bandwidth. Without the PCF, the laser is an es-

tablished self-similar laser [3]. Simulations were performed for varying lengths of PCF. Simulations converge to stable solutions for a range of PCF lengths, with

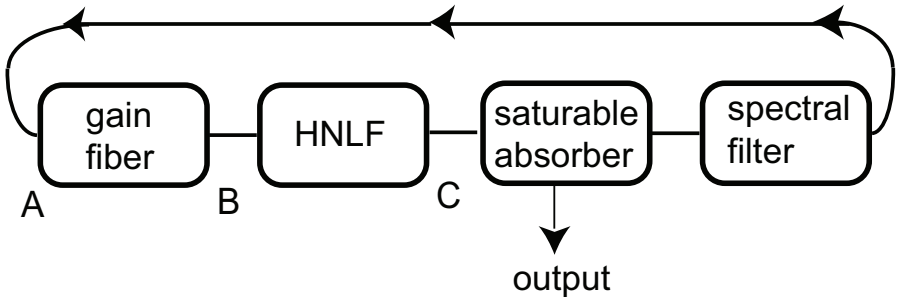

Figure 3.1: Schematic of the simulated laser. HNLF: Highly nonlinear fiber.

the desired pulse evolution occurring for lengths around 2 m. Starting from a narrow Gaussian, the spectrum broadens and develops the structure characteristic of a chirped parabolic pulse [3] (Fig.3. 2, middle row). A parabolic temporal profile is clearly established in the gain fiber (top row of Fig. 3.2). The spectrum broadens further in the passive fiber (Fig. 3.2, middle row). Impressing a quadratic spectral phase on the output produces a dechirped pulse that is close to the transform limit. The 0.6-nJ dechirped pulses are 20-fs long (Fig. 3.2, top row, inset).

3.1.3 Experiment

A PCF (NL-1050-NEG-1 from NKT Photonics A/S) 1.6 m long, with 2.2-μm mode-field diameter and the nonlinear and dispersion parameters assumed in the simulations, is employed in the experimental setup (Fig. 3.3). A 300 l/mm grating and a collimator create a Gaussian spectral filter with 4-nm bandwidth. Nonlinear polarization evolution (NPE) is an effective saturable absorber, im-

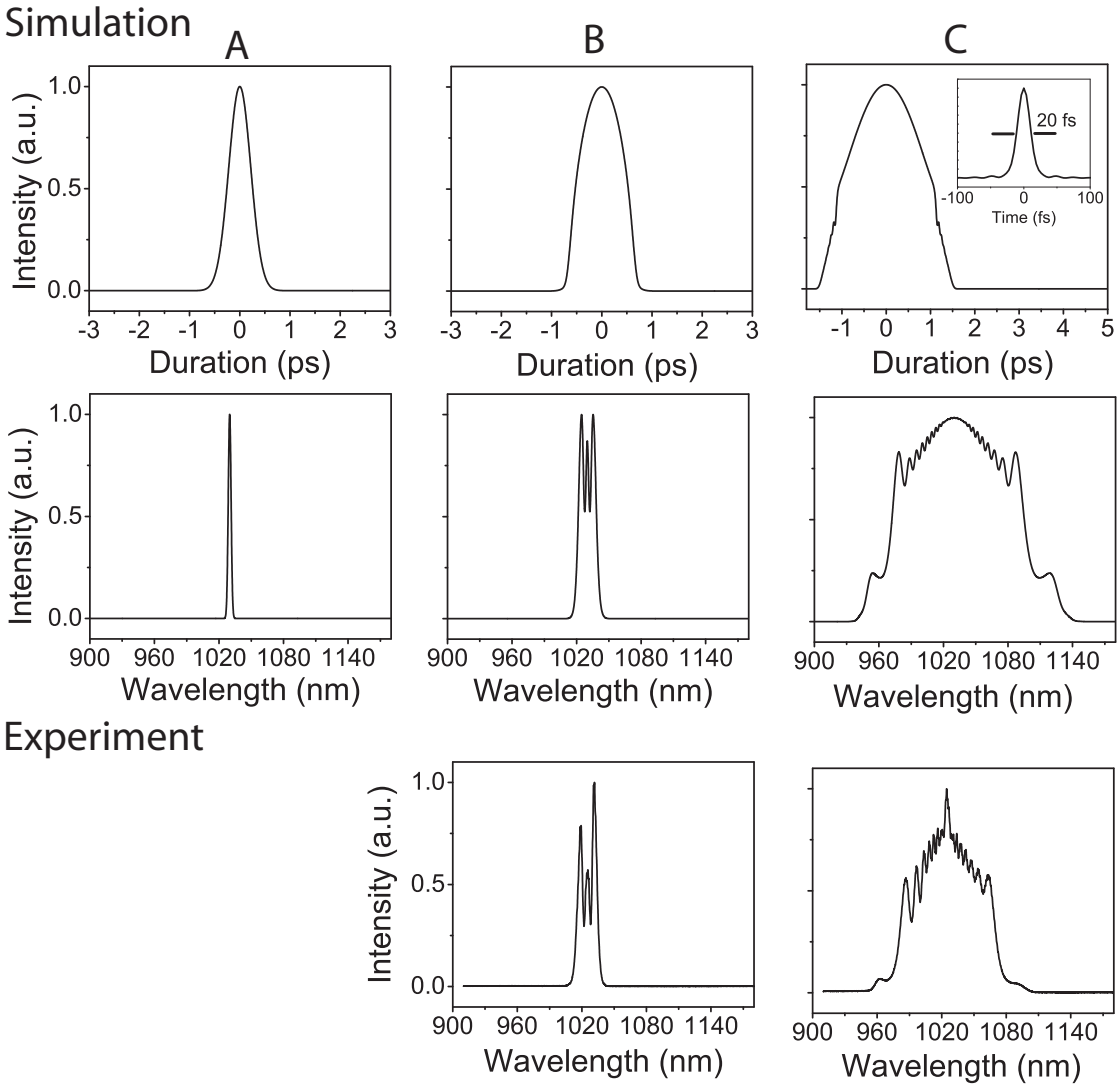

Figure 3.2: Comparison of simulation to experiment at the indicated locations in the cavity. Simulations assume 2 m length of PCF, along with parameters given in text. Top row: simulated chirped pulses. The inset is the numerical transform-limited pulse from location C. Middle row: simulated spectra. Bottom row: experimental spectra.

plemented by the quarter- and half-wave plates and polarizer. The laser is constructed with some bulk components to facilitate variation of the cavity parameters, and sampling beam-splitters allow monitoring of the intra-cavity pulse evolution. The pulse-repetition rate is 62 MHz. Single-pulse operation is veri-

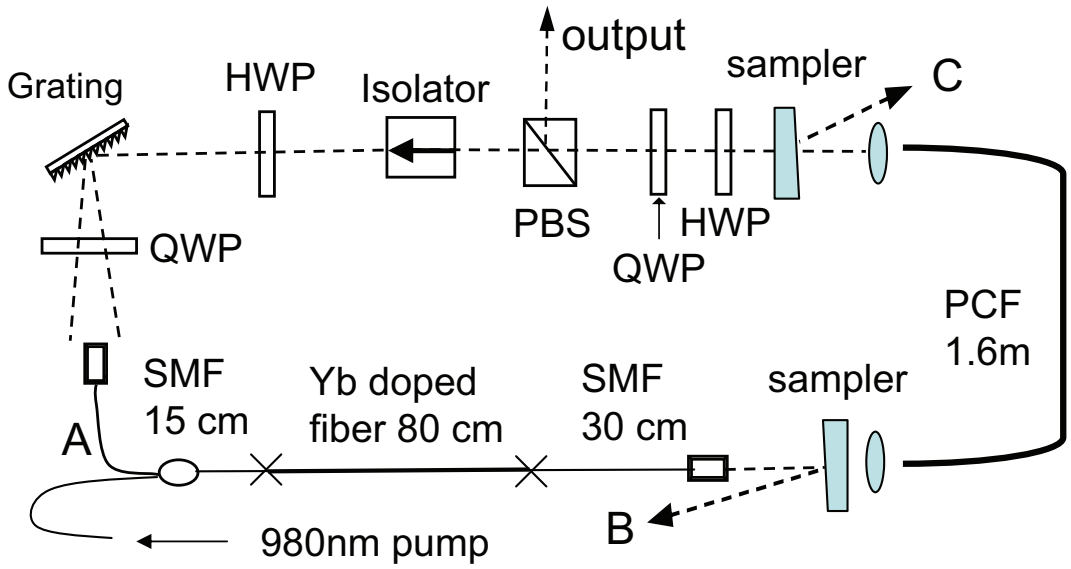

Figure 3.3: Fiber laser schematic. QWP: quarter-waveplate; HWP: half-waveplate; PBS: polarizing beam-splitter.

fied by monitoring the output with a photodetector and sampling oscilloscope with 30-GHz bandwidth and recording the autocorrelation for delays up to ~100 ps.

The laser is mode-locked by adjusting the wave plates. The bottom row of Fig. 3.2 shows the spectra recorded at the indicated points of the cavity. After the gain segment, the spectrum has the structure of a chirped parabolic pulse [3]. The 30-nm bandwidth of the pulse from the gain segment increases dramatically in the PCF. The full-width at half-maximum bandwidth is 100 nm, which exceeds the gain bandwidth. The spectrum exhibits all of the qualitative features of the simulation result, along with a continuous-wave peak near 1025 nm that is difficult to avoid. The pedestals at the base of the spectrum are a signature of incipient wave-breaking, which is also visible in the simulated temporal profile (Fig.3.2, top row, point C).

The chirped output pulse energy is 1 nJ. The energy is limited by the avail-

able pump power, but simulations show multi-pulsing at 2 nJ, so we do not expect much higher energy.

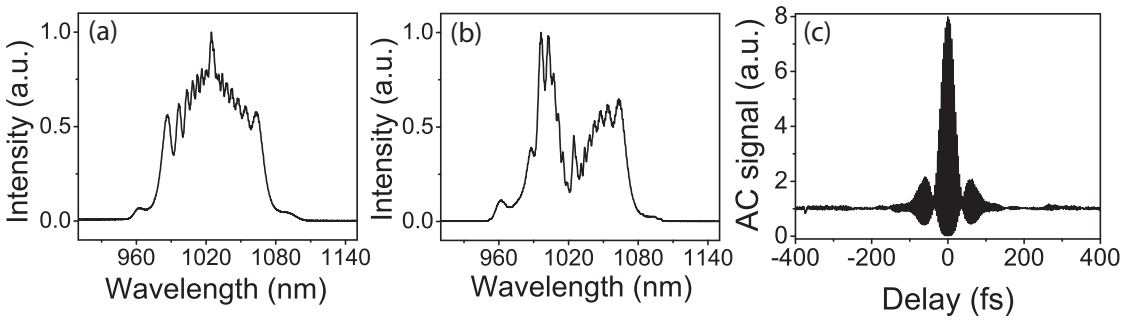

Figure 3.4: Experimental results. a) spectrum after the PCF, b) output spectrum and c) output autocorrelation signal after phase correction by MIIPS for a 25-fs pulse.

The output spectrum (Fig. 3.4(b)) maintains the overall bandwidth, but typically exhibits some modulation, and may become asymmetric. Some spectral structure can be expected to arise from the NPE process. Birefringence of the PCF may play a role, but that remains to be assessed carefully. We used multiphoton intrapulse interference phase scan (MIIPS) [42] to characterize the phase of the output pulse. The quadratic, cubic, and quartic phases are typically 12,000 fs^2, -6×$10^4 fs^3$, and 2×$10^6 fs^4$, respectively. The quadratic phase is smaller than the cavity dispersion, which is typical for amplifier-similariton lasers [3]. The sign and magnitude of the cubic and quartic phases are consistent with the third- and fourth-order dispersion of the PCF. This suggests that the residual phase is accumulated in the PCF without disrupting the intended propagation. After phase correction by MIIPS (Fig. 3.4(c)) the pulse is dechirped to the transform limit, with a full-width at half-maximum (FWHM) duration of 25 fs. The pulse energy after dechirping by the MIIPS apparatus is 0.5 nJ. A consequence of the structured output spectrum is that about 20% of the energy is in the secondary structure. Although the CW peak is certainly undesirable, it

does not seem to have major impact on the pulse quality nor the stability of the laser. Pulses from the laser described here have produced high-resolution images by third-harmonic generation microscopy [43]. Based on the MIIPS results, it should be possible to design a grating compressor, e.g., to dechirp the output pulses.

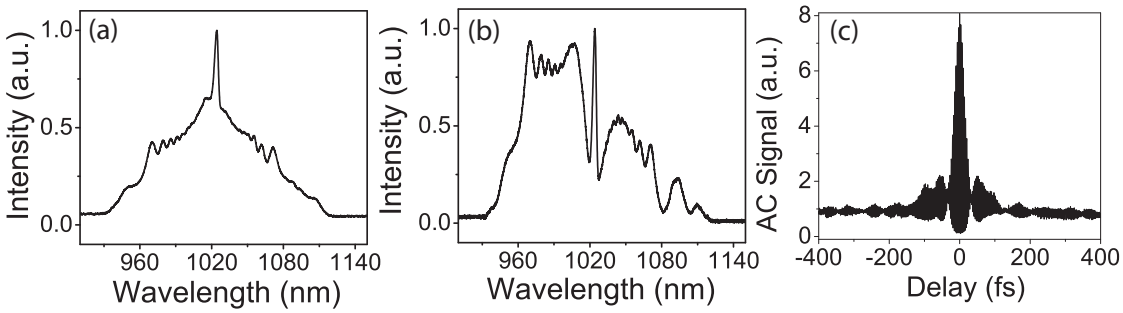

Figure 3.5: Experimental Results of shortest pulse. a) spectrum after the PCF, b) output spectrum and c) output autocorrelation signal after phase correction by MIIPS for a 21-fs pulse.

An example of the broadest spectra that we have observed is shown in Fig.3.5. Significant energy extends over nearly 200 nm at the base of the spectrum. The production of spectra with ~ 20% of the energy below the pump wavelength (where there is no gain) and the excellent agreement between calculated and measured spectra clearly demonstrate that the Yb gain bandwidth does not limit the output spectrum. The FWHM pulse duration is 21 fs, which corresponds to 6 cycles of the field. The pulse does have significant structure in the wings, with energy extending beyond 100 fs from the peak. The pulse evolution in this laser exhibits some remarkable aspects. The spectrum broadens from 4 to 30 nm in the gain fiber, and then to 110 nm in the passive fiber, for an overall spectral breathing ratio of 25. The intracavity pulse duration varies between 1 and 10 ps, yet the pulse can be dechirped outside the cavity to ~20 fs. With respect to that pulse duration, the laser is equivalent to 300 dispersion

lengths of propagation. For comparison, in a 5-fs Ti:sapphire laser the spectrum exceeds the gain bandwidth by ~ 30%, the spectral breathing is less than a factor of 2, and the intracavity pulse duration varies from 10 to 50-fs [44].

3.1.4 Discussion

The results presented here show that substantial bandwidth enhancement by nonlinear pulse propagation can be stabilized in a self-similar laser. However, our understanding of this kind of laser is not complete, and significant improvement on these initial results should be possible. The existence of the CW component, and its influence on the mode-locked state, need to be studied. The parabolic pulse launched into the passive nonlinear segment helps to control the nonlinear phase accumulation, but, as mentioned above, the pulse deviates from a perfect parabola. The influence of higher-order dispersion of the nonlinear segment on the pulse evolution must be determined. It should be possible to produce pulses with more-linear chirp by better design of the nonlinear segment. The PCF has a cut-off wavelength around 300 nm, so extremely broad spectra can be accommodated without risk of multimode propagation. With broader spectra, the loss from filtering will present a challenge.

This work can be extended by continuing the ideal self-similar evolution from the gain segment in a section without bandwidth limitations. This is theoretically possible with a dispersion-decreasing fiber, where the resulting system is formally equivalent to a gain fiber [5]. In addition to the potential of unbounded bandwidth, we expect the pulse to be closer to a parabola and therefore have a nearly-linear chirp. Indeed, initial numerical simulations show that

the use of a dispersion-decreasing fiber should allow the generation of broader and less-structured spectra, with smaller higher-order phase to be corrected. The generation of parabolic pulses in dispersion-decreasing fiber has been reported [45, 46], but the dispersion varies over kilometers. If such a fiber can be fabricated with the dispersion varying on the scale of meters, this will be another promising way to extend the work presented here.

3.1.5 Conclusion

In conclusion, we have shown that the gain bandwidth does not present a fundamental limitation to the minimum pulse duration in an amplifier-similariton laser. The spectrum can be broadened in a separate nonlinear segment, and filtering produces the seed pulse to the amplifier that allows a self-consistent solution. This opens a promising route to the development of few-cycle fiber lasers.

3.2 Extended Self-Similar Pulse Evolution in a Laser with Dispersion-Decreasing Fiber

Following the work from last section, this section introduces a mode locked fiber laser based on self-similar pulse evolution in a segment of dispersion decreasing fiber. We show numerically and experimentally that the dispersion decreasing fiber extends the self-similar propagation after the gain fiber while avoiding the limitations imposed by the gain bandwidth. The 1 nJ pulses generated by this cavity are de-chirped down to 6 cycles (20 fs) with a grating pair, demonstrating

the utility of this concept in creating short pulses from fiber lasers.

3.2.1 Introduction

The development of fiber lasers has been advanced by the discovery of new mode locking mechanisms, and the mathematical study of nonlinear attractors has provided important insights in this area. Soliton lasers operating in the anomalous dispersion regime dominated the field of fiber lasers for 20 years [47]. but the performance of these was limited to low pulse energy. For the last decade, the development of dissipative soliton lasers [48] in the normal dispersion regime has enabled the power level of fiber laser to compete with their solid-state counterparts. Recently, self-similar lasers based on parabolic attraction in the gain fiber have been reported [2, 3] with the gain attractor operating as shown by Fermann's [7]. The generated parabolic pulse has linear chirp and tends to have larger bandwidth, shorter pulses than pulses from dissipative soliton laser [49]. However, the gain bandwidth places a limit on the shortest pulse achievable from this type of laser by interrupting the self-similar propagation in the gain fiber, which eventually leads to wave breaking.

Recently, Chong et. al [4] reported a scheme to broaden the spectrum in a segment of highly nonlinear passive fiber after the gain based through passive self-similar pulse propagation, as described by Anderson in [6], The laser generates 20 fs pulses that were dechirped by a multiphoton intrapulse interference phase scan (MIIPS) device due to excessive nonlinear phase on the pulse accumulated in the high nonlinear fiber.

Another way to extend the self-similar propagation is to use dispersion de-

creasing fiber (DDF). Almost a decade ago, Hirooka and co-workers [5]demonstrated that through an appropriate transformation, a self-similar parabolic pulse solution can be supported by a DDF with an hyperbolic dispersion profile in the normal dispersion regime. Therefore, a DDF with an appropriate dispersion curve placed after the gain would allow for the continuation of self-similar evolution without the limitations of the gain bandwidth and excessive nonlinear phase accumulation. Although the generation of parabolic pulses from DDF through passive propagation have been reported [46], there has been no report of a fiber laser based on it. Whether the self-similar evolution can be extended in a laser through this mechanism, and, more importantly, whether the two local attractors can co-exist in the same cavity are interesting questions with major implications for short-pulse generation. There have been no reports of a fiber laser based on this concept.

Here we report numerical and experimental results of the first fiber laser with DDF to extended self-similar evolution within the cavity. This laser generates the shortest pulses from Yb- doped fiber oscillator to date, and these pulses can be dechirped to close to the transform limit with a grating pair only.

3.2.2 DDF Theory

It has been shown previously [5] that the nonlinear Schrodinger equation (NLSE) with uniform dispersion and gain can be transformed to one with decreasing dispersion and no gain.

$$\frac{\partial A}{\partial z} = \frac{g}{2}A - i\frac{\beta_2}{2}\frac{\partial^2 A}{\partial t^2} + i\gamma(|A|^2)A \tag{3.2}$$

where A is the slowly varying envelope of the pulse, g is the gain per length of the amplifier, β_2 is the constant dispersion of the fiber, γ is the nonlinear coefficient. With some substitutes:

$$\mu = A\sqrt{1+\Gamma z}\ ,\ \ \xi = \frac{\ln(z\Gamma+1)}{\Gamma} \tag{3.3}$$

$$\frac{\partial\mu}{\partial\xi} = \frac{\Gamma}{2}A - i\frac{\beta_{20}}{2}\frac{\partial^2\mu}{\partial t^2} + i\gamma(|\mu|^2)\mu \tag{3.4}$$

where the μ is the substitute of amplitude, ξ is the substitute of propagation distance, β_{20} is the initial dispersion at the beginning of the DDF, γ is the presuedo gain. And the dispersion curve should follow the relation of

$$\beta_2(z) = \frac{\beta_{20}}{1+\Gamma z} \tag{3.5}$$

The transformed equation also has an asymptotic solution of parabolic pulse

$$A(z,t) = \sqrt{A(z)}\{1-[\frac{t}{\tau(z)}^{(}1/2)\}exp[i\phi(z,t)], |t| \le \tau(z) \tag{3.6}$$

which will broaden in both spectral and temporal domain at power of $\frac{1}{3}$:

$$\Delta t \propto (1+\Gamma z)^{\frac{1}{3}}\ \ ,\ \ \Delta\lambda \propto (1+\Gamma z)^{\frac{1}{3}} \tag{3.7}$$

There are several features of this asymptotic solution worth noting. The most important one is that it is not restricted by the gain bandwidth. Although the growth rate of the spectral bandwidth is slower than the exponential rate in the amplifier case [7], the lack of fixed gain gives additional freedom in engineering the desired solution. In addition, the DDF solution also has a fixed chirp determined by the group velocity dispersion (GVD) of the fiber, similar to the case of amplifier.

$$\delta^2\omega = -\frac{3\beta_{20}}{\Gamma} \tag{3.8}$$

This allows the engineering of the pulse chirp but it also bring the question that whether the two local attractor could co- exist within the same cavity, especially when their solution are not fully identical.

3.2.3 Numerical Simulation

Numerical simulations were carried out to study the behavior of a laser with a DDF. More specific simulations with realistic fiber parameters were used to guide the design of the experiment. The simulated cavity consisted 4 fiber segments as shown in Fig.3.6: 30 cm SMF, 80 cm gain, 30 cm SMF, and various lengths of DDF. The DDF is initially 4.3 m with dispersion varying 4 to 74 fs^2/mm along that length. The exactly dispersion decreasing curves have been fitted with hyperbolic curve (γ=0.038/cm) and linear curve (γ=0.044/cm). Despite of the difference of two fitting, they both give similar results compared with experiment. For more controlled study to understand DDF function in the cavity, hyperbolic curve simulation is presented here.

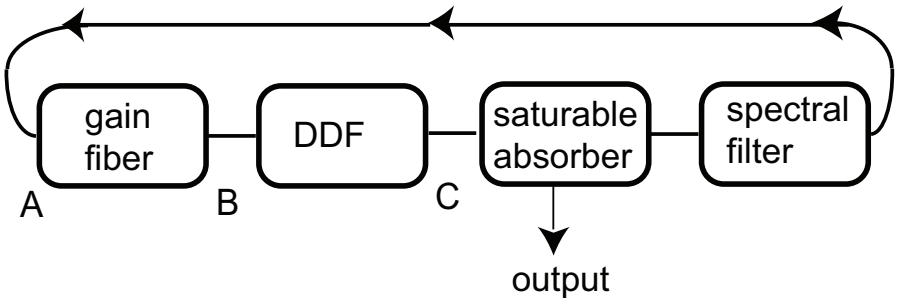

A narrow filter was used before the gain to promote amplifier similariton formation, as described in [3]. The DDF is placed after the gain with an assumed 30 % coupling ratio. An ideal saturable absorber with 100 % modulation depth is used to assist mode locking. Stable solutions were found with various

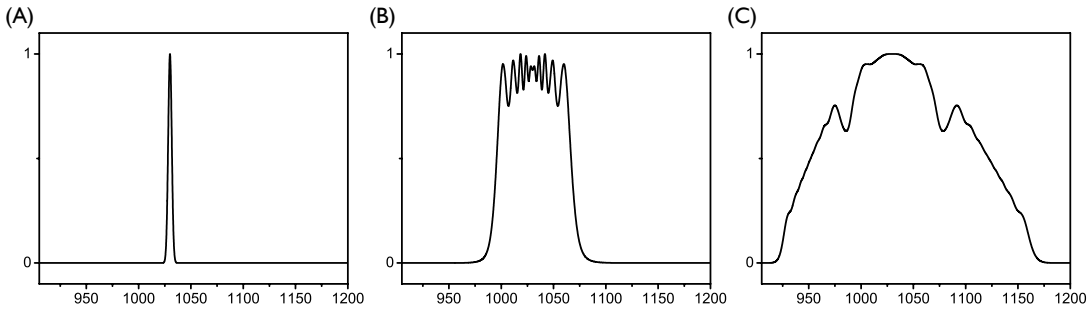

Figure 3.6: Schematic and Pulse spectrum at different location of the cavity.

DDF lengths and the trends agrees with the experiment result (Fig.3.7(a)). Simulations confirm that the chirp of the pulse is close to the theoretical fixed dispersion from a DDF (Fig.3.7(b)), the second attractor of the cavity, as predicted. n the simulations the nonlinearity of the DDF was assumed to be constant since

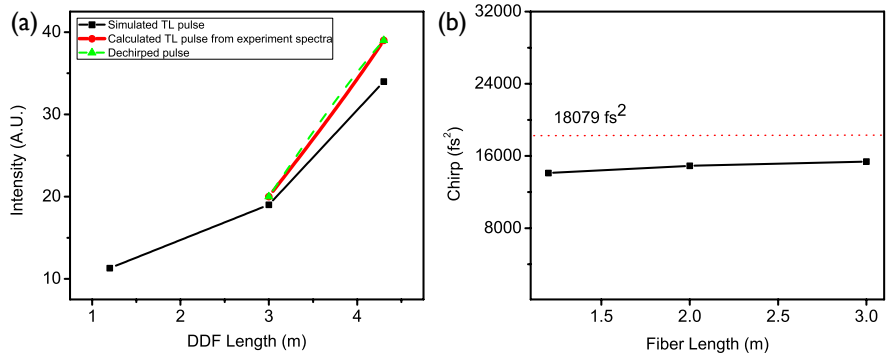

Figure 3.7: DDF cavity properties. (a).Broadest bandwidth generated with various length of DDF. (a)Simulation (black line) and experiment results (Red line: calculated transform limited pulse from spectra. Green Line: Dechirped pulse) with different length of DDF.(b)The amount of chirp for a cavity of fixed DDF initial dispersion β_{20} with various DDF length. Red dotted line is the calculated theoretical value of the constant chirp from DDF.

the variation of core size is small. The best performance is obtained with 1.2 m of DDF, for which the initial dispersion value matches the gain fiber, 23 fs^2 /mm,

Pulses as short as 14 fs are produced in the simulation. Fig.3.8 shows the simulated mode locked results. The pulse has linear chirp and 2 nJ of energy. The transform limited pulse from the spectrum is 14 fs (inset).

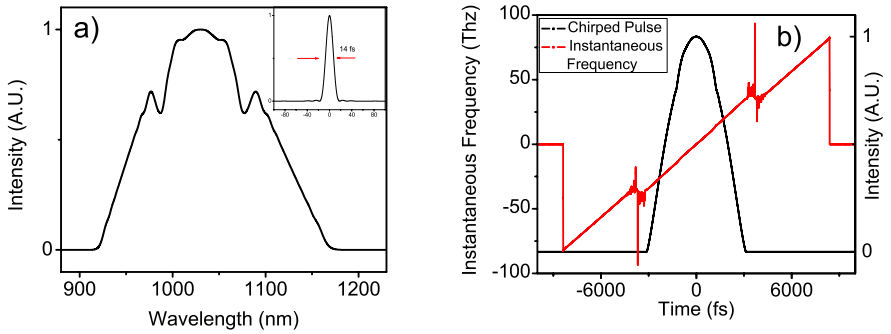

Figure 3.8: Mode locked Simulation Result. (a):Simulated spectrum and its transform limited pulse (inset). (b): Chirped pulse and its spontaneous frequency.

Fig.3.9 show that the spectrum and pulse broaden inside the gain and, after a disruption in a short segment of ordinary fiber,continuously broadening within DDF. This indicates that the parabolic pulse is a nonlinear attractor in both the gain and DDF segments.

3.2.4 Experiment

The experimental design is shown in Fig. 3.10. A 300 lines/mm grating and a collimator form a 4 nm Gaussian filter. 80 cm of Yb-gain fiber is followed by a DDF with free space coupling. The DDF was fabricated at Bath University by tapering a photonic crystal fiber with core size 3.2 μm under computer control during the fiber draw. The change in core size is minimal. Nonlinear polarization evolution (NPE) is employed as the saturable absorber. Mode locking is achieved by adjusting the wave plates. The sampler plates are used to monitor

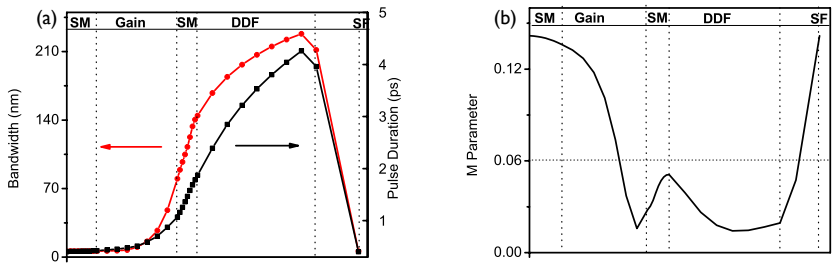

Figure 3.9: Pulse evolution inside the cavity. Left: pulse duration and bandwidth evolution. Right:Pulse shape evolution compared with a parabolic shape with same peak power and energy. $M^2 = \int[|u| - |p|]^2 dt / \int |u|^4 dt$, where u is the pulse being evaluated and p is a parabola with the same energy and peak power.M=0.14 represents Gaussian shape. M<=0.06 represents parabolic shape

the spectral evolution. The length of the DDF has been cut from 4.3 m to 3 m, and the mode locking results have agreed well with the trends from simulation. The spectrum directly after the DDF matches simulation results. However, filtering induced by NPE tends to create structure on the output spectrum since the combined spectrum from PBS and grating reflection always makes the spectrum right after DDF, which is seen in Fig.3.11(d).

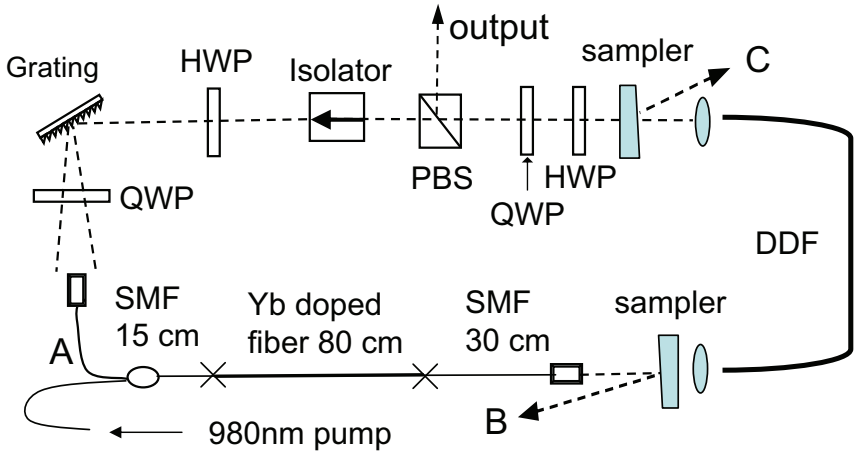

Figure 3.10: Experiment Setup. PBS: polarization beam splitter.

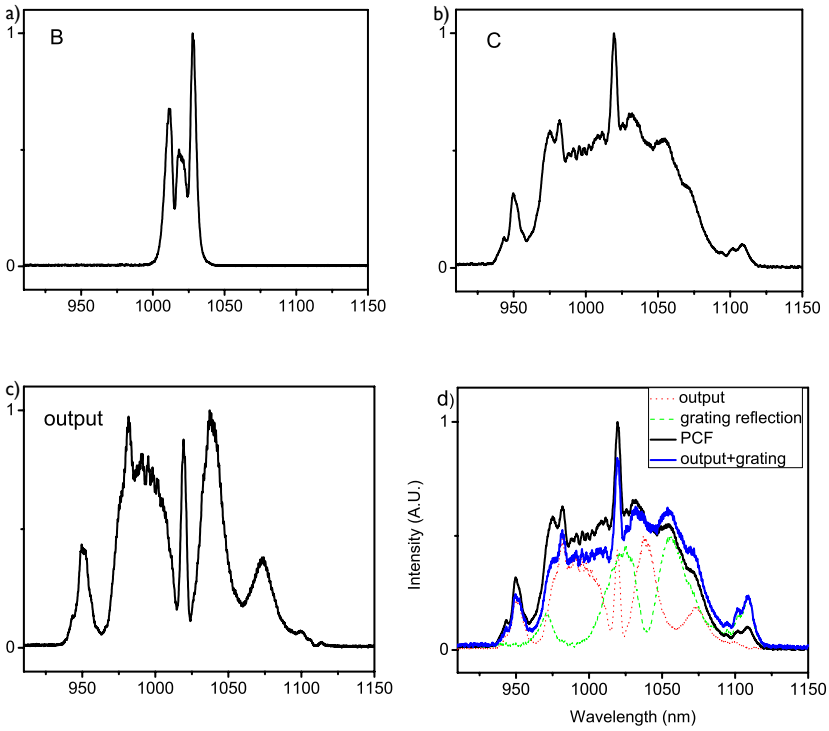

Figure 3.11: Generic spectrum evolution at different location of the cavity.(a) Spectrum from gain.(b) Spectrum from PCF.(c) Spectrum from PBS. (d) Comparison of spectrum from PCF and combined spectrum from PBS and grating reflection.

The shortest pulse from this cavity is shown in Fig.3.12 The output pulses are 1 nJ. The dechirped pulses have a full-width at half-maximum of 20 fs, but exhibit secondary structure.

The total amount of chirp on top of the pulse referred from dechirping stage is 11,300 fs^2. One significant feature of this laser is that the chirped pulse could be dechirped to close to transform limit with a pair of grating, which is a practical improvement over the work described in [4]. The dechirped pulse is 20 fs (6 cycles). The structure of the autocorrelation is due to small amount of uncompensated TOD (600 fs^3) as from calculation. The continuation of the experiment is hindered by self lasing from DDF after a few times burning of the fiber.

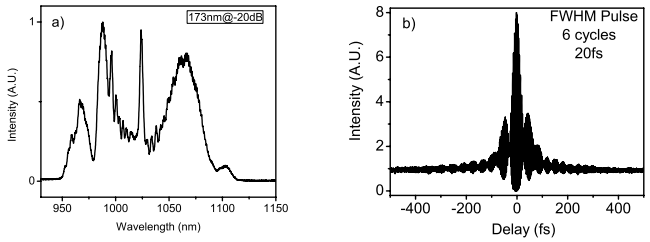

Figure 3.12: Experiment Results. (a): Mode locked spectrum. (b): Dechirped autocorrelation(black line) and calculated transform limited autocorrelation with 600 fs^2 TOD (Redline).

3.2.5 Conclusion

We have demonstrated the use of DDF in a laser cavity to continue the self-similar pulse evolution after the gain fiber. The demonstration of structured 6-cycle pulses shows the promise of this approach. Optimization of the performance based on simulation results and through controlling higher order dispersion in the de-chirping state is expected to produce shorter and cleaner pulses.

3.3 Sub 10-fs pulse generation from DDF

3.3.1 DDF laser features

The success of initial numerical and experimental study of DDF shows that it is a promising way of designing the laser cavity with DDF. The performance of the DDF is limited by loss fundamentally if the DDF curve is designed to control the nonlinear phase well. Fig.3.13 shows the trend of laser performance with increasing the coupling ratio between hi1060 fiber and DDF. The pulse bandwidth and energy increases with reducing the loss of the cavity.

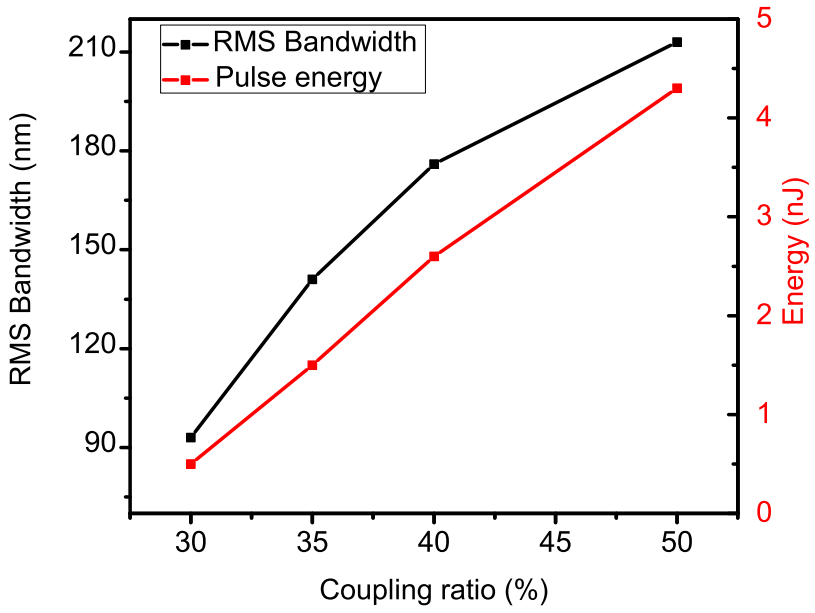

Figure 3.13: Impact of loss on DDF lasers.

When the loss of the cavity is fixed, increasing the pump power will increase the pulse bandwidth and energy as is the case for other types of fiber lasers. However, all other fiber lasers will start to experience wave-breaking or lose mode locking at some pump level. The DDF cavity does not lose mode locking but instead starts to show saturation with increasing pump power as is shown in Fig.3.14. The mode locked pulses show increasing bandwidth and energy with pump power up to a point but reach a saturation state at a certain pump power and keep that state despite the big increase in pump power. This is also the feature of the parabolic pulse propagation in the amplifier case.

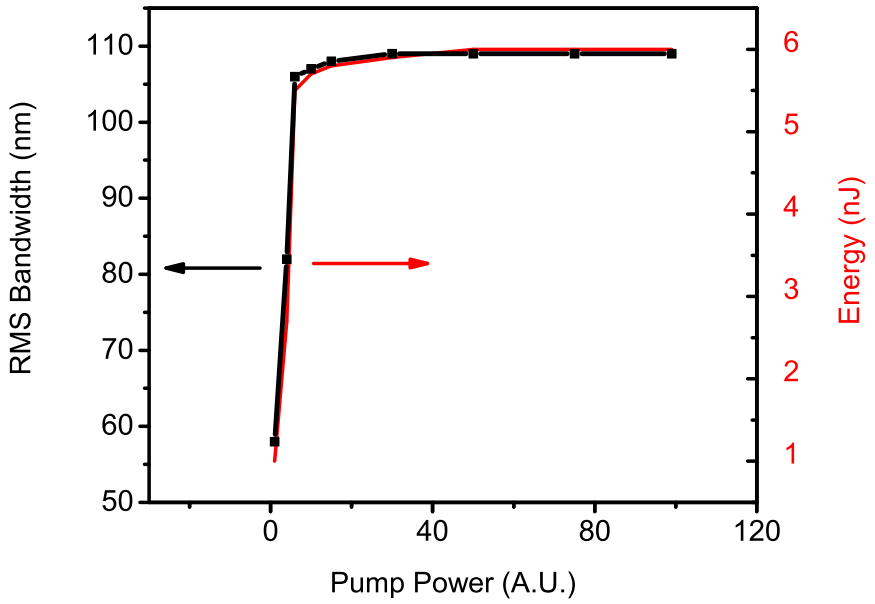

Figure 3.14: Pump power impact on pulse bandwidth and energy.

3.3.2 Octive Span DDF Laser

When the DDF curve is well designed to match the other fibers in the oscillator to avoid wave-breaking , it can control the nonlinear phase so well that an octave spanning spectrum was mode locked in simulation as shown in Fig.3.15. Higher-order dispersion from the fiber (mainly TOD) does not affect the laser performance much since the net cavity dispersion is large. The DDF used in the cavity has a very small initial dispersion value of 3.7 fs^2 and τ=0.038/cm. The length of the DDF is 2 m. The output of the laser cavity is 80%. Octave spanning spectra can be mode locked when the coupling ratio between SMF and DDF is >= 50%. The laser generated 1ps pulses with 4 nJ of energy.

Although the trustworthiness of the simulation needs to be tested for such pulses that clearly violate the slowly varying envelope approximation, it is the

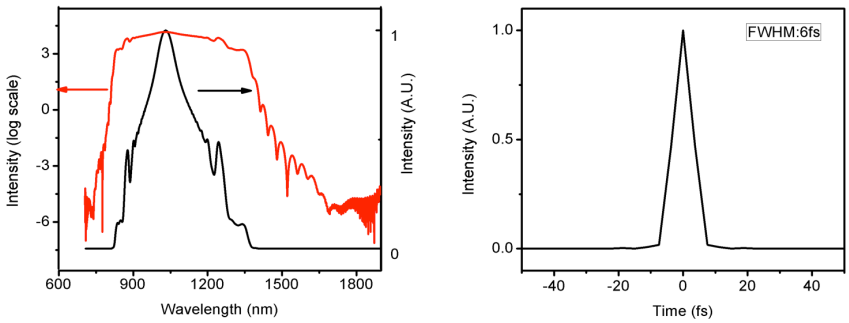

Figure 3.15: DDF Simulation Results. (a): Mode locked spectrum in both linear(black) and log (red) scale. (b): Calculated transform limited autocorrelation.

first time in simulation to see an octave span spectrum from fiber oscillator. It clearly shows that there is potential for fiber laser to reach the performance of the shortest pulses generated from a Ti-sapphire. It is so far the only proposed method to achieve less than 10 fs pulses from a fiber oscillator. Further, the method of achieving such a short pulse is unique to a fiber cavity since solid state lasers typically do not have such a large amount of dispersion. The degrees of freedom in designing the DDF need to be explored as the next step, but this certainly opens a door to a pulse propagation regime that even solid state laser have not reached, such as 10 fs pulses at low repetition rates. This approach could potentially be used to generate frequency combs directly from a fiber oscillator which may have better noise properties than those made from amplified pulses.

3.3.3 Limitations of DDF Laser Cavity

There are two known limitations to DDF laser cavities. One is the free space coupling between SMF(HI1060 fiber) and the DDF. This is not only a limit to the

laser performance, but also brings mechanical instability to the cavity, which will prevent it from being user friendly. This problem can be eventually solved by advanced splicing or a fiber combiner with high transmission efficiency.

The other limitation is from the core size of DDF. Currently the known method of making a DDF for the fiber laser cavity is to taper the fiber to vary the wave-guide dispersion in order to change the total dispersion(material dispersion+waveguide dispersion). This method only works for small core fibers where the contribution of the waveguide dispersion is significant. The maximum simulated pulse energy from this type of laser made of standard SMF is only a few nJ.

3.3.4 Future work for DDF lasers

1. Systematic study design of cavity, such as curve of DDF fiber and length of gain fiber.
2. Cascade DDFs. Try another DDF after the first one.
3. Spectrum compression to reduce the loss and reach even broader spectrum.

3.4 Scaling with CCC fiber

3.4.1 Introduction

To really achieve high energy in a short pulse fiber laser with peak power more than 1 MW, managing nonlinearity has to be done. A standard way to accomplish this in fiber lasers is to use large core fiber. Although the DDF laser has more controlled phase than in a other fiber lasers and can generate extremely short pulses, DDF is not available for the large core size fiber and therefore the output energy is limited to a few nJ due to the small core size as discussed in section above. For applications needing high power, scaling the fiber core size with the extended self-similar propagation with a highly nonlinear fiber design was introduced in Section 3.1. This concept has been studied and initial results shows it is a promising way to generate pulses with 1 MW peak power and sub 40 fs durations.

3.4.2 Numerical Study

Lasers using 30 um core CCC fiber and other single mode fibers have been explored to see the potential of the scaling performance. Fig. 3.16 shows a table of simulated mode locked pulse performance. High energy pulses with peak powers more than 1MW can be generally reached by different combinations.

Simulation results converge to peak powers as high as 10 MW (22 fs, 303 nJ). However, we only consider the cases where the spectrum after the gain is around 40 nm to be modest. It is possible that the excellent performance seen

	hi1060		LMA8	LMA10	LMA25	
	4nm filter				60%	40%
2m	22fs,22nJ	11fs,9nJ	22fs,19nJ	22fs,16nJ	52fs,141nJ	38fs,71nJ
3m	11fs,11nJ	11fs,10nJ	24fs,16nJ	25fs,19nJ	40fs,78nJ	38fs,78nJ

Figure 3.16: Simulated mode locked results with different combination of 2.7 m CCC fiber and other single mode fiber.

in simulation could one day happen in experiment once we understand how the gain spectrum shape affects mode locking. Fig. 3.17 shows the simulated CCC cavity with the highest pulse peak power. It has 2 m of CCC gain fiber and 2 m of LMA25 fiber after the gain. A 60% coupling ratio between the two is assumed considering their relatively big core sizes. The chirped pulse has energy of 141 nJ, and the spectrum corresponds to a 40 fs pulse. The peak power of the pulse is 4.5 MW.

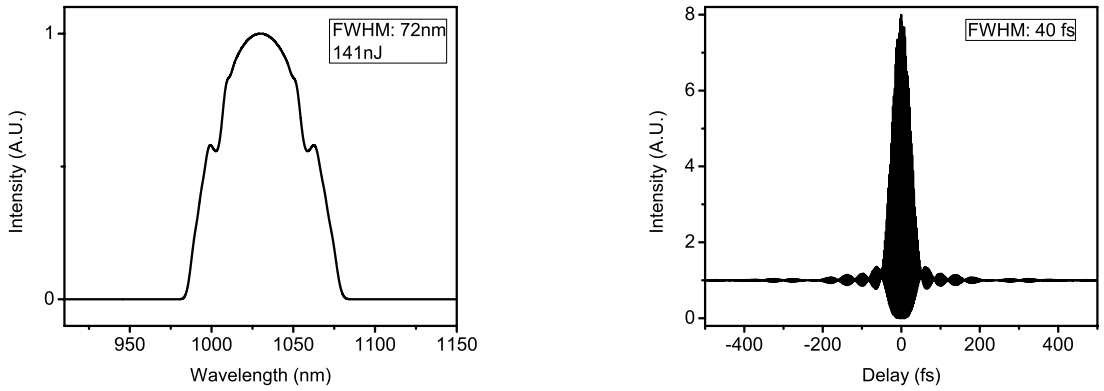

Figure 3.17: Simulated mode locked results with the highest peak power. (a) Mode locked spectrum. (b) Calculated zero phase transform limited autocorrelation.

3.4.3 Initial Experiment

Considering the limited pump power and the construction of the laser cavity, initial experiments are carried out with 2 of CCC fiber(β_2=20 fs^2/mm, A_{eff}=346 μm^2) spliced to 3 m HI1060 (β_2=23 fs^2/mm, A_{eff}=31 μm^2) fiber with a mode filed adapter. The 600/mm grating is used as a 3 nm Gaussian filter. CCC fiber is free space aligned with an f=19 cm focal lens. The laser has a low slope efficiency of about 15% but can mode locked easily. The spectral bandwidth increases as the pump power goes up. However, beyond 15 W of pump power, the laser starts to have burning issue. The highest energy from this laser is 9 nJ with the spectrum shown in Fig. 3.18. The calculated zero phase transform limited pulse is 60 fs. By scaling of the bandwidth and energy, this laser can achieve 30 fs pulses with 18 nJ if the full pump power could be used without burning.

3.5 Conclusion

In this chapter, two methods for short pulse generation from fiber laser cavities based on the self-similar nonlinear attractor in the gain segment were introduced. These two methods show the promise of a fiber laser that can directly compare to a solid laser laser in the combination of short pulse with high energy. Future work needs to be done to improve the performance, and more systematic study is needed to better understand the limitations and potential of these lasers.

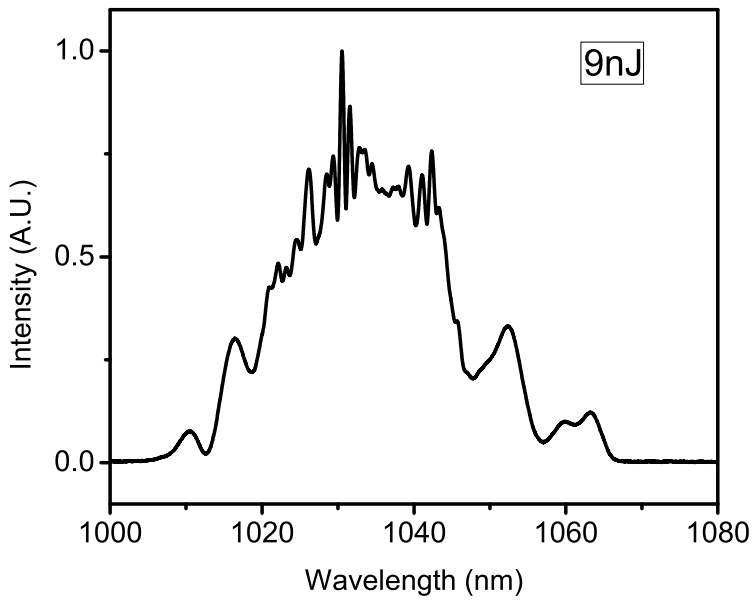

Figure 3.18: Simulated mode locked results with different combination of 2.7 m CCC fiber and other single mode fiber.

CHAPTER 4

TM FIBER LASER

4.1 Introduction

The wavelength of thulium-based lasers has several useful features that have drawn a lot of attention over the past five years. First, it is at eye-safe range (>1.4 μm) for applications where human exposure is not avoidable. Second, it is very efficient for superficial ablation of tissue, with minimal coagulation depth in air or water. This makes thulium lasers attractive for laser-based surgery. The other applications of 2 um Tm lasers include but are not limited to high efficiency THz generation, 3-5 micron super-continuum generation, time-resolved molecular spectroscopy, optical frequency combs, Light Detection and Ranging (LIDAR), free space communication, higher-order harmonic generation, MID-IR frequency conversion, air pollution monitoring, and high efficiency soft X-ray generation.

The recent progress in Tm-doped fiber has enabled the wide study of Tm fiber lasers. Tm-doped gain has a relative broad spectrum of around 200 nm and a large mode field diameter, which are useful for both short pulse duration and high energy pulse generation.

In this chapter, Tm fiber lasers from anomalous dispersion to large normal dispersion will be introduced. The performance of these lasers is limited by technical issues such as fiber cooling and lossy components.

4.2 Tm Soliton Laser

As a first step in exploring a new wavelength regime, we first make a soliton laser. Khanh Kieu made a CNT mode locked soliton laser [50]. However, to fully access the mode locking states and explore the physics, a Tm fiber laser with NPE as the saturable absorber is built with an isolator centered at 1950 nm and mode locked. The schematic of the laser setup is shown in Fig.4.1.

4.2.1 Experiment

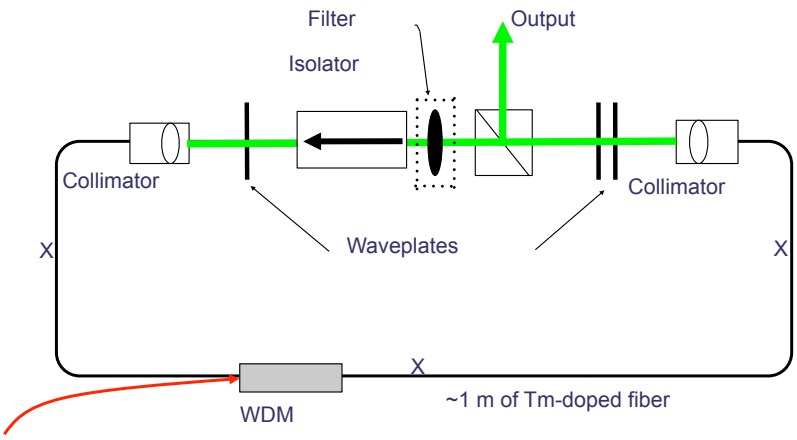

Figure 4.1: Experimental Setup. The Filter was added later.

The laser consists of 1m of Tm-doped fiber and 1 m of SMF28 from the collimator and WDM fiber pigtails. The WDM is a 980/1550 nm coupler with 1550 nm as the pump end and 980 nm as the signal end. The laser is pumped by a 1 W Er laser at 1569 nm. The CW efficiency of the Tm laser is about 20%. The cavity has net dispersion of -0.18 ps^2 with the fiber parameters listed below:
SMF28: β_2=-60 fs^2/mm, A_{eff}= 93μm^2

Tm512: β_2=-120 fs^2/mm, A_{eff}= 78μm^2

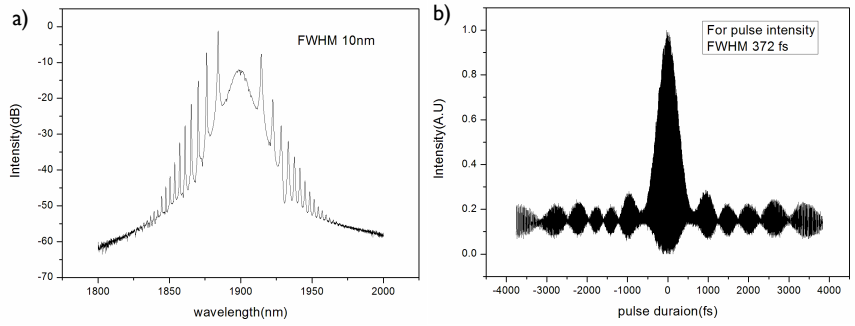

Figure 4.2: Experimental Result. (a):Mode locked spectrum.(b) Autocorrelation

The mode locked results from this laser are shown in Fig. 4.2. The mode locking was hard to find and existed only within a narrow range of NPE settings. The FWHM of the spectrum is 10 *nm*, with a pulse width of about 400 fs. The pulse is slightly chirped. The spectrum has less side band compared with Khanh's laser [50] could be due to more efficient pumping at 1570 *nm* with a tunable pump source and a more matched isolator to the gain spectrum, which results in better efficiency in the cavity. The single pulsing output power is 25-30 *mW*. From the sideband positions and the dispersion of SMF at 2*um* as measured by other groups, we calculated the dispersion of the gain fiber to be -120ps^2/km if the dispersion of SMF is as assumed to be -60ps^2/km. WIth these dispersion parameters, the pulse duration and energy also match the soliton area theorem. The laser can also be mode-locked at other center wavelength such as 1950 *nm* due to the broad bandwidth of gain spectrum.

4.2.2 Tm Soliton Laser with a Filter

Due to the strong sidebands and difficulty in mode-locking seen in the result in the previous section, we add a filter to the cavity. From the past experience, we expect the filter to stabilize the pulse also cut off the sidebands. The previous result for a soliton laser around 2 um with a 10T birefriengent filter before shows spectral distortions [51]. We tried the filter they used but could not get mode-locking. After change to a 15T filter, the mode-locking gets much easier and the spectrum exhibits fewer sidebands than the one presented in Fig. 5.2. The filter is added after the output and before the isolator, as shown is Fig. 4.1 (the dotted line). The slope efficiency of the cavity is around 25%. The tunability for some mode is large, and the center wavelength of the spectrum can be continuously tuned for 40 nm. The pulse usually mode locked with a center wavelength around 1900 nm, although it can mode-lock around 1950 nm too due to the sinusoid transmission curve of the quartz filter having a bandwidth of about 50 nm. The mode locked pulse in Fig. 4.3 is verified to be single pulse by our fast detector and autocorrelator. Various mode locking states exist in this cavity. By adjusting the waveplates continuously and slowly, mode locked spectrum with weaker sidebands and higher energy can be found. The highest output power for single pulsing is 30 mw, which occurs with a pump power of 400 mW. This corresponds to 0.42 nJ of pulse energy at the 71.4 MHZ reputation rate. The mode-locking is not self-starting. However, by continuously turning up the pump power to 1 W, the laser would mode-lock with multi-pulsing and then become single pulsing again when the power is turned down without any adjustment of the wave-plates.

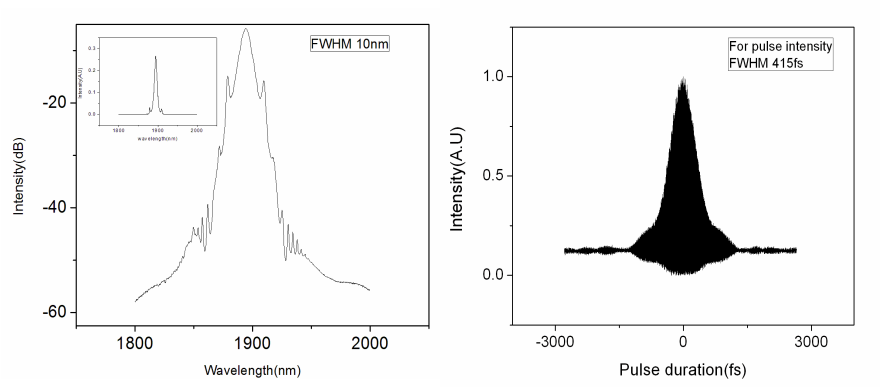

Figure 4.3: Experimental Result of Tm soliton laser With a filter. Left: Mode locked spectrum. Right: Autocorrelation.

4.2.3 Dispersion Managed (DM) Tm Soliton

Next, a DM soliton Tm fiber laser is designed with dispersion compensation from a high NA fiber (UHNA7). This fiber has a large waveguide dispersion which compensate the well-known negative material dispersion at this wavelength regime. The parameters of UHNA7 fiber at 2 μm are : β_2=90 fs^2/mm and A_{eff}= 11 μm^2. Due to the small mode filed diameter, UHNA7 fiber is placed before the gain fiber to avoid the excessive nonlinearity. In addition, the splicing loss between UHNA7 fiber and other fibers in the cavity is not negligible, so it is better for the cavity efficiency to have the extra loss before the gain also. The 15T filter was kept inside the cavity based on the experience with soliton lasers.

A piece of 1.5 normal dispersion fiber for 2um was added inside the cavity for the next step as shown in Fig.4.4. The net cavity dispersion is -0.045 ps^2. The cavity has a CW efficiency of 25%. Fig.4.5 shows the mode locked experiment result. The FWHM of the spectrum is 15 nm. The pulse has 46 mW of average power at a 46 MHz reputation rate, which gives 1nJ of pulse energy. The autocorrelation indicates that the pulse is slightly chirped. If we still assume a $Sech^2$

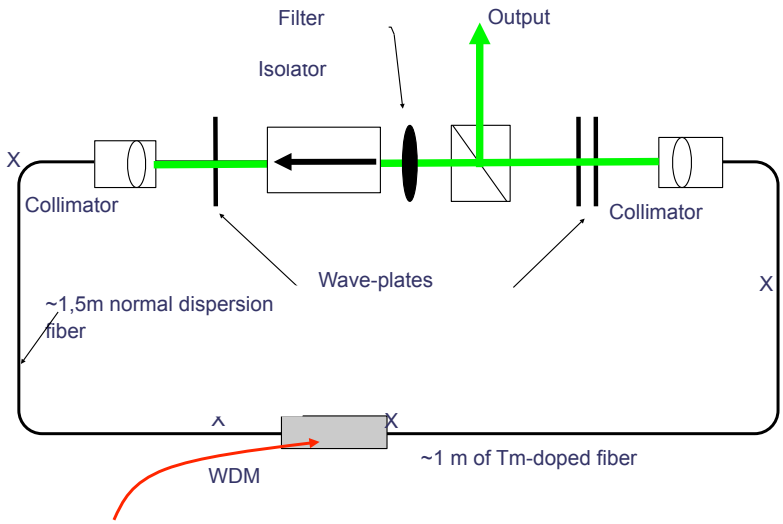

Figure 4.4: DM Tm Soliton Experimental Setup with a 15T filter.

conversion, for the autocorrelation, the pulse duration is about 340 fs. This is one of the best Tm fiber oscillators so far in terms of pulse duration and energy.

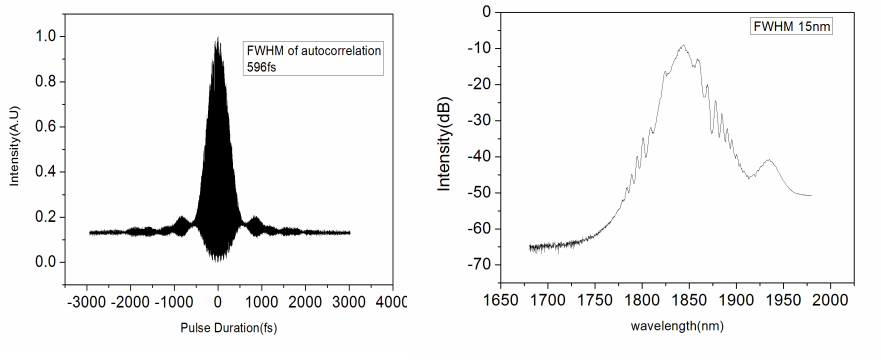

Figure 4.5: Experimental Result. (a):Mode locked spectrum.(b) Autocorrelation

The influence of the filter can be observed as a sinusoid modulation for the whole gain bandwidth. The mode locked spectrum can also be centered at various wavelengths.

4.3 Large Normal Dispersion Tm Laser

To make the Tm laser have net normal dispersion, more UHNA7 fiber was added before the gain for dispersion compensation. However, no mode locking was found initially. We suspect this is caused by low saturable absorption from the NPE due to low pump powers. We solve this by adding passive fibers both before and after gain to lower the repetition rate for higher pulse energy and for more accumulated nonlinear phase to drive the NPE saturable absorption. Due to the splicing loss between UHNA7 and other fibers in the cavity, SMF28 was added after the gain and more UHNA7 was added before the gain. This section demonstrated a mode-locked Tm fiber laser at large normal dispersion, generating 0.4 nJ pules that dechirp to 470 fs with a pair of gratings. The dispersion inside the cavity is controlled in an all fiber format.

4.3.1 Introduction

Tm fiber lasers are currently attracting attention for use as short-pulse infrared sources. The broad (200 nm) and relatively smooth fluorescence spectrum of Tm-doped fiber has the potential to generate very short pulses and could be the basis of frequency combs. 2 um lasers can also be used as pumps to generate supercontinuum between 3-5 μm [52]. To date, mode-locked Tm fiber lasers have included soliton lasers with nonlinear polarization evolution (NPE) [51], SESAM [53] or carbon nanotubes [50] acting as saturable absorbers. Engelbrecht et al. [54] used a grating−telescope combination inside the cavity to create a dispersion map in a double-clad Tm-doped fiber, and stretched-pulse operation was observed with excellent performance. Normal-dispersion cavities with

pulse-shaping based on spectral filtering produce the highest-energy pulses for a given mode area [21]. Tm fiber lasers should be capable of performance levels comparable to Yb fiber lasers. Here we present initial results from a mode-locked Tm laser in the large normal dispersion regime, with a spectral filter assisting the pulse evolution. In a cavity with all-fiber dispersion control, pulses with 0.4 nJ energy and dechirping down to 470 fs are obtained. Factors that limit the performance will be discussed.

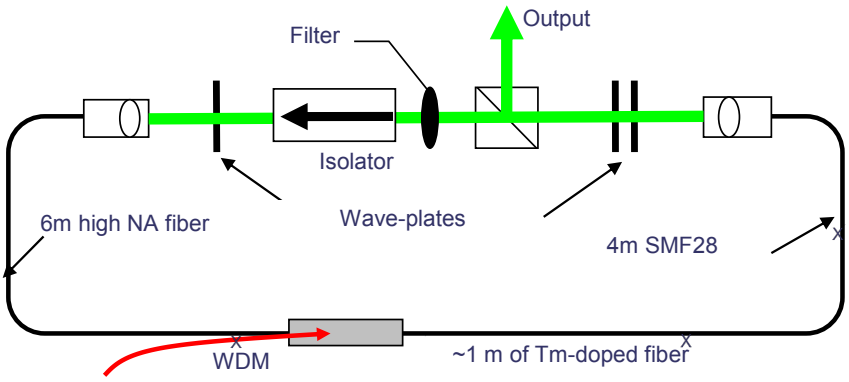

Figure 4.6: Experimental Setup

4.3.2 Experiment

Standard fibers have large anomalous dispersion at 2 um, so it is a challenge to design a fiber cavity with a dispersion map or large normal dispersion. In prior work, a grating pair and telescope were used to introduce normal dispersion [54]. To date, there is no report of accomplishing this with fiber, which would have the obvious advantages of integration, efficiency, and compactness. We employ a high-NA fiber with a very small core and correspondingly large waveguide dispersion to introduce normal dispersion at 2 μm. Our goal

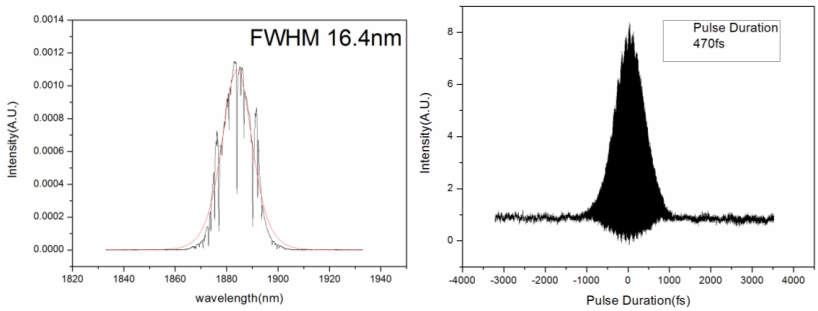

Figure 4.7: Experimental Results.Left: Mode locked spectrum in log scale. Right: Autocorrelation

is to construct a dissipative-soliton laser. Before this, we also mode-locked a stretched-pulse laser in the same fiber format with 1.5m of high-NA fiber. The laser (Fig. 4.6.) consists of 6 m of the high-NA single-mode fiber (SMF) with large normal dispersion (90 fs^2/mm at 2 μm), 1 m of Tm-doped gain fiber with anomalous dispersion, and another 4 m of SMF-28 with anomalous dispersion. The cavity has the large net normal dispersion of 0.24 ps^2 . The total length of the cavity is 11 m, chosen for a relatively low repetition rate (17 MHz), which reduces the pump power requirement. The Tm fiber is pumped by 1 W from an Er fiber laser-amplifier system. The normal-dispersion fiber also introduces large nonlinearity through its small core, and the mismatch of core sizes leads to significant loss when it is spliced to the gain fiber. For these reasons, we avoid the use of the normal-dispersion fiber after the gain segment. A birefringence filter with 22 nm bandwidth is used, and wave plates and beam splitter implement NPE as the saturable absorber. A 28 nm bandwidth filter was first tried but the laser could not mode- lock.

The long segment of normal-dispersion fiber before the gain is intended to facilitate chirped-pulse evolution inside the cavity. After the output coupling,

the pulse energy is low, so in the normal-dispersion fiber the pulse accumulates linear phase and broadens in time. In the anomalous-dispersion segments (gain and SMF-28), the pulse will compress. However, the large normal dispersion cannot be fully compensated, and the filter shapes the pulse in both time and frequency, and takes it back to the initial state. The SMF after the gain provides nonlinearity for NPE.

Self-starting and single-pulsing mode-locking is observed (Fig. 4.7) with appropriate adjustment of the wave plates. The spectrum is about 16 nm wide. The pulse could be dechirped by passing it through anomalous dispersion to 470 fs, which is near the transform limit. The energy before dechirping is 0.35 nJ, which is lower than expected from normal dispersion lasers. Double pulsing is observed when pump power is increased. Numerical simulations match the pulse evolution inside the cavity. We suspect that the long stretch of anomalous-dispersion fiber after the gain may limit the pulse energy. The pulse will tend to a soliton solution, which has low energy, and will be distorted or will break up at higher energy. We believe that by optimizing the fiber length there or even replacing it with a normal-dispersion fiber that better matches the gain fiber, higher pulse energy and broader spectra will be possible.

4.3.3 Discussion

The simulated results are actually very close to the experiment results as shown in Fig.4.8. This cavity has the feature of passive self similar laser with large normal dispersion before the gain where the parabolic pulse tries to form (Fig.4.8(c). There is not much spectral breathing in this cavity.

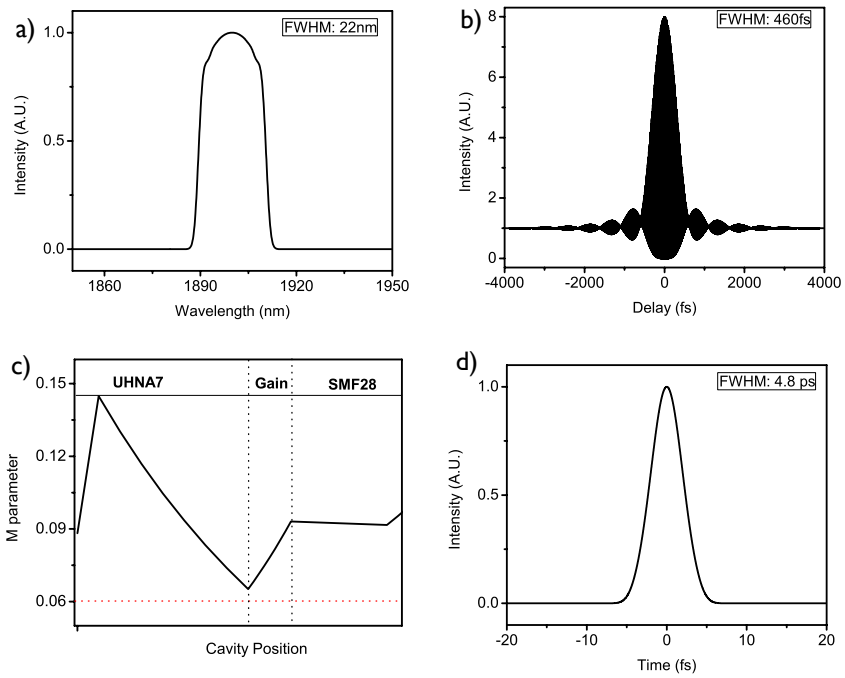

Figure 4.8: Simulation Results. (a) Mode locked spectrum. (b) Autocorrelation of calculated zero phase pulse. (c) M parameter evolution within the cavity. (d) Chirped pulse

This cavity is not optimized for either the pulse energy or the pulse duration, but rather it is designed to operate with available pump power and components. But it offers a way to mode lock at large normal dispersion, which helps to understand the reason for difficult mode locking of Tm laser and verify our pulse propagation understanding in this new wavelength regime. There are several directions to optimize this cavity:

1. Reduce the fiber after the gain.

2.Replace some of the SMF28 after the gain with some Er-doped fiber that has small normal dispersion at 2 um to avoid soliton formation.

3. Use a narrower bandwidth filter since the current filter is broader than the mode locked spectrum. A narrower filter may increase spectral breathing and

allow more nonlinear phase accumulation.

4.3.4 Conclusion

In summary, successful mode-locking of a Tm fiber laser with fiber-based large normal dispersion was achieved. The initial performance is modest, but better results can be expected with further optimization of the cavity, fiber matching and filtering to fully take advantage of the potential of all-normal dispersion mode-locking.

4.4 Conclusion and Future Direction

Currently, there has been no published Tm fiber oscillator with good performance. The handling of Tm fiber laser is trickier than Yb and Er lasers. The cavities with NPE based saturable absorbers are also harder to mode lock than lasers at other wavelengths. One of the reasons is that the life time of Thulium is short at room temperature and the laser has a tendency to Q-switch. The accumulated common knowledge says to cool the fiber for better performance. In addition, higher pump power will be needed in order to operate in normal dispersion regime with health pulse energy.

Based on experience at other wavelengths, we expect to achieve higher performance fiber laser is when operating in the normal dispersion regime, particularly with normal dispersion gain fiber. The current method uses UHNA7 fiber or other high NA to provide normal dispersion. However, those fibers have both high propagation loss and bending loss at 2 μm. Further techniques need

to be developed for providing normal dispersion at 2 μm in order to achieve better performance. Recently, Advalue Photonics developed normal dispersion silicate fiber (both doped and passive) for 2 μm. It opens the opportunity for both dissipative soliton and amplifier similariton lasers at 2 μm. An example of a dissipative soliton simulation based on the normal dispersion silicate fiber is shown below. The laser cavity consists of 50 cm of passive fiber, 1 m of Tm fiber and anther 50 cm of passive fiber. The dispersion of the fiber is 120 fs^2/mm. The mode field area A_{eff}=100μm^2. Filters from 10 nm to 50 nm are used for mode locking. For the 50 nm filter (which is equivalent to a 15 nm filter at 1 um), the laser can generate 1 μJ and 112 fs pulses directly from oscillators (assuming that self-focusing is not a problem and that sufficient pump is available) as shown in figure below. The spectrum has the signature batman ears and an 80 nm bandwidth. Future increases in energy are possible in simulation but will be subject to self-focusing in experiment.

This is truly an encouraging result to be follow up in experiment. It also shows the importance of Tm fiber lasers in terms of performance. With all the technical problem to be solved, Tm fiber lasers could be strong candidates for many applications requiring high energy and short pulses.

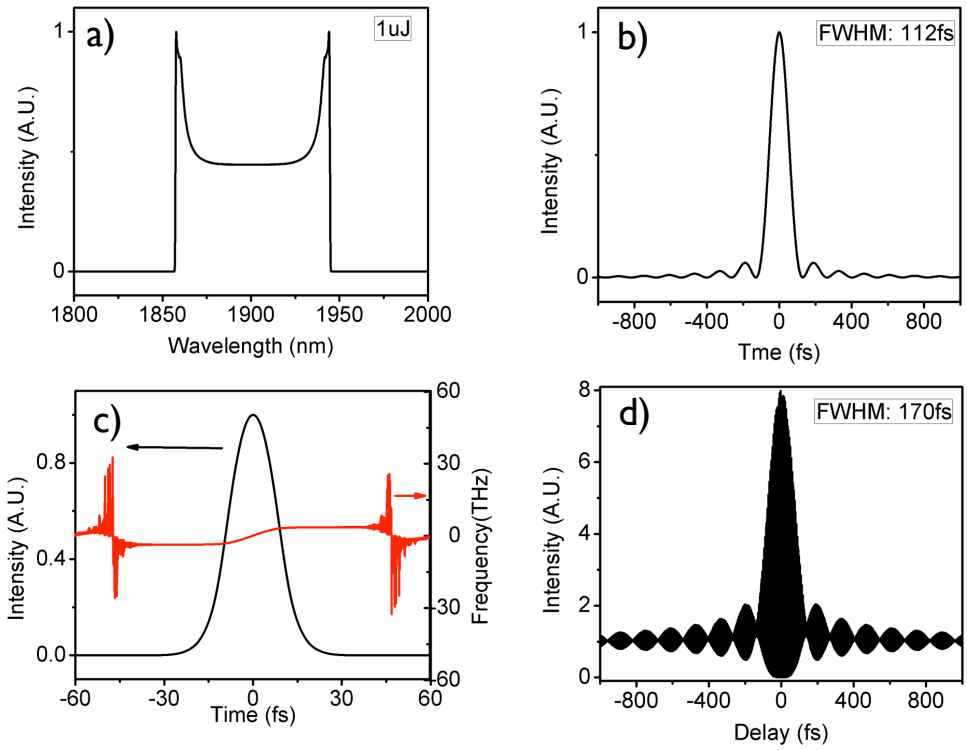

Figure 4.9: Simulation Results of a cavity made from Advalue Photonics normal dispersion fiber.(a) Mode locked spectrum.(b) Calculated transform limited pulse. (d) Chirped pulse and its spontaneous frequency. (d) Autocorrelation of transform limited pulse

CHAPTER 5

FUTURE DIRECTIONS

In this chapter, future work based on current study will be presented including spectral compression to replace narrow filter for amplifier similariton laser and more importantly for extended self similar lasers, as well as new mode locking lasers near zero dispersion regimes and hybrid evolution of dissipative soliton laser and amplifier similariton laser at large normal dispersion regimes. The discussion is to understand the nonlinear wave propagation for mode locked lasers and to explore the potential fiber lasers with higher performance.

5.1 Spectral Compression within Gain Attractor

One of the potential concerns with using a narrow filter inside the laser cavity is the large loss introduced by the narrow filter when strong spectral breathing exist as in the case of amplifier similariton and more significantly its extended cavity. Spectral compression is a way to avoid the loss while support large spectral breathing within the cavity [28]. The schematic of the idea is shown in Fig. 5.1. They have demonstrated in simulation that by replacing narrow filter with this type of spectral compression, the laser can get mode locked and moreover the desired self similar evolution could happen within the gain segment.

For amplifier similariton laser itself, the ultimate pulse performance is set by gain fiber parameters (dispersion, nonlinearity and bandwidth) as discussed before. Reducing the loss may help with the laser noise but is not necessarily leading to higher performance. However, for extended self similar cavities,

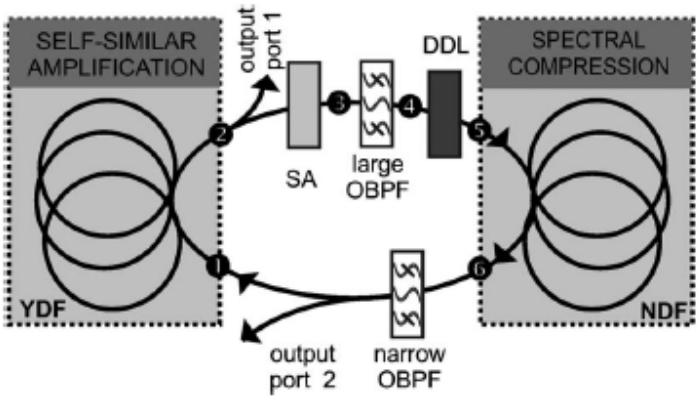

Figure 5.1: Spectral compression within a laser schematic

the loss is one of the limiting factors of the laser performance when the pulse bandwidth gets much broader than the gain bandwidth. By introducing spectral compression, this type of lasers are expected to reach higher performance. Initial simulation was carried out and confirmed the assumption. Fig. 5.2 shows the schematic of a simulated oscillator.

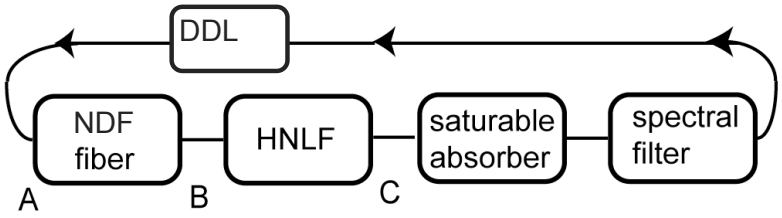

Figure 5.2: Schematic of an extended self similar laser with spectral compression

Simulation was converged and the mode locked results are shown in Fig. 5.3. Despite of the dramatic changes in pulse shape (Fig. 5.3 (a)), the pulse is able to reach and keep parabola within the gain segment. The pulse duration evolution has some features of DM soliton due to the dispersion map (Fig. 5.3 (b)). The

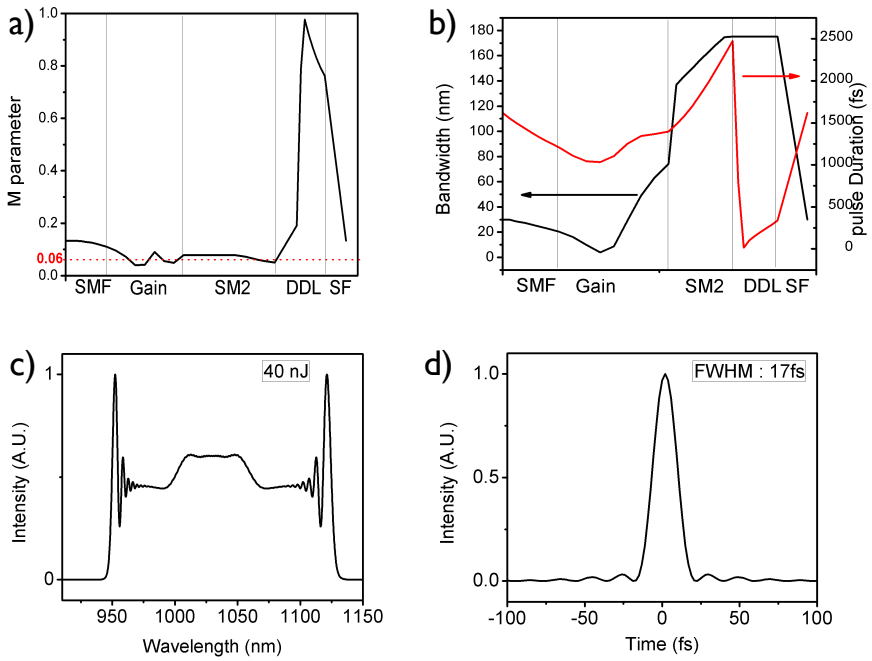

Figure 5.3: (a) Pulse shape evolution inside the cavity. (b) Pulse bandwidth and duration evolution. (c) Mode locked spectrum. (d) Calculated transform limited pulse.

mode locked spectrum has close to 200 nm bandwidth with 40 nJ pulse energy. The pulse is no longer parabola but rather a Gaussian (Fig. 5.3 (a)). The sharp edges of the spectrum along with high pulse energy is similar to the dissipative soliton laser. The spectrum corresponds to a calculated transform limited 17 fs pulse (Fig. 5.3 (d)).

This laser has features of several different evolutions and pulse shaping mechanisms including: self similar evolution inside the gain, dispersion managed soliton for pulse duration evolution and dissipative soliton for the spectral feature and pulse energy. The performance of the laser also has the advantages of all those evolutions in terms of high energy and short pulse duration. To better understand this laser, we first review different mode locking mechanism in term of their dispersion regimes as shown in Fig. 5.4.

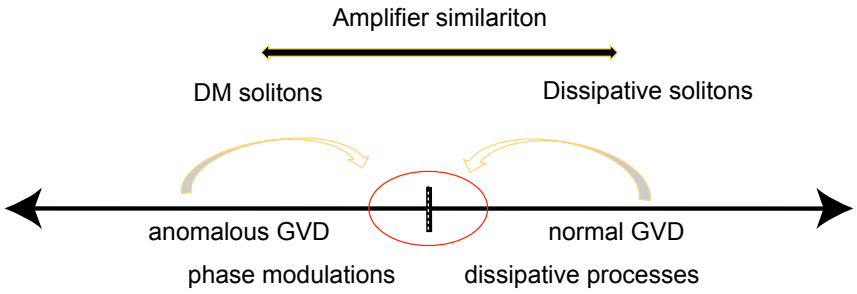

Figure 5.4: Dispersion regimes of mode locking lasers

DM soliton works at anomalous dispersion regimes and dissipative soliton works at normal dispersion regimes. However, both have higher performance towards near zero dispersion. Amplifier similariton could work at any net dispersion regimes with the proper initial condition before the gain since it is a local solution of the gain attractor. The near zero dispersion regimes are where all kinds of evolution could happen. The problem at this regime is that traditionally lasers start to become hard to mode lock because the effective gain for CW will be bigger than it is for pulses. Because of the dispersion map for the spectral compression, the laser in Fig. 5.3 is unavoidable working around near zero dispersion. However, when the right initial condition is prepared, the gain attractor can act as additional force for pulse shaping and to help pulses win over CW. If our understanding is correct, this type of performance with short pulse and high energy could happen even without the extra fiber after the gain for the extended self similar evolution since the DM soliton element could allow very short pulses.

Based on the assumption, the extra piece of fiber after the gain is taken away from the oscillator as is shown in Fig. 5.5 (a). The mode locked pulse has 80 nJ with spectrum broad enough to support a 14 fs transform limited pulse (Fig. 5.5 (b)(c)).

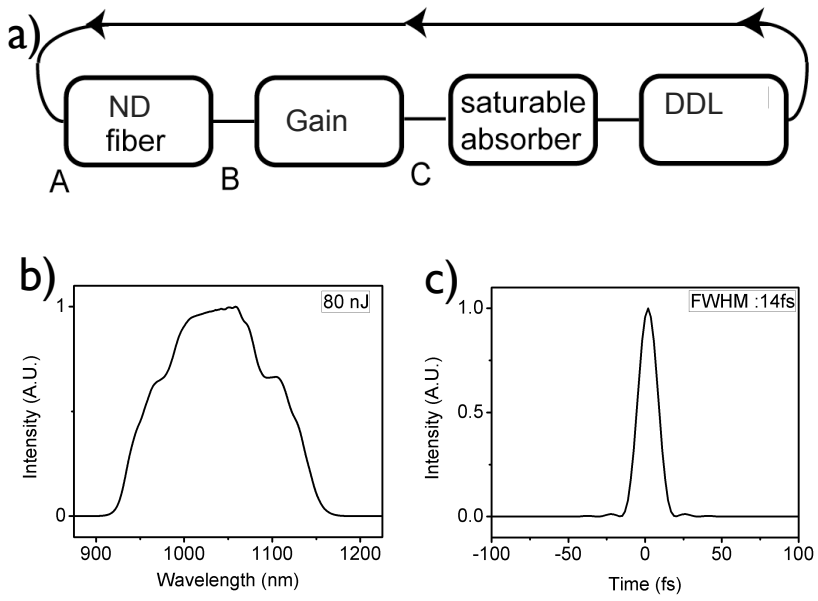

Figure 5.5: (a) Schematic of self similar laser with spectral compression near zero GVD. (b) Mode locked spectrum. (c) Calculated transform limited pulse

5.2 Experimental Design of a Laser with Spectral Compression

Systematic experiment work needs to be done to further confirm the assumption and simulation results in section 5.1. However, some initial experiment work by Lan and coworks [17]has shown that this type of laser could work. They used GTI to introduce large anomalous dispersion after output to have spectral compression at the beginning of the gain segment. The experimental cavity design is shown in Fig. 5.6 below. A 30 nm bandpass filter is placed before GTI to assist mode locking and bring some dissipation to the system.

The gain segment of this cavity is only 23 cm and it is not ideal to form an amplifier similariton. The pulse did not evolve into parabola indeed [17]. Simulation with 173 cm gain fiber for the same cavity design was carried out to see how the spectral compression works for amplifier similariton. The simulated

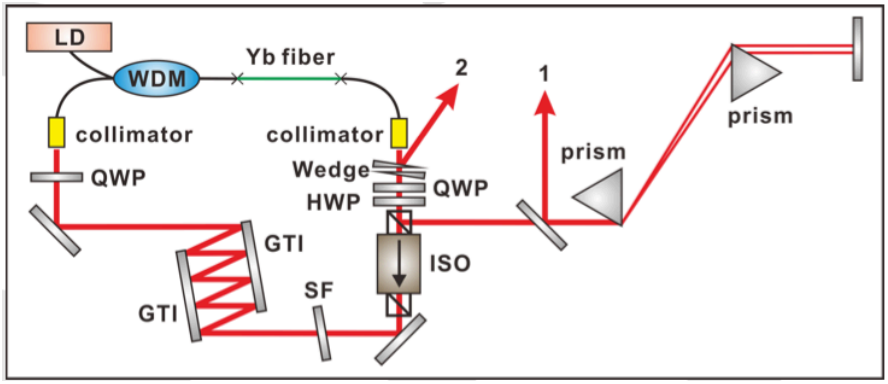

Figure 5.6: Experiment Setup

result is shown in Fig. 5.7 (a)(b). More GTI bounces were used in order to have enough spectral compression. For control, a standard amplifier similariton laser with a narrow filter (same bandwidth as the spectral compression effect) was shown in Fig. 5.3 (c)(d). Although the two cavities have different net dispersion (one is 523 fs^2 and the other is 51520 fs^2), their mode locked spectra shapes and performance are similar. So we can conclude that spectral compression from this type of experimental cavity design can be used for amplifier similariton lasers.

5.3 "Hybrid" Evolution

5.3.1 DM Soliton and Amplifier Similariton

When the spectral compression is introduced to the cavity, it enforces the cavity to work at near zero dispersion regime. At this regime, many mode locking solutions could exist including DM soliton, passive self similar laser, DM dissipative soliton(Renninger's thesis) and DM amplifier similariton. Each solution

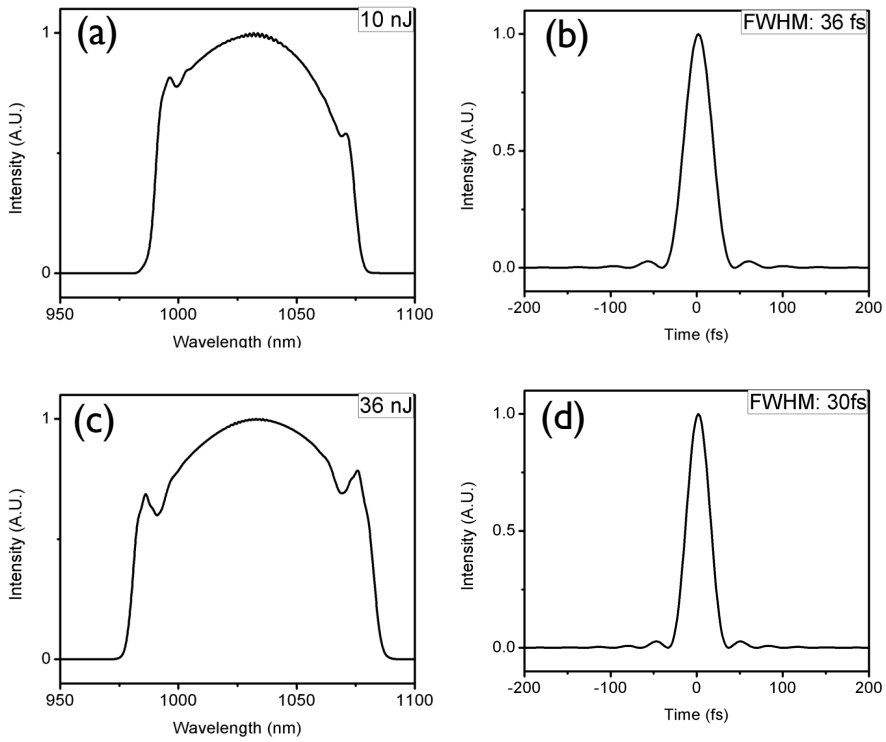

Figure 5.7: Simulation Results of amplifier similariton laser with spectral compression. (a) Spectrum compression laser mode locked spectrum (b) Spectrum compression laser calculated transform limited pulse. (c) Narrow filter cavity mode locked spectrum. (d) Narrow filter cavity calculated transform limited pulse.

can be identified by its featured evolution. However, when the cavity condition satisfy more than one evolutions, mode locking could still happen in a "hybrid" evolution with features of different evolutions. For example, Lan reported a laser (Fig. 5.6) which has both features of DM soliton with two times temporal breathing and of amplifier similariton with large spectral breathing and attracting towards parabola pulse [17]. The performance of the laser is better than both the DM soliton and amplifier similariton laser along in terms of pulse duration and energy. Stating from there, initial systematic study of this cavity was carried out to understand this new evolution.

First controlled study in simulation is to vary the bounces of GTI. Fig. 5.8 shows the impact of amount of bounces(anomalous dispersion) on the equivalent spectral compression filtering and unavoidably the net cavity dispersion. It

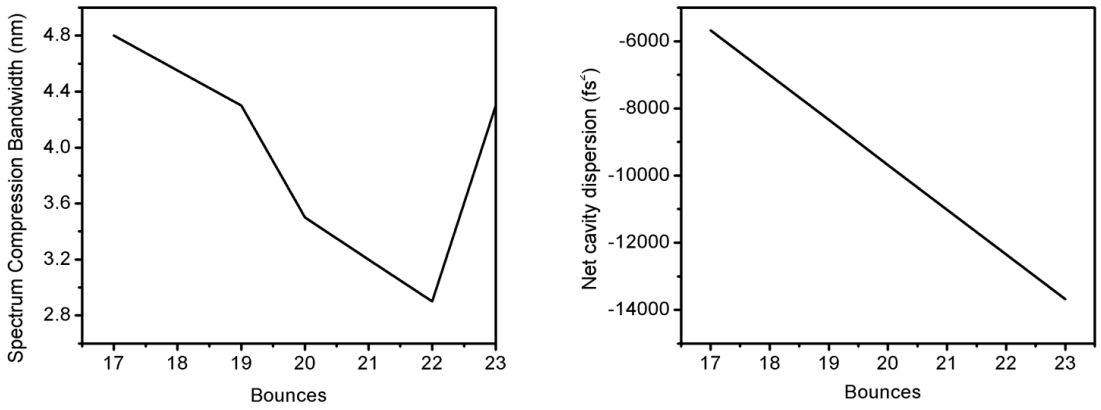

Figure 5.8: Controlled spectral compression study by changing the GTI bounces. Left: spectral compression bandwidth v.s total bounces. Right: Net cavity dispersion v.s. total bounces

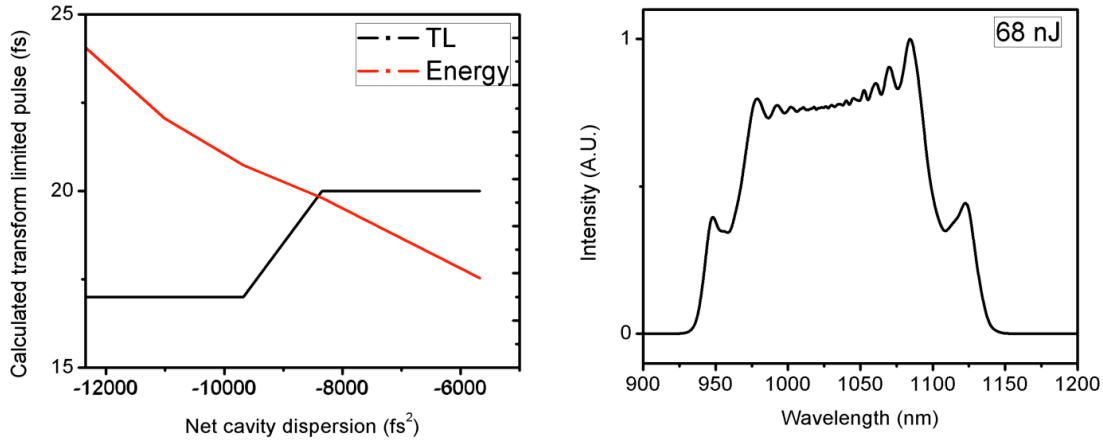

Figure 5.9: Laser performance with controlled net cavity dispersion

shows that within certain range(between 17 and 22 bounces which corresponds to -5000 -13000 fs^2), the more anomalous dispersion from GTI, the narrower the spectral compression bandwidth is. Too much anomalous dispersion will

impact the strength of spectral compression. So we focus the evolution trend between 17 to 22 bounces (between -12000 fs^2 and -5000 fs^2). Fig. 5.9 shows the pulse performance trend in this regime. It shows that the more the net anomalous dispersion, which also corresponds to narrower the spectral compression bandwidth, the higher pulse energy and shorter pulse duration can be achieved.

Fig. 5.10 shows the mode locked results from the cavity with 22 bounces. The laser can support 17 fs pulses with 68 nJ pulse energy. Consider a factor of 10 of pulse energy difference from simulation to experiment as was the case in Fig. 5.6, the result is still directly comparable with solid state lasers. The pulse

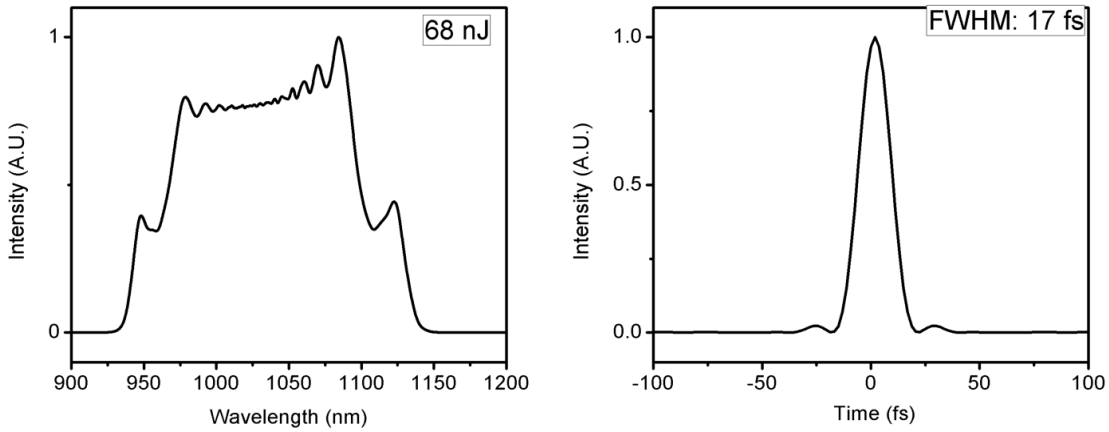

Figure 5.10: Simulated mode locked results from the cavity with 22 GTI bounces. Left: mode locked spectrum. Right: Calculated transform limited pulse.

evolution of this cavity is shown in Fig. 5.11. The pulse has temporal breathing twice as in the case of DM soliton but the two breathings have different amplitude. Large spectral breathing with a ratio of 45 is supported by the cavity which is a feature of amplifier similariton. The pulse shape from output is very close to parabola(Fig. 5.12)

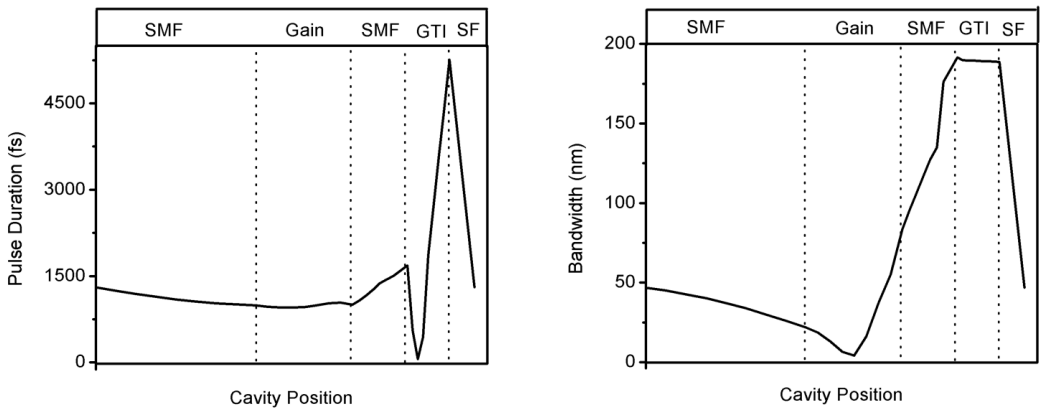

Figure 5.11: Pulse evolution from the cavity with 22 GTI bounces. Left: pulse duration evolution. Right: spectrum bandwidth evolution.

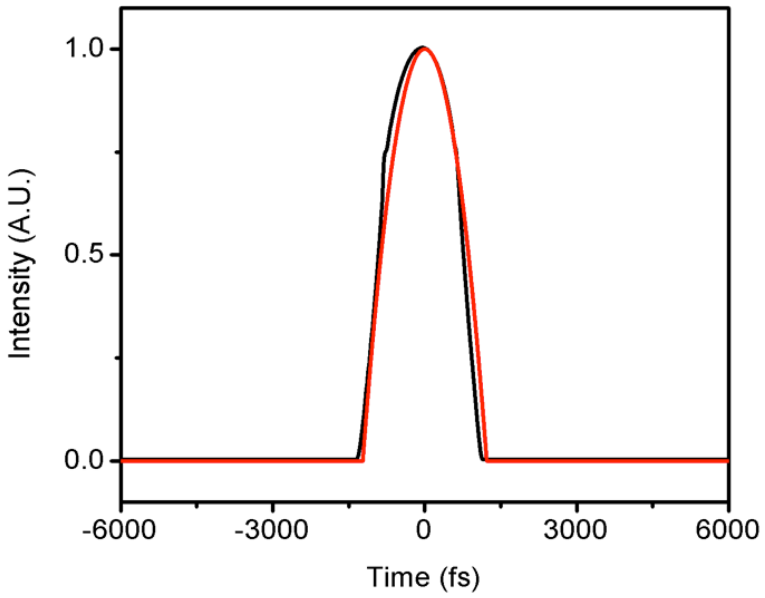

Figure 5.12: Simulated output pulse (black line) and a parabola pulse with the same peak power and energy(red line)

5.3.2 Dissipative Soliton and Amplifier Similariton

At large normal dispersion regimes, dissipative soliton and amplifier similariton both exist. The differences of those two include the bandwidth of the filter

used, the ratio of spectral breathing and pulse shape. Some laser has features of two evolutions. The dissipative soliton Er laser in Section 3.2 has some features of amplifier similariton in its spectrum. Indeed, simulation shows that the pulse was drawn to parabola by the end (Fig. 5.13) of gain segment, although it has very little spectra breathing (a factor of 2) compared with routine amplifier similariton case.

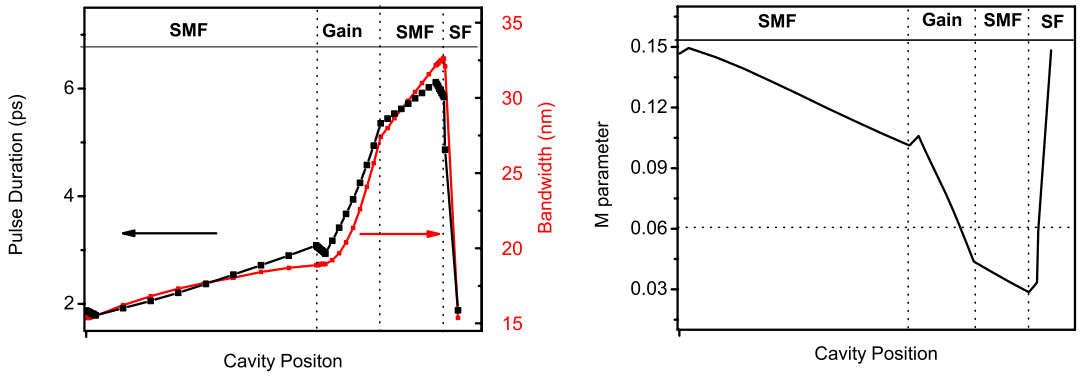

Figure 5.13: Simulation of pulse evolution of Er dissipative soliton laser from Section 3.2. Left: bandwidth and pulse duration evolution. Right: M parameter evolution to compare with parabolic pulse. M≤0.06 indicates parabolic pulse.

5.4 Conclusion

It is interesting and important to know that when there are more than one solutions or even nonlinear attractors inside the cavity, how the pulse formation and evolution are impacted. The examples in section 5.1 and 5.3 show that they can work together to assist pulse shaping and give better performance than previous known evolutions along. One regime particularly interesting is the near zero dispersion regime, where the performance of the laser is hard to

predict and also where the maximum numbers of attractors could exist (DM soliton, dissipative soliton and amplifier similariton). Better understanding of how those combined evolution can stabilize the cavity and form the pulse will bring new insights to nonlinear pulse propagation of mode locked lasers and generate pulses with higher performance.

BIBLIOGRAPHY

[1] Andy Chong, Joel Buckley, Will Renninger, and Frank Wise. All-normal-dispersion femtosecond fiber laser. *Opt. Express*, 14(21):10095–10100, 2006.

[2] Bulent Oktem, Coskun Ulgudur, and F Omer Ilday. Soliton-similariton fibre laser. *Nat Photon*, 4(5):307–311, May 2010.

[3] Frank W. Renninger, William H. and Chong, Andy and Wise. Self-similar pulse evolution in an all-normal-dispersion laserv. *Phys. Rev. A*, 82(2):021805, 2010.

[4] A Chong, H Liu, B Nie, B G Bale, S Wabnitz, W H Renninger, M Dantus, and F W Wise. Pulse generation without gain-bandwidth limitation in a laser with self-similar evolution. *Opt. Express*, 20(13):14213–14220, June 2012.

[5] Toshihiko Hirooka and Masataka Nakazawa. Parabolic pulse generation by use of a dispersion-decreasing fiber with normal group-velocity dispersion. *Opt. Lett.*, 29(5):498–500, March 2004.

[6] D Anderson, M Desaix, M Karlsson, M Lisak, and M L Quiroga-Teixeiro. Wave-breaking-free pulses in nonlinear-optical fibers. *J. Opt. Soc. Am. B*, 10(7):1185–1190, July 1993.

[7] M E Fermann, V I Kruglov, B C Thomsen, J M Dudley, and J D Harvey. Self-Similar Propagation and Amplification of Parabolic Pulses in Optical Fibers. *Phys. Rev. Lett.*, 84(26):6010–6013, June 2000.

[8] D E Spence, P N Kean, and W Sibbett. 60-fsec pulse generation from a self-mode-locked Ti:sapphire laser. *Opt. Lett.*, 16(1):42–44, January 1991.

[9] K Tamura, E P Ippen, H A Haus, and L E Nelson. 77-fs pulse generation from a stretched-pulse mode-locked all-fiber ring laser. *Optics Letters*, 18(13):1080, 1993.

[10] Nikolai B Chichkov, Christian Hapke, Jörg Neumann, Dietmar Kracht, Dieter Wandt, and Uwe Morgner. Pulse duration and energy scaling of femtosecond all-normal dispersion fiber oscillators. *Opt. Express*, 20(4):3844–3852, February 2012.

[11] H A Haus and M Nakazawa. Theory of the fiber Raman soliton laser. *J. Opt. Soc. Am. B*, 4(5):652–660, May 1987.

[12] J. D. Kruglov, V. I. and M\'echin, D. and Harvey. All-fiber ring Raman laser generating parabolic pulses. *Phys. Rev. A*, 81(2):023815, 2010.

[13] Khanh Kieu and Masud Mansuripur. Femtosecond laser pulse generation with a fiber taper embedded in carbon nanotube/polymer composite. *Opt. Lett.*, 32(15):2242–2244, August 2007.

[14] N J Doran and David Wood. Nonlinear-optical loop mirror. *Opt. Lett.*, 13(1):56–58, January 1988.

[15] L M Zhao, A C Bartnik, Q Q Tai, and F W Wise. Generation of 8 nJ pulses from a dissipative-soliton fiber laser with a nonlinear optical loop mirror. *Opt. Lett.*, 38(11):1942–1944, June 2013.

[16] M.E. Hofer, M. and Ober, M.H. and Haberl, F. and Fermann. Characterization of ultrashort pulse formation in passively mode-locked fiber lasers. *Quantum Electronics, IEEE Journal of*, 28(3):720–728, 1992.

[17] Yang Lan, Youjian Song, Minglie Hu, Bowen Liu, Lu Chai, and Chingyue Wang. Enhanced spectral breathing for sub-25 fs pulse generation in a Yb-fiber laser. *Optics letters*, 38(8):1292–4, 2013.

[18] Andy Chong, William H Renninger, and Frank W Wise. All-normal-dispersion femtosecond fiber laser with pulse energy above 20nJ. *Opt. Lett.*, 32(16):2408–2410, August 2007.

[19] L M Zhao, D Y Tang, and J Wu. Gain-guided soliton in a positive group-dispersion fiber laser. *Opt. Lett.*, 31(12):1788–1790, June 2006.

[20] L M Zhao, D Y Tang, T H Cheng, and C Lu. Gain-guided solitons in dispersion-managed fiber lasers with large net cavity dispersion. *Opt. Lett.*, 31(20):2957–2959, October 2006.

[21] Andy Chong, William H Renninger, and Frank W Wise. Properties of normal-dispersion femtosecond fiber lasers. *J. Opt. Soc. Am. B*, 25(2):140–148, 2008.

[22] F O Ilday, J R Buckley, W G Clark, and F W Wise. Self-Similar Evolution of Parabolic Pulses in a Laser. *Physical Review Letters*, 92:4, 2004.

[23] William H Renninger, Andy Chong, and Frank W Wise. Amplifier similaritons in a dispersion-mapped fiber laser \[Invited\]. *Opt. Express*, 19(23):22496–22501, 2011.

[24] Ding Ma, Yue Cai, Chun Zhou, Weijian Zong, Lingling Chen, and Zhigang Zhang. 37.4 fs pulse generation in an Er:fiber laser at a 225 MHz repetition rate. *Opt. Lett.*, 35(17):2858–2860, 2010.

[25] Andy Chong, William H Renninger, and Frank W Wise. Route to the minimum pulse duration in normal-dispersion fiber lasers. *Opt. Lett.*, 33(22):2638–2640, November 2008.

[26] Nikolai B Chichkov, Katharina Hausmann, Dieter Wandt, Uwe Morgner, Jörg Neumann, and Dietmar Kracht. 50 Fs Pulses From an All-Normal Dispersion Erbium Fiber Oscillator. *Optics Letters*, 35(18):3081–3083, 2010.

[27] Claude Aguergaray, David Méchin, Vladimir Kruglov, and John D Harvey. Experimental realization of a Mode-locked parabolic Raman fiber oscillator. *Opt. Express*, 18(8):8680–8687, 2010.

[28] Sonia Boscolo, Sergei K Turitsyn, and Christophe Finot. Amplifier similariton fiber laser with nonlinear spectral compression. *Opt. Lett.*, 37(21):4531–4533, 2012.

[29] Stefan Rausch, Thomas Binhammer, Anne Harth, Jungwon Kim, Richard Ell, Franz X Kärtner, and Uwe Morgner. Controlled waveforms on the single-cycle scale from a femtosecond oscillator. *Opt. Express*, 16(13):9739–9745, June 2008.

[30] H A Haus, J G Fujimoto, and E P Ippen. Structures for additive pulse mode locking. *J. Opt. Soc. Am. B*, 8(10):2068–2076, October 1991.

[31] Ferenc Spielmann, Christian and Curley, P.F. and Brabec, T. and Krausz. Ultrabroadband femtosecond lasers. *Quantum Electronics, IEEE Journal of*, 30(4):1100–1114, 1994.

[32] Gunther Krauss, Sebastian Lohss, Tobias Hanke, Alexander Sell, Stefan Eggert, Rupert Huber, and Alfred Leitenstorfer. Synthesis of a single cycle of light with compact erbium-doped fibre technology. *Nat Photon*, 4(1):33–36, January 2010.

[33] Peng Xi, Yair Andegeko, Lindsay R Weisel, Vadim V Lozovoy, and Mar-

cos Dantus. Greater signal, increased depth, and less photobleaching in two-photon microscopy with 10 fs pulses. *Optics Communications*, 281(7):1841–1849, 2008.

[34] D.C. Paschotta, R. and Nilsson, J. and Tropper, A.C. and Hanna. Ytterbium-doped fiber amplifiers. *Quantum Electronics, IEEE Journal of*, 33(7):1049–1056, 1997.

[35] F.W. Ding, E. and Lefrancois, S. and Kutz, J.N. and Wise. Scaling fiber lasers to large mode area: an investigation of passive mode-locking using a multi-mode fiber. *Quantum Electronics, IEEE Journal of*, 47(5):597–606, 2011.

[36] J R Buckley, S W Clark, and F W Wise. Generation of ten-cycle pulses from an ytterbium fiber laser with cubic phase compensation. *Opt. Lett.*, 31(9):1340–1342, May 2006.

[37] Xiangyu Zhou, Dai Yoshitomi, Yohei Kobayashi, and Kenji Torizuka. Generation of 28-fs pulses from a mode-locked ytterbium fiber oscillator. *Opt. Express*, 16(10):7055–7059, May 2008.

[38] Peter Adel and C Fallnich. High-power ultra-broadband mode-locked Yb3+-fiber laser with 118 nm bandwidth. *Opt. Express*, 10(14):622–627, July 2002.

[39] L M Zhao, D Y Tang, T H Cheng, H Y Tam, and C Lu. 120 nm bandwidth noise-like pulse generation in an erbium-doped fiber laser. *Optics Communications*, 281(1):157–161, 2008.

[40] Brandon G Bale and Stefan Wabnitz. Strong spectral filtering for a mode-locked similariton fiber laser. *Opt. Lett.*, 35(14):2466–2468, July 2010.

[41] A C Peacock, R J Kruhlak, J D Harvey, and J M Dudley. Solitary pulse propagation in high gain optical fiber amplifiers with normal group velocity dispersion. *Optics Communications*, 206(13):171–177, 2002.

[42] Yves Coello, Vadim V Lozovoy, Tissa C Gunaratne, Bingwei Xu, Ian Borukhovich, Chien-hung Tseng, Thomas Weinacht, and Marcos Dantus. Interference without an interferometer: a different approach to measuring, compressing, and shaping ultrashort laser pulses. *J. Opt. Soc. Am. B*, 25(6):A140—-A150, June 2008.

[43] Ilyas Saytashev, Bai Nie, Andy Chong, Hui Liu, Sergey Arkhipov, Frank W

Wise, and Marcos Dantus. Multiphoton imaging with sub-30 fs Yb fiber laser, 2012.

[44] Michelle Y Sander, Jonathan Birge, Andrew Benedick, Helder M Crespo, and Franz X Kärtner. Dynamics of dispersion managed octave-spanning titanium:sapphire lasers. *J. Opt. Soc. Am. B*, 26(4):743–749, April 2009.

[45] A. Plocky, A. A. Sysoliatin, A. I. Latkin, V. F. Khopin, P. Harper, J. Harrison and S. K. Turitsyn. Experiments on the generation of parabolic pulses in fibers with length-varying normal chromatic dispersion. *JETP Lett*, 85:319–322, 2007.

[46] Christophe Finot, Beno\^it Barviau, Guy Millot, Alexej Guryanov, Alexej Sysoliatin, and Stefan Wabnitz. Parabolic pulse generation with active or passive dispersion decreasing optical fibers. *Opt. Express*, 15(24):15824–15835, November 2007.

[47] L F Mollenauer and R H Stolen. The soliton laser. *Opt. Lett.*, 9(1):13–15, January 1984.

[48] K Kieu, W H Renninger, A Chong, and F W Wise. Sub-100 fs pulses at watt-level powers from a dissipative-soliton fiber laser. *Opt. Lett.*, 34(5):593–595, March 2009.

[49] Bai Nie, Dmitry Pestov, Frank W Wise, and Marcos Dantus. Generation of 42-fs and 10-nJ pulses from a fiber laser with self-similar evolution in the gain segment. *Opt. Express*, 19(13):12074–12080, June 2011.

[50] F.W. Kieu, K. and Wise. Soliton Thulium-Doped Fiber Laser With Carbon Nanotube Saturable Absorber. *Photonics Technology Letters, IEEE*, 21(3):128–130, 2009.

[51] L. E. Nelson, E. P. Ippen, and H. a. Haus. Broadly tunable sub-500 fs pulses from an additive-pulse mode-locked thulium-doped fiber ring laser. *Applied Physics Letters*, 67(1):19, 1995.

[52] Jonathan Hu, Curtis R Menyuk, L Brandon Shaw, Jasbinder S Sanghera, and Ishwar D Aggarwal. Computational study of 3–5 μm source created by using supercontinuum generation in As2S3 chalcogenide fibers with a pump at 2 μm. *Opt. Lett.*, 35(17):2907–2909, 2010.

[53] R C Sharp, D E Spock, N Pan, and J Elliot. 190-fs passively mode-locked thulium fiber laser with a low threshold. *Opt. Lett.*, 21(12):881–883, 1996.

[54] Martin Engelbrecht, Frithjof Haxsen, Axel Ruehl, Dieter Wandt, and Dietmar Kracht. Ultrafast thulium-doped fiber-oscillator with pulse energy of 4.3 nJ. *Opt. Lett.*, 33(7):690–692, 2008.